The maintenance of sustained high frequency discharges in gases

S. N. Goswami

THE MAINTENANCE OF SUSTAINED HIGH FREQUENCY DISCHARGES IN GASES

TO

SARASHI

THE MAINTENANCE OF

SUSTAINED HIGH FREQUENCY

DISCHARGES IN GASES

by

S. N. GOSWAMI, M.Sc.

being a thesis submitted for the
Degree of Doctor of Philosophy
in the University of Durham.

June 1966.

PREFACE

The work presented in this thesis was carried out in the University of Durham during the period of study leave granted to me by the Government of West Bengal, India and I take this opportunity of expressing my gratitude to them.

I am very much indebted to the University of Durham for providing me with all the resources of the Physics Department and to the Senate for doing me a great honour by designating me as a Visiting Fellow of the University.

Thanks are due to the Central Electricity Generating Board for generous financial help towards apparatus and technical assistance and also for contribution to my maintenance.

I wish to record my sincerest thanks to my Supervisor, Dr. W. A. Prowse for advice, encouragement and guidance during the course of the work. Thanks are also due to Dr. M. Breare and my colleagues for many illuminating discussions.

SATYENDRANATH GOSWAMI.

TABLE OF SYMBOLS

A	- Area of electrodes " discharge space.
a	- Electron ambit. Constant.
b	- Constant
C	- Capacitance
c	- Velocity of light Constant.
$\bar{c}$	- Mean velocity
D	- Diameter of tubes
D^-, D^+	- Diffusion coefficient of electrons and positive ions respectively.
D_a	- Ambipolar diffusion coefficient.
D_s	- Effective diffusion coefficient.
d	- Distance between electrodes Ammeter deflection.
d_1, d_2	- Lengths of Zones I and II in the discharge space.
E	- Magnitude of the electric field.
E_e	- Effective field
E_g	- Axial electric field in the gas.
E_p	- Peak value of the electric field.
E_R	- Electric field at the wall of tube of radius R.
E_r	- Radial electric field at a distance r from the axis.
e	- Charge of an electron.
f_o	- Natural frequency of oscillation of the ellipsoid.
f	- Frequency of oscillation of the ellipsoid in the r.f. field.
i	- Current. Imaginary ($\sqrt{-1}$)
i_c	- Conduction current.
i_d	- Displacement current.
J_o, J_1	- Bessel functions of the zeroeth and first order respectively.
j^+, j^-	- Current density of positive ions and electrons respectively.

K - Constant. Boltzmann's constant.

K_1 - Constant

L - Inductance

l - length of the discharge tube.

m - Mass of electron.

N^+, N^- - Number density of positive ions and electrons respectively.

N_o - Number density of electrons in the central plasma.

p - Pressure in mm.Hg.

p_o - Pressure reduced to 0^oC.

R - Resistance.

r - Radius of the tube.

S - Space charge density.

T - Period of the applied electric field.

T^+, T_e - Ion and electron temperature respectively.

u_i - Ionisation potential in volts.

V - Potential.

V_o - Observed potential drop.

V_g - Voltage drop in the gas

$V_1(t), V_2(t)$ - Instantaneous voltages in zones I and II respectively.

V_{end}, V_{oend} - Instantaneous and peak value of the end drop of potential.

v_d - Drift velocity.

v_{diff} - Velocity of diffusion.

t_{glass} - Thickness of glass.

$\frac{dV}{dx}$ - Voltage gradient in the x-direction.

$\frac{dN}{dx}$ - Concentration gradient in the x-direction.

α - Probability that an electron will be swept out of the discharge space by the h.f. field.

α_1 - Ratio of negative ion to electron concentration.

γ - Ratio of electron to ion temperature.

ε_r Permittivity of mediu

ξ - H.F. ionisation coefficient.

Λ - Characteristic diffusion length of the discharge vessel.

λ - Wave-length of the applied field.

λ_e - electronic mean free path.

μ_+, μ_- - Ionic and electronic mobility respectively.

μ^o - Reduced mobility of positive ions.

ν - Collision frequency.

ν_i - Ionising collision frequency.

σ_o - Electrical conductivity at the central plasma.

θ - torque.

ω - Angular frequency of the applied field.

ω_r, ω_p - series and parallel resonance frequency.

CONTENTS

CHAPTER IV. INSTRUMENTATION

CHAPTER - I

INTRODUCTION.

1.1 General Considerations.

Studies in the h.f. discharge in gases have aroused interest in relatively recent years compared to studies in d.c. discharge. The processes of ionisation and deionisation and hence the maintenance conditions in the h.f. and d.c. cases are fundamentally different in many important respects; those in the former type of discharge appear to be much less complicated compared to those in the latter type. In fact, there is a domain of the h.f. discharge where there are only two processes competing with each other, namely, gain by collisional ionisation and loss by diffusion. This is, therefore, the simplest type of the h.f. discharge. This happens when both the mean free path of the electrons and their amplitude of oscillation are much smaller than the gap dimensions.

Numerous experiments have been performed to explore the mechanism of h.f. breakdown. There are three major variables and their relative values determine the relative importance of the various physical processes operating.

These are: (a) the gas pressure p (and hence the mean free path of electrons and their collision frequency ν with the gas molecules); (b) the dimensions of the gap and (c) the frequency ω of the applied field.

The mechanism of discharge for various ranges of p, ν and ω may be so different that it is difficult, if not impossible, to formulate a unique theory covering the entire range of observations done so far. The problem has been attacked by different schools of workers by means of variations in respect of the gap geometry, amplitude and frequency of the applied field, the nature and pressure of the gas, nature and shape of the electrodes (both internal and external) and their separations. Nevertheless, one is not sure how, when the discharge has started and reached equilibrium condition the boundary voltage drop compares with the voltage drop in the gas and what their phase relationship is. One may, further, ask a simple question as to how the conductivity of the gas changes with gap current, the answer to which is far from simple. It is known that the conductivity of the gas is a complex quantity, there being both an in phase (real) and an out of phase (imaginary)

component of current. In order to ascertain the conductivity of the gas at any stage after breakdown, one needs to know the current-voltage characteristics of the conducting gas, of which very little is known.

The current-voltage relations were examined by the Townsend (1) school of workers. Their experimental results, with external electrodes fitted to cylindrical vessels of different gap geometry show that within a limited range of pressure and gap current, the characteristic is approximately a straight line. Observations were also made with internal electrodes. In order to compare the results with the elctrodeless case considerations of the voltage drop between the external electrodes and the inner surface of the discharge tube was necessary. Townsend and his associates treated this in a simple way, neglecting the inherent phase quadrature between this drop and that along the gas column so that an error of uncertain magnitude was introduced. The results presented in this thesis all take account of the phase relation between the dielectric voltage drop (between the external electrodes and the inner surface of the discharge tube) and the voltage drop along the gas column.

As a result of study by a great many workers, plenty of experimental data are available now relating the breakdown and maintenance potentials and fields to the various similarity parameters, e.g. $p\Lambda$, $p\lambda$, $E\Lambda$, etc., where E and λ are the magnitude and wave-length of the applied field respectively and Λ is the characteristic diffusion length of the discharge vessel. For a cylindrical discharge tube of radius r and length ℓ, the characteristic diffusion length Λ is defined by

$$\frac{1}{\Lambda^2} = \left(\frac{\pi}{\ell}\right)^2 + \left(\frac{2.405}{r}\right)^2 \qquad (1.1)$$

From a study of extensive data obtained from various sources it is possible to distinguish certain limiting regions of the diffusion-controlled h.f. discharge. These limits are concerned with (i) the uniformity of the field; (ii) the electronic mean free path, (iii) the oscillation amplitude of the electrons and (iv) collision frequency. A good review on this aspect has been given by S.C.Brown (2). Data have been collected and shown to be lying within these various limits. It has also been shown that even when the breakdown is other than diffusion-controlled,

it is possible to represent all data by a $p\Lambda$ - $p\lambda$ - $E\Lambda$ surface model. For each gas such a surface is unique. This surface model is such a useful thing that not only pure h.f. discharges but also those with superposed d.c. and/or a.c. and/or magnetic fields can be taken account of by such surfaces, by using modified values of the characteristic diffusion lengths (Λ) under corresponding conditions.

One of the important problems of the h.f. discharge is that of determining the electronic concentration N in the gap and its spatial distribution. A few other fundamental quantities like the breakdown and maintenance potentials, frequency of ionisation ν_i, the electron temperature T_e, the coefficient of diffusion D, the electrical conductivity σ etc. are also of importance. The values of all these parameters at any point in the gap are known to be functions of the spatial co-ordinates of the point in the gap, as well as of the ratio E/p, where E is the breakdown field.

We are, however, here concerned with the maintenance conditions of the sustained discharge rather than the conditions leading to breakdown. In fact, one does not know how the voltage in the gap adjusts itself to the

steady state current flowing in the gap. Does the gap, after breakdown, behave as a pure resistance, or a pure reactance, or a simple L,C, R circuit, or a combination of some or all of them, in a simple or intricate manner? Disregarding drift, recombination or attachment we can arrive at a reasonable answer to these questions by assuming that diffusion is the only loss process to compete with electron generation by the applied field. One has also to bear in mind that when the steady state is attained the charge density is favourable for the transition of free electron diffusion to the so-called ambipolar diffusion, which arises as follows (3).

Let us assume that the applied field is slightly less than that necessary for breakdown. There may be only a few electron-ion pairs produced by the small energy transfer from the field to the chance electron and the loss by diffusion stops the development of the discharge, which, therefore, cannot maintain itself. When the applied potential is of the right value for breakdown to occur, the loss by diffusion is equal to the gain from the field. With the onset of breakdown, the concentration of electrons and ions in the plasma

reaches a very high value quickly. Now, the electrons diffuse out of the gap very much faster than the ions. This causes a gradual building up of a positive space charge and thus creates an electrostatic field between the body of the plasma and the walls of the container. This means that soon after breakdown the electrons are slowed down and the positive ions are speeded up by this electrostatic field, and after a while, there is a compromise so that both the electrons and positive ions diffuse out of the gap at the same rate. This fact has been taken account of, by defining an effective diffusion co-efficient of both electrons and positive ions, the ambipolar diffusion co-efficient D_a. In the free limit, therefore, when the discharge just starts or is about to start, the loss is purely by electron diffusion, the charge density in the gap is low and diffusive velocity high. In the ambipolar limit, on the other hand, when the discharge reaches a steady state, the loss is by ambipolar diffusion, the charge density is high and diffusive velocity is one or two orders of magnitude lower than in the former case. The diffusive losses in the steady state being thus much reduced, the maintenance potential is much less than the breakdown

potential.

In the diffusion-controlled, steady-state, h.f. discharge as has been studied by the author, it is, therefore, the value of the ambipolar diffusion, and not that of the free electron diffusion that is of the utmost significance. The role of the ambipolar diffusion in various discharge configurations has been studied in great details in recent years. A knowledge of this is essential for the interpretation of experimental results.

The variation of D_a has been mostly studied in the afterglow of various gases mainly by microwave techniques. For example, for a plasma consisting of electrons and one type of positive ion, Oskam and Mittlestadt (4) found that D_a is independent of time; for plasma containing electrons and several types of positive ions, however, D_a decreases with time and approaches the value corresponding to that in the presence of the slowest type of positive ion; in a plasma consisting of both positive and negative ions and electrons, D_a is found to increase with increasing ratio of negative ion to electron concentration. Mulcahy and Lennon (5) have studied also the variation of this co-efficient with pressure. Further, in many h.f. discharges, the spatial

distribution of electrons has a maximum at the centre and approaches zero at the walls. Thus, there is a transition region on either side of the central plasma where ambipolar diffusion changes into free electron diffusion (6). Owing to these important facts, a review of recent literature on this co-efficient with particular attention to the h.f. discharge phenomena would be useful and is given in Chapter II.

In Chapter III, the description of the experimental conditions imperative with our main assumption that ambipolar diffusion is the only loss process will be given. An oscillator of the dielectric heater type capable of delivering high power (3.5 KW) at 17 Mc/s was available in the laboratory; for this frequency the necessary pressure range and the gap dimensions are discussed.

Chapter IV deals with the instrumentation. This is a major part of the work; as this was a new experiment altogether, everything had to be assembled from the very start. The development of the voltage and current measuring circuits, effective screening of the discharge tube and its associated circuit etc. are described

chronologically as far as possible.

In Chapter V, some observations on the stationary and moving striations are reported. The explanation of their formation in an h.f. discharge is far from clear. Their study is in itself an important subject and should be taken separately. Nevertheless, some interesting photographs are presented as a matter of general interest. A short discussion of the existing literature on the h.f. striations has also been included.

In Chapters VI - IX, the main results of the experiments are shown graphically. As will be explained in section 1.2 below, our basic assumption was that ambipolar diffusion is the major electron removal process and if that is so, one should expect a constant potential gradient in long cylindrical tubes and a constant current density in flat cavities, where respectively, the current and voltage are maintained constants. The experimental results are in good agreement with these expectations.

Finally, in Chapter X, general discussion of results has been made. Values of some important quantities, namely, the ambipolar diffusion co-efficient, the h.f. ionisation co-efficient and the number density of electrons

in the central plasma have been calculated as a function of the gap current and the gas pressure. The meaning of the end-drop of potential, possible application of the Langmuir probe theory, treating the electrodes as probes, for determining the electron concentration and electron temperature in the plasma, comparison of power dissipation in the long cylindrical tubes and flat cavities and lastly, application of Poisson's equation to find the density of charges near the electrodes, have been discussed in detail. Also, some of the limitations of the present experiments have been pointed out.

1.2 The Problem

Results of investigations on the h.f. discharge by previous workers (1), (7), (8), reveal a few things which are common in them: (a) there exist two sharply defined regions in the discharge space, the end regions where the field is high and the charge density low, and the central region where the field is low and the charge density high; (b) the two potential drops, large at the ends and small at the centre, have a phase relationship between them. One of the problems is what their phase

relation is. Also, one does not know how the current-voltage relation in the gap is determined by the pressure and nature of the gas, or by the gap geometry.

Let us make the hypothesis that the maintenance of discharges at ultra-high frequencies in suitable conditions is a matter of the balance between generation of electrons and ions by ionising collisions on the one hand and their removal by ambipolar diffusion to the walls or the end plates on the other. Two types of geometry are suitable for testing the above hypothesis, e.g. long cylindrical tubes of which the radius is small in comparison with the length, and parallel plate systems in which the radius of the plates is large compared with the separation.

In the long cylindrical geometry, diffusion to the cylindrical walls is the operative removal process and it is to be expected that, provided the electron population is not too dense, one length of the tube should be like any other length, since, as can be seen from Eq. (1.1), when $r \ll \ell$, the characteristic diffusion length Λ is $r/2.405$ and is, therefore, independent of length. One can, therefore, expect constant potential gradient along the column. Here, we must make the assumption that we are

dealing with discharges in which the electron temperatures are the same. This is to be expected with discharges in which the same current is used for a tube of a given radius whatever the length of the tube, provided the expected result is obtained, namely, that the potential gradient in the tube is, in fact constant. In particular, discharge observations on the potential gradient in tubes of various diameters should tell us whether in fact diffusion is the controlling process. It is expected that in experiments of this type the regions around the electrodes will have different properties from the column as a whole, and observations of this kind are valuable.

When parallel plate electrodes are employed, it is conceived that in the case of plates whose distance apart is small compared to their radii, diffusion to the plates themselves is the operative removal process. In this case, since $r >> \ell$, the characteristic diffusion length Λ is ℓ/π, and is, therefore, independent of the radius. Thus, for a given flat cavity, if the potential drop between the electrodes is the same, one should expect constant current density for all electrode areas, to satisfy the assumption that electron temperatures must be the same in comparable systems.

It is expected that these diffusion-controlled discharges will fill the whole of the interelectrode space in most cases. But at higher pressures, the discharges are much more likely to be filamentary than diffuse in form and it will be a matter of great interest to observe the transition, if any, from the uniform glow type of discharge to the filamentary one and to try to ascertain the mechanism for this transition.

It is likely that these simple conceptions will be interfered with and the experimental results masked by occasional incidence of plasma oscillations.

CHAPTER - II

REVIEW OF LITERATURE ON AMBIPOLAR DIFFUSION

2.1 The Basic Concepts.

The coefficient of ambipolar diffusion is rather a concept than a separate physical entity, which takes into account the mobility and diffusion coefficient of electrons and positive ions. If μ^+, μ^- are the mobilities and D^+, D^-, the coefficients of diffusion of ions and electrons respectively, then the coefficient of ambipolar (meaning "on both sides of the axis") diffusion is defined by

$$D_a = \frac{D^+\mu^- + D^-\mu^+}{\mu^+ + \mu^-} \qquad (2.1)$$

This definition arises from the following considerations: If N^+ be the number density (i.e. number per unit volume) of positive ions, then the number of positive ions diffusing per second through unit area perpendicular to the x-axis (say) is

$$N^+ v^+_{diff} = -D^+ \frac{dN^+}{dx} \qquad (2.2)$$

where $\frac{dN^+}{dx}$ is the concentration gradient necessary for diffusion to occur. The negative sign appears because diffusion takes place in the direction of decreasing concentration.

Now, if the applied field E is also in the x-direction, then the drift velocity v_d^+ (say) of the positive ions is defined by

$$v_d^+ = \mu^+ E \tag{2.3}$$

Thus, considering diffusion taking place only along the field direction, the total velocity of the ions is given by

$$v^+ = v_{diff}^+ + v_d^+ \tag{2.4}$$

Therefore, the positive ionic current density

$$j^+ = N^+ v^+ = -D^+ \frac{dN^+}{dx} + N^+ \mu^+ E \tag{2.5}$$

Similarly, if N^- be the number density of electrons, one can write

$$j^- = N^- v^- = -D^- \frac{dN^-}{dx} - N^- \mu^- E \tag{2.6}$$

In the steady state, the flow (or the particle current density) of both types of particles is the same i.e. $j^+ = j^- = j$ (say). Assuming that

$$\frac{dN^+}{dx} = \frac{dN^-}{dx} = \frac{dN}{dx} \quad \text{(say)} \tag{2.7}$$

one can eliminate E from (2.5) and (2.6) and obtain

$$j = -\left(\frac{D^+\mu^- + D^-\mu^+}{\mu^+ + \mu^-}\right) \frac{dN}{dx} \tag{2.8}$$

which is of the same form as (2.2).

The expression within brackets on the right hand side of (2.8), therefore, can be shortened into D_a so that

$$D_a = \frac{D^+\mu^- + D^-\mu^+}{\mu^+ + \mu^-} \tag{2.1}$$

It is an effective diffusion co-efficient of both electrons and positive ions.

It may not be irrelevant if a few notes on Eq.(2.1) and the concept of the ambipolar diffusion are added here. These are enumerated overleaf:

(i) The values of the mobility and diffusion co-efficient of electrons in terms of the electronic mean free path λ_e and mean velocity $\bar{c}$ are respectively given by

$$\mu^- = \frac{e\lambda_e}{m\bar{c}} \qquad (2.9)$$

and

$$D^- = \frac{\bar{c}\lambda_e}{3} \qquad (2.10)$$

so that

$$\frac{D^-}{\mu^-} = \frac{m\bar{c}^2}{3e} = \frac{KT_e}{e} \qquad (2.11)$$

where T_e is the electron temperature. This definition of T_e assumes that the velocity distribution of electrons is Maxwellian.

For positive ions, one can similarly write

$$\frac{D^+}{\mu^+} = \frac{KT^+}{e} \qquad (2.12)$$

T^+ being the positive ion temperature, again assuming that the velocity distribution of ions also is Maxwellian.

Now, experimentally, $\mu^- >> \mu^+$. Therefore, when

$T_e >> T^+$, it follows from (2.1) that

$$D_a = D^+ + \frac{D^- \mu^+}{\mu^-} \simeq \frac{D^- \mu^+}{\mu^-} = \frac{KT_e}{e} \mu^+ \quad (2.13)$$

When, however, $T_e \simeq T^+$,

$$D_a = \frac{2KT_e}{e} \mu^+ \quad (2.14)$$

i.e. twice the value given by (2.13).

(ii) In the body of the plasma, $N^+ - N^- << N^+$ or N^-. If this is not so, the differences in N^+ and N^- may create a space charge field of such a magnitude as can possibly annul the gradient of concentration responsible for the diffusive flow; i.e. the system is self-adjusting.

(iii) Though one freely uses the term 'electronic mobility' in h.f. fields, it must be realised that the concept is rather a fiction than a reality. Further, even in the d.c. case, except in the molecular gases, the ratio of the drift velocity of electrons to the applied field, that is, the mobility is not a constant quantity. Since constant electronic mobility has been assumed above, the implication is that either the electric field variation

should be small or the curvature of the electronic drift velocity function against E/p should be negligible, as is true in the case of molecular gases. If, instead of writing $\mu^{-}E$ in Eq.(2.6) one writes $c\sqrt{E}$ (where c is a constant) for electrons, which is probably in better agreement with experiment, the resulting expression for the ambipolar diffusion becomes rather cumbrous and inconvenient for physical interpretation. In h.f. fields nearly all electron drift takes place near the peak of a sine-curve, i.e. the error introduced by disregarding the higher mobility at low fields is smaller than might be expected.

(iv) T_e is known to have a spatial variation; this means that D_a should vary in the same way and that when we talk of ambipolar diffusion co-efficient Da, we really mean a sort of average value of it within the discharge system.

(v) At very low pressures, the idea of diffusion is no longer valid, since then there really occurs many more collisions on the walls of the discharge tube than in the volume. The loss of electrons to the walls is still governed in this case by the random velocity of the electrons

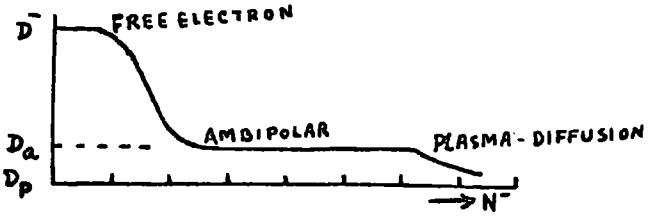

FIG. 2.1. FREE ELECTRON (D^-), AMBIPOLAR (D_a) AND FULLY IONISED PLASMA (D_p) DIFFUSION CO-EFFICIENTS AS A FUNCTION OF ELECTRON CONCENTRATION (N^-) AT A CONSTANT ELECTRON TEMPERATURE (AFTER VON ENGEL)[9]

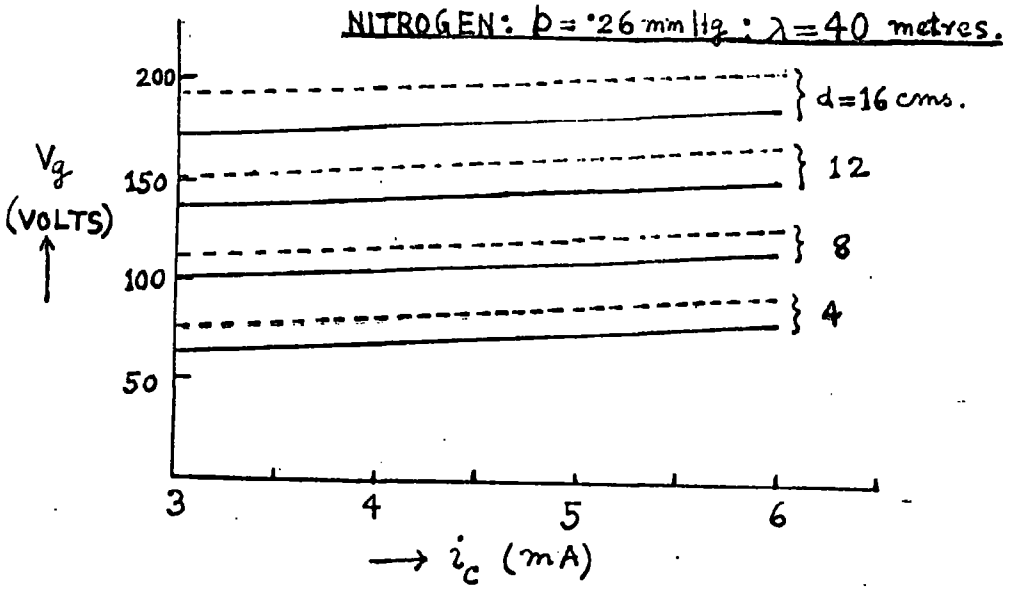

FIG. 2.2. CURRENT-VOLTAGE CURVES (DOTTED-FOR TUBE DIAMETER 2·9 cm; CONTINUOUS – FOR TUBE DIAMETER 3·9 cm.) d = DISTANCE BETWEEN ELECTRODES (AFTER TOWNSEND AND NETHERCOT)[1]

but it is not the value of the pressure alone, but rather the ratio ω/p, (where ω is the angular frequency of the applied field) that determines the h.f. drift loss factor. At low charge densities free electron diffusion operates. Since the concept of ambipolar diffusion refers to a state of statistical equilibrium in the discharge, there should be high enough gas density to provide sufficient number of collisions per second.

If, however, the plasma is too dense, i.e. if $N^+ = N^-$ is too high, the density of neutral molecules may be so small that electron-ion collision will far exceed those with the neutrals. The diffusion then is better known as the plasma diffusion rather than ambipolar diffusion. Thus, ambipolar diffusion is midway between the electron diffusion and the plasma diffusion on the low and high charge density regions respectively(9)(Fig.2.1). It may, further be noted that when the charge density is too high i.e. in the plasma diffusion region, the assumption of Maxwellian distribution for electronic and ionic velocities, is no longer valid and hence we cannot properly talk of the terms like T^+, T_e etc..

(vi) As p is raised, atomic ions are said to be replaced

by molecular ions. As we shall see later, when there are two types of ions, there will be two values Da_1 and Da_2 of ambipolar diffusion co-efficient. In addition, the presence of negative ions will also introduce another ambipolar diffusion co-efficient for them.

(viii) Referring to Eq. (2.13), one should note that both theory and experiment have established the inverse dependence of μ^+ with pressure, and hence $D_a p$ is constant.

(viii) Some workers (5) have experimentally found that D_a decreases with increase of the molecular weight of the experimental gas.

(ix) The concept of ambipolar diffusion is only a method of eliminating the use of the radial field.

After enumerating the basic facts concerning this co-efficient, it is now proposed to give a short review of literature where ambipolar diffusion is the primary electron removal process under different experimental conditions.

2.2 The Review

As early as 1928-29, Townsend and his associates (1) investigated certain properties of the h.f. discharge

under conditions where ambipolar diffusion is the main operating process. They used long cylindrical tubes fitted with external electrodes in the form of slideable sleeves as well as with electrodes immersed in the experimental gases which were He, N_2 and Ne. They not only measured the starting and maintenance potentials, but also extended their investigations to obtain current-voltage characteristics in the discharge for a uniform glow. They found that these characteristics were positive (Fig. 2.2); also, that over a limited range of currents the field in the gap was found to be independent of the current and the frequency of the applied field. With large currents, however, the field was found to diminish with the current. The change of field with the current was found to be smaller in wide tubes than in narrow tubes under otherwise unaltered conditions. This fact led Townsend to propose that the change in the field was probably due to the increase of temperature with the large currents; an increase of temperature means a decrease in the density of the gas, which, in turn, means a diminuition in pressure and hence a smaller field to maintain the current, since at low pressures, the field is less when the temperature is constant.

An explanation of the mechanism of the h.f. discharge was given on the same principles as the d.c. discharge. They affirmed that the mean value of the electric field in the uniform h.f. glow should be the same as that in the uniform positive column of a d.c. discharge. The electric field in the latter is governed by the condition that supply of ions by collisional ionisation is balanced by the loss due to diffusion. Townsend remarks that this hypothesis means "there must be a positive charge in the gas which repels positive ions towards the surface and retards the rate at which the electrons reach the surface by diffusion so that the positive ions reach the surface at the same rate as electrons". This is precisely ambipolar diffusion, though Townsend did not use the term.

Thus, N^+ exceeds N^-, but the difference $N^+-N^- << N^+$ or N^-. Also, the charge $e(N^+-N^-)$ is independent of N^+ or N^-.

Therefore, there are two fields in the positive column, the axial field and the radial field. The latter effectively increases the conductivity of the gas by reducing the diffusion loss of electrons.* There is also a charge, Townsend states, on the inner surface of the tube which tends to become distributed so that the axial field is

* See bottom of next two pages

uniform in the uniform glow. The explanation of the h.f. discharge is based on the above principles of a d.c. discharge.

An empirical relation between the observed potential difference V and the current i was given in the form

$$\left.\begin{aligned} V &= E_g(x+a) + b\lambda i \\ &= E_g x + E_g a + b\lambda i \end{aligned}\right\} \qquad (2.15)$$

where E_g is the axial field in the central plasma and a,b are constants depending upon the pressure of the gas and the diameter of the tube and λ is the wave-length of the applied field. Eq. (2.15) indicates that the total potential is divisible into a fall along the column corresponding to a gradient $\frac{dv}{dx} = E_g$, together with a component $(E_g a+b\lambda i)$ of the general nature of an end-effect (namely, the drop between the sleeves and inner surface of the tube and in the gas near the electrodes where the electric field is different). This is supported by the observation that E_g was found to be the same whether internal or external electrodes were used.

---

* This means that there is probably another cause of the reduction of field intensity with increase in current. The charge density increases with current and this probably reduces the value of Da (Fig.2.1). The loss of charged particles being thus reduced, the maintaining field should

It may be remarked here that Townsend's proposition of the two potential drops in phase (i.e. in the column and at the ends) is an over-simplification of the real situation: that at least one of them (the potential drop between the sleeve electrodes and the inner surface of the tube) being a drop across the tube capacitance should be in phase quadrature with the voltage drop in the central plasma. This is further discussed in Chapter VI.

When the current is high, both E_g and b in Eq. (2.15) decrease with further increase in current. These changes are enhanced at higher pressures.

Townsend's results in nitrogen with external and internal electrodes show that at pressures above 1.6 cm, the potential difference between the internal electrodes is smaller than that between external electrodes. Below 1.6 mm, the reverse is true. No explanation of this was given by the authors.

For a given current, the potential V is greater in the

---

* be less. Yet another possible cause may be the secondary emission from the electrodes or the walls of the tube, or even the thermal ionisation if the temperature of the plasma is high enough at the large currents.

electrodeless case than that with immersed electrodes. This difference is attributed to the potential drop across the tube capacitance, which is proportional to the current. Since the effect is small with small currents, the maintenance of the current, it is stated, cannot be due to the secondary emission from the internal electrodes, unless in the electrodeless case too there is secondary emission from glass, which, according to Townsend, is highly improbable. Subsequent works by von Engel and his associates (10-11) and Hatch and Williams (12), however, have beyond doubt established that secondary emission from glass is quite a probable phenomenon.

Some qualitative observations were also made by Townsend and Jones(13) regarding the intensity characteristics of the glow as a function of the change in current. For example, the glow is uniform along the whole length of the tube and its intensity increases with the current. The glow, however, disappears from the middle part of the tube, when the current is below a certain value, the two ends remaining luminous. The minimum potential necessary to maintain a current of uniform glow can be easily determined. When the applied power is reduced, there is an abrupt diminuition of current and an increase in the

potential drop between the electrodes.

Regarding the qualitative study of the h.f. electrodeless glow discharge (with movable external electrodes fitted to cylindrical discharge tubes) the work of R.L. Hayman (14) (1929) in He and Ne contains some valuable information. He observed that -----

(a) the radial distribution of the luminosity in the discharge is dependent upon the pressure of the gas as well as the current flowing through the gap.

(b) the ratio of the intensity near the axis to that near the wall is greatest at high pressure and weak discharges; also it appears to increase with the wavelength.

(c) the colour of the discharge depends upon the pressure as well as the electric field intensity -- for higher pressure and low field, there is a shift towards the red end and for lower pressure and high field, towards the blue end of the spectrum.

Some of the main problems of the h.f. discharge are the determination of the distribution of the field in the gap, variation of the ionisation rates in the different regions of the discharge space, and the spatial distribution of the electron density. Allis, Brown and Everhart (8) studied these problems in systems where ambipolar diffusion

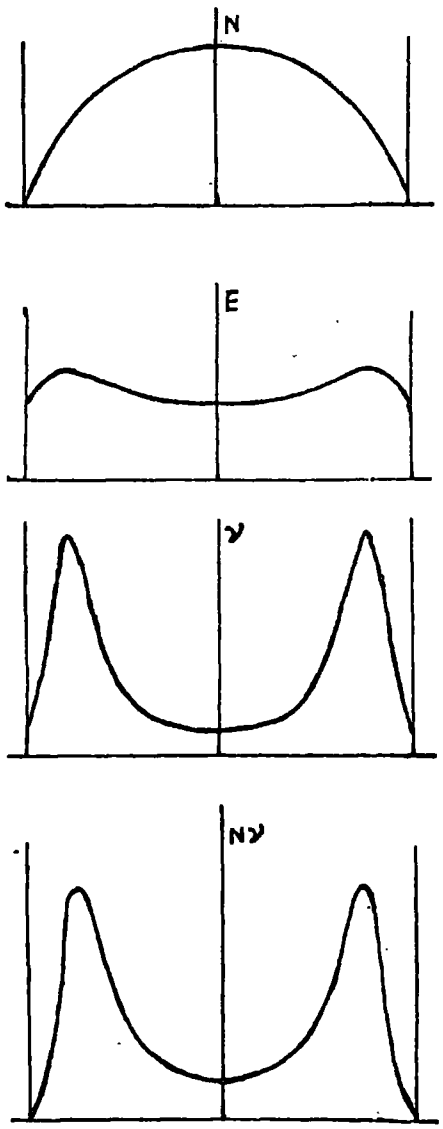

FIG. 2.3. VARIATION OF ELECTRON DENSITY N, ELECTRIC FIELD E, IONISATION RATE PER ELECTRON ν AND IONISATION RATE PER UNIT VOLUME $N\nu$ FOR A HELIUM DISCHARGE. THE ELECTRODES ARE REPRESENTED BY VERTICAL LINES. (AFTER ALLIS, BROWN AND EVERHART[8])

is the main operating mechanism. It is known that when an h.f. field is applied to a plasma of high electron concentration, plasma resonance maximises the field i.e. the field intensity tends to become a maximum where the plasma is resonant. The effect of this resonance on the electron distribution and ionisation in the simplest case of a parallel plane discharge was calculated. Their calculations are in agreement with the fact that the intensity of the high-frequency glow is a minimum at the centre (Fig.2.3).

This phenomenon of plasma resonance can be very important. In a valuable paper dealing with phenomena of this kind, Schneider(7) has shown that the discharge in the case of plane parallel electrodes can be represented by an equivalent circuit (Fig.2.4) which possesses both series and parallel resonances. The parallel resonance frequency ω_p is given by that part of the equivalent circuit representing the body of the plasma and is the same as the ordinary plasma resonance frequency, given by

$$\omega_p^2 = \frac{N_o e^2}{m\epsilon_o} \qquad (2.16)$$

where N_o is the maximum density of the electrons in the centre of the plasma and ϵ_o is the permitivity of the

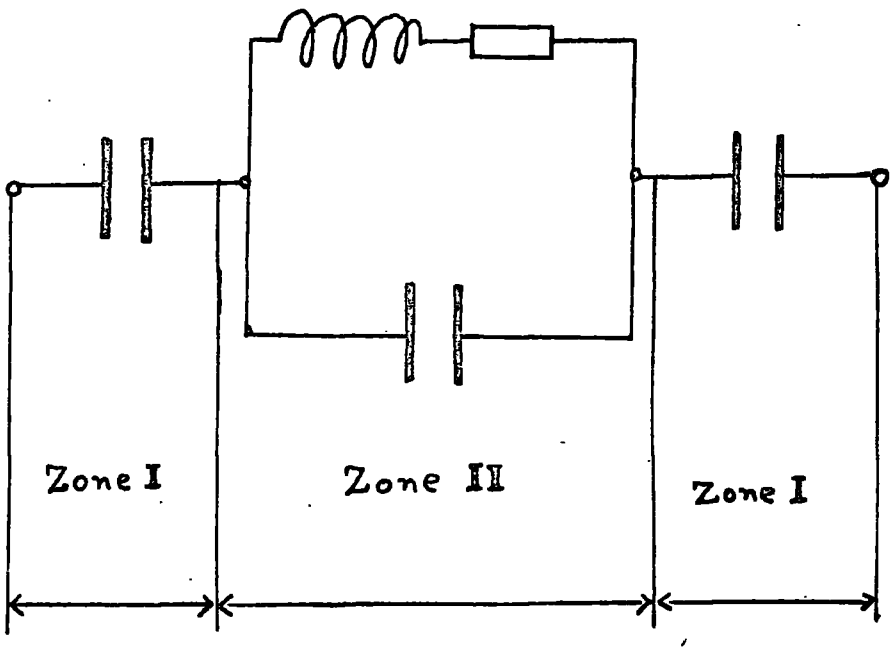

FIG. 2.4. EQUIVALENT CIRCUIT OF H.F. DISCHARGE (AFTER SCHNEIDER)[7]

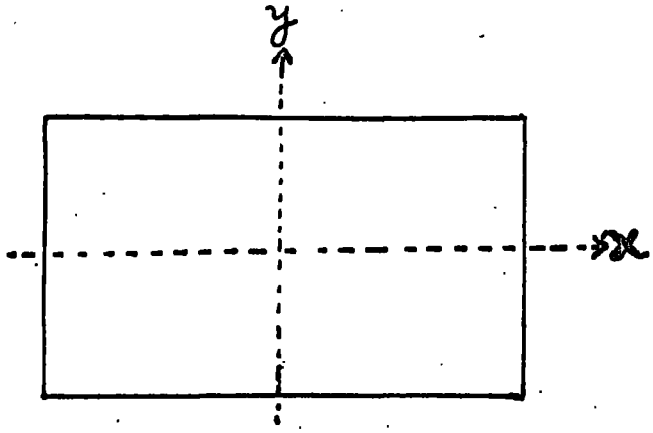

FIG. 2.5. THE DISCHARGE TUBE AND ITS AXES OF CO-ORDINATES.

discharge space. According to Schneider, one is, however, more concerned with the series resonance given by the entire equivalent circuit i.e. the central plasma (zone II) as well as the two end regions (zone I), the series resonance frequency ω_r being given by

$$\omega_r^2 = \frac{N_o e^2}{m\varepsilon_o} \frac{2d_1}{d_2 - 2d_1} \qquad (2.17)$$

which is of the same form as Eq. (2.16); d_1 and d_2 are the breadths of zones I and II respectively. The plasma resonance frequency is, therefore, modified by the factor $2d_1/d_2-2d_1$. It is evident that occurrence of plasma resonance necessitates the existence of the two end zones (for if $d_1 = 0, \omega_r = 0$) and vice versa. Further, if $d_2 \simeq 2d_1$, the plasma resonance frequency is very high.

A particular point should be specially noted here, namely that Schneider's starting equation for j^- is modified by the addition of an extra loss term $\alpha x N$, where N is the plasma density and αx is the probability that an electron will be swept out of the discharge space by the h.f field, x being measured from the centre of the plasma (Fig. 2.5). The origin of this loss term has been explained by him as follows:

In the gap electrons which are at a distance less than their amplitude of oscillation from either electrode will touch the electrode and be lost, whereas those much further away, right into the middle of the gap, will not be cleared by drift motion. This means that in the steady state, the electron density in the middle region of the gap should be independent of time. The greater the field strength, the greater the random motion of the electrons, and hence the greater is the probability of diffusion to the walls i.e. this loss term and hence α should increase with increasing field strength.

The value of α determines the spatial distribution of electrons and as it depends on E, also determines the character of the h.f. discharge. When α=o, i.e. an undistorted plasma, the electron distribution is represented by a cosine function: when $\alpha = \frac{(\mu^+ + \mu^-)\nu}{3\mu^+}$, ν being the collision frequency, the spatial distribution curve of electrons is parabolic. For higher values of α, the distribution curve is more and more of a square shape. The distribution curves for various values of α are given in Fig. (2.6). Measurements agree better with curve III or IV, so that approximately homogeneous charge density can be assumed in the centre of the plasma. The discharge space can then be divided into two zones: zone I at the ends where

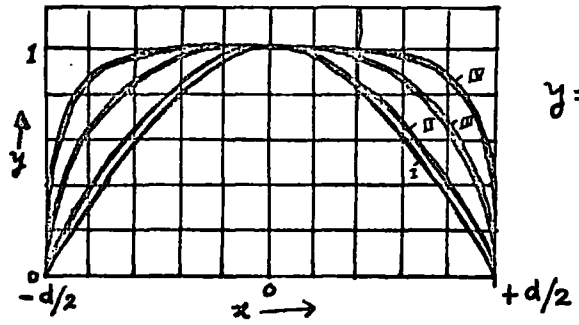

$y = \left(\frac{N}{N_0}\right) = 0$, AT $x = \pm d/2$.
$= 1$, AT $x = 0$.

FIG. 2.6. SPATIAL DISTRIBUTION OF ELECTRON DENSITY. (AFTER SCHNEIDER[7])

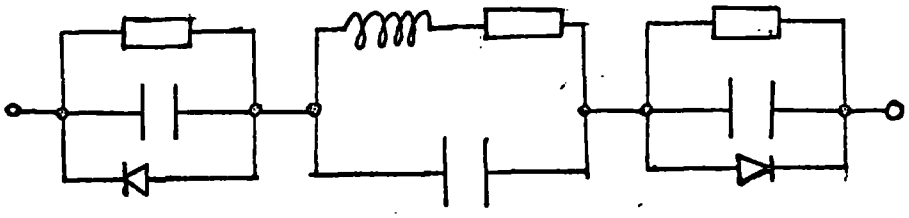

FIG. 2.7. MODIFIED EQUIVALENT CIRCUIT (AFTER SCHNEIDER.[7])

N approaches zero and zone II at the centre where N is a constant. Applying Maxwell's equation for conservation of total current to the two zones, the equivalent circuit of Fig.(2.4) and hence expressions for ω_p and ω_r as given by Eqs.(2.16) and (2.17) can be obtained.

There is a rectifying effect at the boundary regions of the discharge. This arises from the difference in mobility between electrons and positive ions. This can be taken account of by a modification of the equivalent circuit of Fig.(2.4) at the boundary regions, as shown in Fig.(2.7).

Observations on discharge admittance and average potential of the plasma with probes were in agreement with theory.

In a gas containing more than one type of positive ion, there arises the question of more than one ambipolar diffusion co-efficient, e.g. D_{a1}, D_{a2} etc. Phelps and Brown(15) considered this point when both the atomic and molecular ions are present in a system. For example, in an afterglow of a low pressure helium discharge, both He^+ and He_2^+ exist simultaneously. The two types of ions diffuse independently of each other with ambipolar diffusion co-efficients D_{a1} and D_{a2}. It has been shown that the ambipolar diffusion co-efficient decreases with

time and approaches the value corresponding to the slower ions, which are He^+ ions.

If one of the two types of ions is negative, the ambipolar diffusion conditions should be naturally affected. The problem was dealt with by J.B. Thompson (16). When a low pressure discharge is run in an electro-negative gas, negative ions are formed by attachment of electrons to atoms or molecules. While the electrons due to their small mass move rapidly to the walls and form a negative surface charge, the negative ions being much heavier remain in the volume. The negative potential of the wall (due to the deposition of electrons) also retards the escape of the negative ions from the plasma. The concentration of the negative ions, therefore gradually builds up, until they are lost by volume recombination with positive ions.

In a study of the oxygen discharge, these negative ions were detected and their temperature determined by probe techniques. Three ambipolar diffusion co-efficients appear in such cases, i.e. D_a^+, D_a^- and D_a^e for positive ions, negative ions and electrons respectively. Assuming $N^+ = N^- + N_e$ approximately, and denoting the ratio of electron to ion temperature, and negative ion to electron

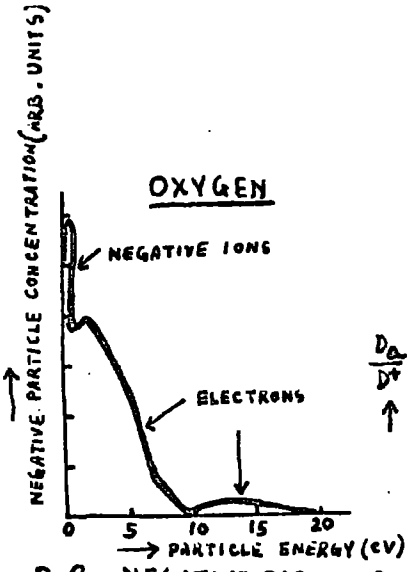

FIG. 2.8. NEGATIVE PARTICLE ENERGY DISTRIBUTION (AFTER THOMPSON)[16]

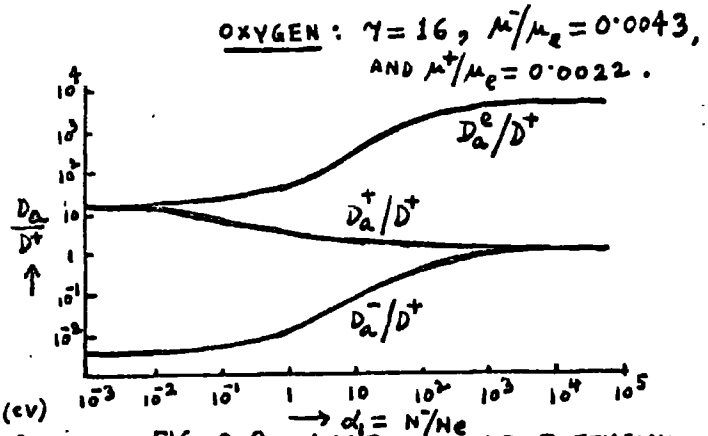

FIG. 2.9. AMBIPOLAR DIFFUSION CO-EFFICIENTS AS A FUNCTION OF $\alpha_1 = N^-/N_e$ (AFTER THOMPSON)[16].

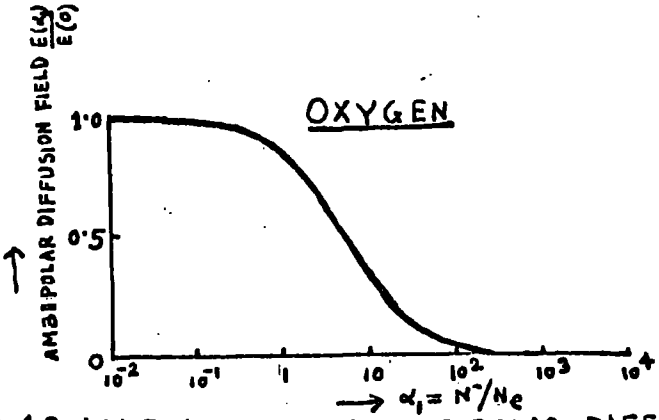

FIG. 2.10. VARIATION OF AMBIPOLAR DIFFUSION FIELD $E(\alpha_1)/E(0)$ WITH α_1 (AFTER THOMPSON)[16]

concentration by γ and α_1 respectively, Thompson showed

$$\left.\begin{aligned} D_a^{+} &= D^{+}\left[\frac{(1+\gamma+2\alpha_1\gamma)\ (1+\alpha_1\mu^{-}/\mu_e)}{(1+\alpha_1\gamma)\ \left\{1+\mu^{+}(1+\alpha_1)/\mu_e+\alpha_1\mu^{-}/\mu_e\right\}}\right] \\ D_a^{-} &= D^{+}\left[\frac{1}{\gamma}\ \ \frac{\mu^{-}}{\mu_e}\ \ \frac{1+\gamma+2\alpha_1\gamma}{1+\mu^{+}(1+\alpha_1)/\mu_e+\alpha_1\mu^{-}/\mu_e}\right] \\ D_a^{e} &= D^{+}\left[\frac{1+\gamma+2\alpha_1\gamma}{1+\mu^{+}(1+\alpha_1)/\mu_e+\alpha_1\mu^{-}/\mu_e}\right] \end{aligned}\right\} \qquad (2.18)$$

The negative particle concentration as a function of the particle energy is shown in Fig.(2.8) and from this Fig.(2.9) has been obtained. It may be remarked here that Fig(2.8) shows three peaks, the origin of which is not known.

The ambipolar field E may be expressed as a function of α_1 by the expression

$$\frac{E(\alpha_1)}{E(0)} = \frac{1-D^{+}/D_a^{+}}{1+\alpha_1}\left(\frac{1+\gamma}{\gamma}\right) \qquad (2.19)$$

where E(0) is the normal ambipolar diffusion field when there are no negative ions ($\alpha_1 = 0$). Its variation with

α_1 is shown in Fig(2.10).

The variations of D_a^+, D_a^- and D_a^e as well as $E(\alpha_1)$ with α_1 are as expected. The increase in α_1 i.e. increase in the negative ionic concentration in the volume, will enhance the ambipolar diffusion rate of both negative ions and electrons, but discourage the rate of ambipolar diffusion of the positive ions because of the increase of the probability of volume recombination with negative ions. Because of the increased volume recombination, the net ambipolar (radial) field due to the separated charges will be reduced. At a very low α_1, this field remains unaffected; at $\alpha_1 \approx 10$, it falls to quite low values and for $\alpha_1 \approx 100$, it falls practically to zero. Measurements of radial distribution of particle density have been found to be in agreement with theory.

The matter becomes further complicated when in addition to the above situation there is a probability of existence of more than one type of positive ion, i.e. when two types of positive ions, one type of negative ion and electrons exist together. There should then be four ambipolar diffusion co-efficients, namely D_{a1}^+, D_{a2}^+ D_a^- and D_a^e. This has been treated in some detail by E. Schulz-Du Bois(17) in the case of decaying plasmas in

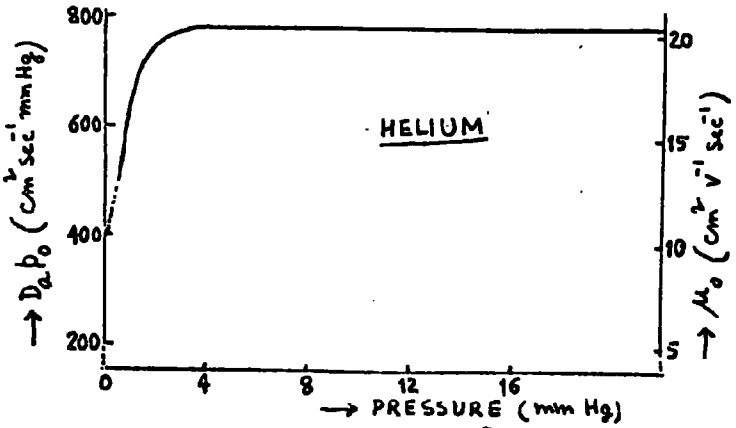

FIG. 2.11 (AFTER MULCAHY AND LENNON[5])

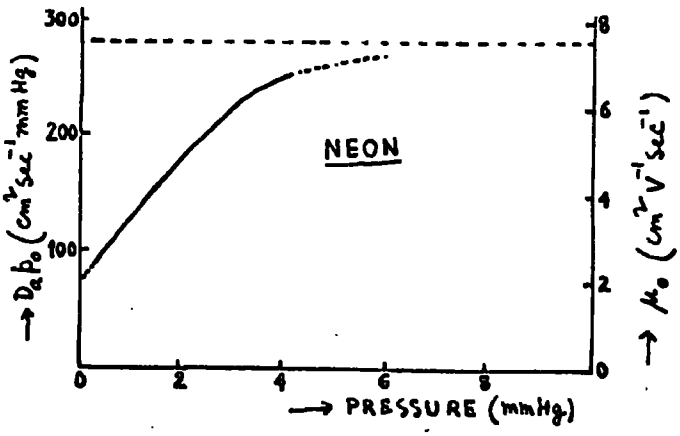

FIG. 2.12 (AFTER MULCAHY AND LENNON[5])

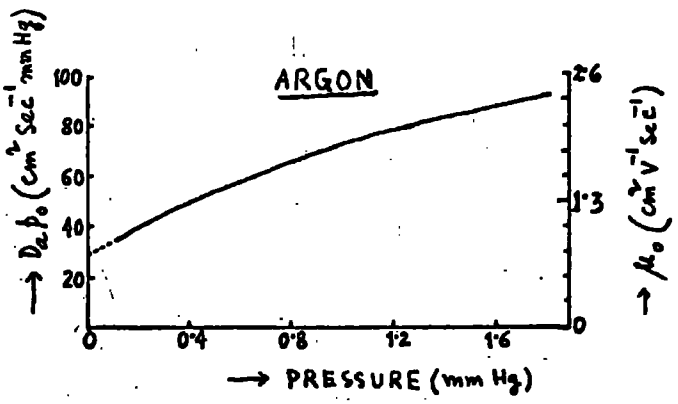

FIG. 2.13 (AFTER MULCAHY AND LENNON[5])

oxygen where O^+, O_2^+ and O_2^- are present. Curves relating electron densities with time and diffusion co-efficient data etc. are shown graphically and discussed in detail.

2.3 Variation of D_a with Pressure and Calculation of Ionic Mobility

It is generally considered that the co-efficient of ambipolar diffusion D_a varies inversely with the pressure. However, Mulcahy and Lennon's (5) results of investigations of the afterglows of low pressure pulsed discharges in the rare gases He, Ne and Ar show marked deviations from this simple relation. One obtains a straight line when a log-linear plot of electron density against time is carried out, which shows that in the afterglows, the ambipolar diffusion of electrons and positive ions is the principal electron removal process. By applying Eq. (2.13) one can obtain the value of the positive ion mobility from the measured value of D_a. In order to remove the dependence of D_a on the gas density, however, values of $D_a p_o$ were calculated, where p_o is the pressure reduced to 0°C. This leads to calculation of μ_o, the reduced mobility i.e. mobility of positive ions at 760 mm Hg. and at 0°C. The results are graphically shown in Figs. (2.11)-(2.13). It is found that in helium,

$D_a p_o$ remains constant between 3 and 22 mm Hg and below 3 mm, $D_a p_o$ decreases with decrease in pressure. In neon, below 5 mm Hg, electron density decays exponentially indicating that the afterglow is diffusion-controlled. At higher pressures, recombination was noticed in the early afterglow. In Ar, recombination with positive ions was found to be dominant for pressures greater than 3 mm Hg. Between 1 and 3 mm Hg, both diffusion and recombination occur and below 1 mm Hg, diffusion alone is responsible for electron removal. This means that there is a transition region in pressure below which diffusion and above which recombination predominates as the electron removal process.

Their experimental results also seem to predict that the higher the molecular weight of the gas used, the less should be the value of $D_a p_o$ at a given pressure.

2.4 High-Frequency Discharge with Axial Flow.

We have so far discussed the various characteristics of the steady state h.f. discharge, in which ambipolar diffusion is the main operating process. Since the ambipolar speed is low, it would be interesting to see how the discharge properties are affected when such a

discharge is subjected to a uniform axial motion (impressed from outside) of which the speed is comparable with the ambipolar speed. Such a study was taken up by Romig (18) The main results of his analysis are quoted below:

(i) Due to the axial flow the active discharge volume is decreased and hence to sustain the steady-state discharge a larger field will be necessary.

(ii) The axial flow causes a shift of the maximum charge density towards the edge of the discharge region. The amount of shift for a given flow depends on the cavity length, pressure in the cavity and the diffusion co-efficient of electrons.

(iii) Calculations in helium show that the effect is much more pronounced in the ambipolar limit than in the free electron diffusion limit of breakdown. This is as expected, since ambipolar diffusion velocity is much lower, by an order of magnitude or two, than the free diffusion velocity and the axial gas velocity which is comparable with the former will, therefore, affect the discharge more effectively.

2.5 Transition from Free to Ambipolar Diffusion.

From the well-known facts that (a) the particle charge density at any point within a steady state discharge system is a function of the space co-ordinates of the point and that (b) the value of the operating diffusion co-efficient, in turn, depends on the particle charge density, it is evident that within a given steady state discharge, there are regions where there will be transitions from free to ambipolar diffusion and vice versa. Allis and Rose (19) undertook an analysis of the general situation in a glow discharge where this transition occurs. They defined an effective diffusion co-efficient D_s which takes into account the combined effects of ambipolar diffusion D_a and space charge fields, by the relation

$$D_s = D_a \left(1+\mu^- \frac{s}{6}\right) \qquad (2.20)$$

where s is the space charge density and ^{6} is the conductivity. On the assumption that the ratio of electron to positive ion density is a constant for any point in the discharge, Eckert (6) used Eq.(2.20) to obtain

$$D_s = D_a \left[\frac{D^- + 4\pi\sigma_o \Lambda^2}{D_a + 4\pi\sigma_o \Lambda^2} \right] \qquad (2.21)$$

where σ_o is the conductivity in the centre and Λ, the characteristic diffusion length of the discharge tube.

For a steady state discharge, the electron continuity equation requires

$$\Lambda^2 = \frac{D_s}{\nu_i} \qquad (2.22)$$

where ν_i is the ionisation frequency per average electron. Eckert deduced expressions for ν_i and D_a in terms of the electric field at the tube wall E_R. It is found that with the increase of the tube radius R, the equilibrium electric field at the tube wall diminishes. The transition from the ambipolar to the free diffusion occurs when for a given value of E_R, the tube radius R is increased, or when for a given R, the value of E_R is greater. These results are as expected.

2.6 Refinements of Schottky's Theory.

The ambipolar diffusion which is the basic physical process of loss of electrons and ions in a positive

column and related discharges was first taken account of by Schottky. This theory had a remarkable achievement in accounting for the spatial distribution of ions and for the electron temperature in the discharge. The value of the radial electric field in the discharge, however, which is the cause of the ambipolar diffusion disagrees with experimental results in some cases. Attempts at improvement led to non-linearities in the basic equations and hence to difficulty of solution. Fowler (20) has arrived at a higher order solution by a straightforward means. He has shown that the problem of the radial electric field in the positive column is essentially reduced to the solution of a second-order linear differential equation. The detailed analysis is outside the scope of this thesis. However, his main points can be enumerated as follows:

(i) Eqs. (2.5) and (2.6) are applicable only in the absence of electro-negative gases and temperature gradients.

(ii) Each ion is ultimately produced through a process which, however complex, involves a single electron collision: volume recombination is negligible.

(iii) The field E in the gap must conform with the relation

$$\text{div } E = 4\pi e (N^+ - N^-) \qquad (2.23)$$

The Schottky solution is obtained by assuming local neutrality of charges (i.e. $N^+ = N^-$), which is in agreement with experiments. Applying this condition i.e. $N^+ = N^-$ and the condition of ambipolarity of the current i.e. that the net radial component of current must be zero, Schottky obtained an expression for the radial field

$$E_r = \frac{KT_e}{e}\left(\frac{\nu_i}{D_a}\right)^{\frac{1}{2}} J_1\left\{\left(\frac{\nu_i}{D_a}\right)^{\frac{1}{2}} r\right\} \Big/ J_o\left\{\left(\frac{\nu_i}{D_a}\right)^{\frac{1}{2}} r\right\} \qquad (2.24)$$

where J_o and J_1 are the Bessel functions of the zeroeth and the first order respectively and ν_i is the ionisation frequency. Fowler has shown that Eq.(2.24) which has been widely used by workers is not compatible with the approximations made in deriving Schottky's equation and the terms neglected in deriving (2.24) are far from negligible in any domain of the discharge carrying a low current. The way out of the difficulty has been suggested by saying that though the relation $N^+ = N^-$ is accurate over the discharge as a whole, nevertheless div E is not zero over essential

portions of the discharge.

(iv) The solution to Schottky's equation given by the first root of the Bessel function of the zeroeth order, used by von Engel and Steenbeck to evaluate electron temperature in the positive column, is hardly accurate. Fowler points out that the success of von Engel and Steenbeck in this regard is rather accidental in that the function J_o changes most rapidly near its root, while its argument changes very slowly.

2.7 Effect of an Inhomogeneous H.F. Field.

There is a considerable amount of literature coming out very recently on this aspect of the high-frequency discharge, namely, the effect of inhomogeneity of the high-frequency field on the discharge. No attempt will be made to give an exhaustive description of such discharges. We shall, however, mention two typical works which are considered to be of some relevance to our work reported in this thesis:

In a recent communication, Golovanivskii and Kuzovnikov(21) have discussed the problem of contraction of the positive column by an inhomogeneous h.f. field. From the elementary

particle density equations, they arrived at the conclusion that it is possible to choose the amplitude of the high-frequency field so that the current of charged particles to the wall is suppressed, if the following relation is satisfied, i.e.

$$- \frac{\nabla N}{N} D_a \cong \frac{\mu^- \mu^+}{\mu^+ + \mu^-} (E^+ + E^-) \qquad (2.25)$$

where E^+, E^- are the fields acting on the positive and negative ions respectively, since $E^+ \neq E^-$, as the field is not homogeneous. If the field amplitude is higher, the condition of zero current is satisfied somewhere between the axis of the discharge tube and the wall. Then the positive column will contract. The higher the chosen field, the greater the compression. As far as can be seen, no account of the change in the value of the ambipolar diffusion co-efficient with radial distance has been taken.

Another important work on this aspect has been recently reported by Perel' and Pinskii (22). They have considered a high-frequency discharge between plane electrodes. By purely analytical methods, they obtained an

expression for the average force exerted on an electron by the inhomogeneous high-frequency field in the presence of collisions and arrived at a number of important conclusions as enumerated below:

(i) It is shown that the plasma is concentrated in the central region of the discharge, which is sharply separated from the electrode regions. In the electrode regions, the charge density is appreciably smaller and the field amplitude is appreciably higher than in the central region where reverse is the case. This is in agreement with the results of previous workers [7,8].

(ii) The inhomogeneity of the high-frequency field has an important effect on the diffusion of the charged particles to the electrodes.

(iii) The potential difference V consists of two parts V_1 and V_2 so that $V = V_1 + V_2$ where V_1 and V_2 are the potential drops in the central and electrode regions respectively. In the high-density case, the basic voltage drop occurs in the electrode region, so that $V \simeq V_2$. This conclusion is in contradiction with Schneider's observation, who found that the electrode regions can be

represented by a capacitance (see F.g 2.4). If Schneider's analysis is correct, which we think likely, the two voltage drops should be in phase quadrature rather than in phase.

(iv) Expressions for instantaneous voltages $V_1(t)$ and $V_2(t)$ are deduced which involve among other quantities, the ambipolar diffusion co-efficient D_a. For a given electrode voltage and gas pressure, these expressions can also be used to find the electron density at the centre and the current flowing in the gap. It is stated that in order to do so, one must know the relation between the ionisation rate and electron temperature as well as the relation between the electron temperature and the high-frequency field. Since the high-frequency field is not uniform, electron temperature should be different in different regions of the discharge. One must also note that the ionisation rates are different in different regions of the discharge. This chain of uncertainty, therefore, leaves one in an unsatisfactory state regarding any clue to the voltage-current characteristics in the discharge.

CHAPTER - III

THE EXPERIMENTAL CONDITIONS.

3.1. Introduction.

In the statement of the problem (sec.1.2) we have drawn the main line of our approach, namely that we want to see whether ambipolar diffusion alone is the main electron removal process in the sustained h.f. discharge. From the assumption that the electron temperature (and hence the electron energy) in comparable discharges should be the same, the expected results should be as follows :

(i) In the long cylindrical system, where the radius of the tube is much smaller than its length, the loss of electrons and ions by diffusion is entirely to the side wall and so, for a given current, a change in length should not affect the maintaining field, since whatever be the length of the tube, provided that the length is always much greater than the radius, the characteristic diffusion length which determines the maintaining field is a constant.

(ii) In the flat cavities, where the radius of the cavity is much larger than the gap width, the entire loss

is due to diffusion to the end-walls. The characteristic diffusion length is determined by the gap width only and so, for a given gap voltage and a given cavity, provided its radius is much larger than its width, the number of electrons and ions diffusing out per second per unit area of the gap along its axis i.e. the current density should be a constant.

If, then, the above expected results are obtained experimentally, one can draw the conclusion that diffusion is probably the only loss mechanism which determines the character of the discharge.

Now, in order that the above hypothesis be tested, one should use tubes which are sufficiently long and cavities which are sufficiently flat, so that the conditions $r \ll \ell$ and $r \gg \ell$ are satisfied respectively. Secondly, one should not choose an electron attaching gas like oxygen or the halogens. It is known that excepting these gases, attachment, if present at all, is negligible[23]; so far as recombination is concerned, very little evidence of this has been found in experiments done so far, except at higher pressures,[24, 25]. It is, therefore, advisable

to begin working at lower pressure range.

The main criteria, however, of the applicability of the diffusion theory are that (i) the mean free path and (ii) the ambit of the electron, should be both small in comparison with the dimensions of the tube. These criteria are not exclusively related with the pressure p or the frequency ω of the applied field, but rather with the ratio of ω/p. That is to say, for a given pressure, there is a frequency range and for a given frequency, there is a pressure range, for the diffusion theory to hold.

A powerful oscillator of the dielectric heater type capable of delivering an output power of about 3.5 KW at 17 Mc/s was available. This fixed frequency restricted our choice of the pressure range for investigation. To begin with, only moderate power was used. This was done in stages, partly by placing a high resistance in the anode lead of the oscillator valve and partly by tuning of the grid circuit of the oscillator, which was of the tuned-anode, tuned-grid type.

3.2. Calculation of the Necessary Pressure Range.

For long cylindrical tubes, the minimum diameter

used was 0.525 cm and for the flat cavity, the maximum gap separation was 2.03 cm. Now, when the electronic mean free path λ_e is to be appreciably small in comparison with the values of the diameter and gap separation, respectively, let us suppose that λ_e should be one-fifth of these values. Accordingly, $\lambda_e \approx 0.1$ cm and 0.4 cm in the long cylindrical tube and flat cavity respectively. Now, taking data from von Engel (9) for the atomic mean free paths λ in Ne and H_2, which gases we studied, e.g.

$$\left.\begin{aligned} \lambda \text{ in } H_2 &= 14 \times 10^{-3} \text{ cm} \\ \lambda \text{ in Ne} &= 12 \times 10^{-3} \text{ cm} \end{aligned}\right\} \text{ at 1 mm Hg and at } 0^{\circ}\text{C}$$

and using the approximation that

$$\lambda_e = 4\sqrt{2}\, \lambda_{atom}$$

and correcting for the average temperature of the gas, we have

$$\lambda_e \text{(at 1 mm Hg) in } H_2 \approx 0.08 \text{ cm}$$

and

$$\lambda_e \text{(at 1 mm Hg) in Ne} \approx 0.07 \text{ cm}$$

This means that for λ_e not to be greater than 0.1 cm in long tubes and 0.4 cm in flat cavities, the pressures in the long and flat cavity systems should not be less than

0.8 mm and 0.2 mm Hg respectively. Now, the characteristic diffusion lengths of the long and flat systems are of the order of 0.1 cm and 0.4 cm respectively so that in either system $p\Lambda \simeq 0.08$ cm. mm. Hg and hence $E\Lambda$ in either system should be $\simeq$ 10 Volts i.e. $E_{flat} \simeq 25$ Volts/cm and $E_{long} = 100$ Volts/cm and $E/p = \frac{100}{0.8} = \frac{25}{0.2} = 125$ Volts/cm mm Hg so that the drift velocity of electrons at E/p = 125 Volts/cm mm Hg would be of the order of 10^7 cm/sec; the half-period of the field is about 0.5×10^{-8} sec.; the electron ambit, therefore, is of the order of 0.05 cm which is negligible in comparison with the long tube or the flat cavity dimensions. Thus, with the working frequency of 17 Mc/s and for the tube and cavity dimensions used, the lowest limit of pressure as discussed above should be something like 0.2 mm Hg.

Thus, since we are concerned with the minimum pressure of about 0.2 mm Hg and we want to study the basic characteristics and test our hypothesis of ambipolar diffusion, it would suffice to study the characteristics up to a few mms of Hg; a McLeod gauge was, therefore, thought to serve the purpose. At a later stage, when it was necessary to push the range of observations to higher pressures than that given by the McLeod gauge, an ordinary U-tube manometer

was fitted to the system.

3.3 Nature of the Gas Used.

Regarding the choice of the experimental gas, hydrogen and neon were selected mainly because these gases had been extensively studied before and represent typical molecular and monatomic gases. Preliminary observations were taken in air first, to ascertain the necessary modifications in the experimental arrangements.

3.4 Nature of the Electrodes.

Both internal and external electrodes were used. For the long cylindrical tubes, close-fitting external sleeve electrodes about 1 cm wide were used, so that the spacing was readily adjustable. For flat cavities, thin circular discs of copper were used as external electrodes.

The immersed electrodes in either system were in the form of thick circular discs of mild steel having grooves for 'O' rings (see Chap.IV).

3.5 The Vacuum System.

(a) The cold trap.

As the total volume of the discharge system was not very large (1000 c.c. approximately), one cold trap

between the discharge tube and the manometer was considered sufficient.

(b) Compression taps.

In order to eliminate the possibility of contamination of the system by grease vapour, nearly all the taps were of the grease-free compression type. It was eventually found necessary to use one cone joint for quick and easy fitting of the different discharge tubes and cavities.

(c) Pumping, washing and filling.

A single rotary pump was employed. The system was at first evacuated to about 0.005 mm Hg; it was then filled with the chosen gas to about 10 mm Hg, pumped down again and refilled, and the process repeated several times.

CHAPTER - IV

INSTRUMENTATION

4.1 Introduction.

In the following sections, various problems encountered on the instrumentation side of the work will be described.

4.2 Adaptation of the Oscillator.

The frequency of the oscillator which was stated to be 17 Mc/s was checked by a wavemeter and found correct.

The range of working of the oscillator was at first examined, using an ellipsoid voltmeter method (26,27). Accordingly, an ellipsoid of brass having its major and minor axes of the order of 1 cm was suspended by means of a thin quartz fibre between the oven electrodes mounted vertically (Fig.4.1). The potential difference V in volts between the electrodes is given by (28)

$$V = Kd\ (f^2-f_o^2)^{\frac{1}{2}} \times c \times 10^{-8} \text{ volts r.m.s} \quad (4.1)$$

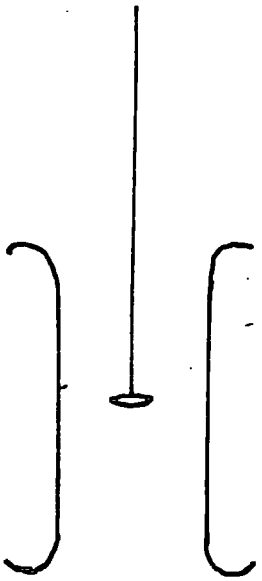

FIG. 4.1. MEASUREMENT OF VOLTAGE BY ELLIPSOID VOLTMETER.

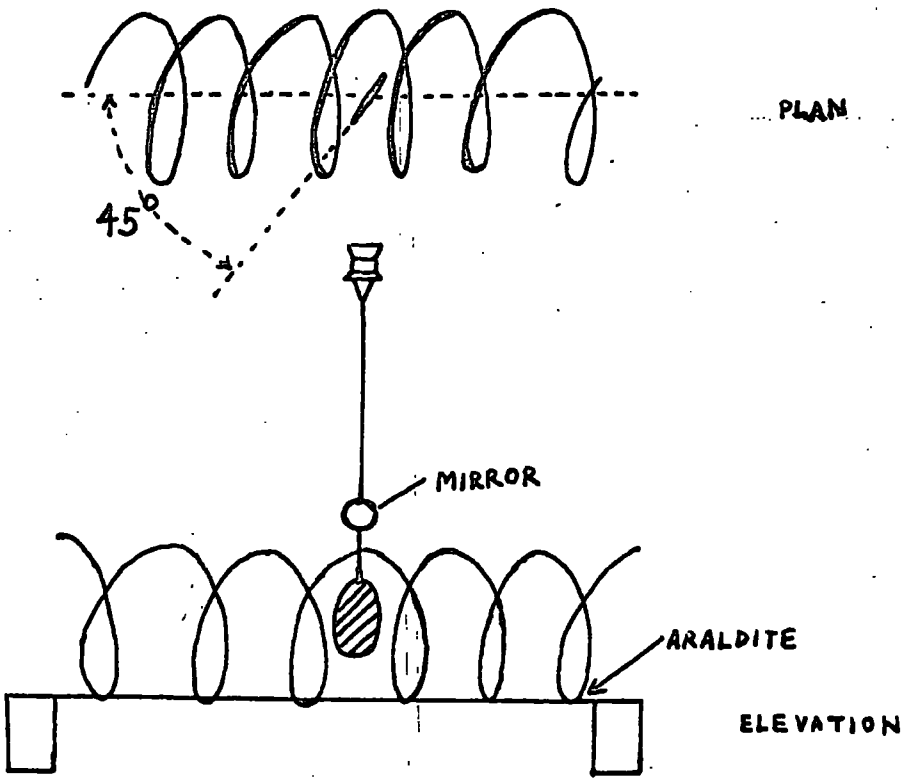

FIG. 4.2. THE EDDY CURRENT GALVANOMETER.

where

d = distance between the electrodes in cm,

f_o = natural frequency of oscillation of the ellipsoid in c/s,

f = frequency of oscillation of the ellipsoid in the r.f. field in c/s,

c = velocity of light in vacuum in cm/sec

and K = a constant depending upon the geometrical dimensions and the mass of the ellipsoid.

From the measurements of the two frequencies of oscillation, f_o and f, and the physical dimensions of the ellipsoid, the potential drop between the electrodes wascalculated and found to be about 20 KV r.m.s. From the fact that when a thick copper wire loop was placed on top of the live electrode set horizontally, an instantaneously luminous snake-like discharge at atmospheric pressure was obtained at its tip, this value appeared to be a probable one. The luminous snake was about 10 cms long and about 1 cm wide.

4.3 The Current Measuring Instrument.

At 17 Mc/s the most suitable current measuring device is the vacuum thermo-junction, but its low overload capacity makes it unsuitable for exploratory work.

Considerable advantage seemed to attach to the high-frequency ring galvanometer (29) and a preliminary study of this instrument was made. The construction and the working principle of this galvanometer are described below:

It consists of a few turns of copper wire mounted on an insulating stand Fig.(4.2). At the centre of coil and at 45^{o} to its axis, a thin copper disc is suspended by means of an extra-thin quartz fibre. When a radio frequency current i passes through the coil, the interaction between the magnetic field and the eddy current produced exerts a torque θ on the disc proportional to the square of the current i and to the frequency ω: or,

$$\theta = K_1 i^2 \omega \qquad (4.2)$$

where K_1 can be determined by calibration using a vacuum thermo-junction. At first, three copper turns were tried and a copper disc of 1 cm diameter was suspended by a fairly thin quartz fibre carefully drawn. This was not sensitive enough to give any response to the output of a signal generator, but doubling the number

of turns raised the sensitivity sufficiently.

Next a mirror was fitted to a suitable quartz fibre satisfying the following conditions:

(i) The copper disc should be at 45^{o} to the axis of the coil:

(ii) The mirror should be outside the coil and

(iii) the quartz fibre should be thin for high sensitivity.

The whole assembly, e.g. the quartz fibre fitted with mirror and copper disc and the copper coil mounted on an insulating stand --- was housed in a rectangular perspex box, having a slideable front door and an adjustable screw, to which the quartz fibre was cemented, for lowering or raising the position of the disc within the coil, or for rotating it about a vertical axis so as to bring it to 45^{o} with the axis of the coil. A metre scale was placed at a suitable distance from the galvanometer mirror so as to read its deflection d.

4.4 Electrodes for Tuning.

The oscillator was found to work satisfactorily only into a proper load; thus a suitable tuning device was needed. Two pairs of copper plates approximating to Rogowski profile were made. This was done (construction

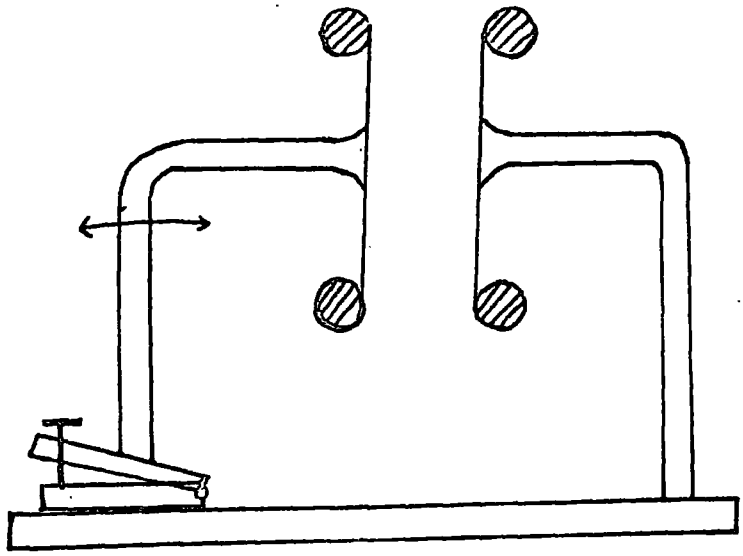

FIG. 4.3. THE TUNING CAPACITOR.

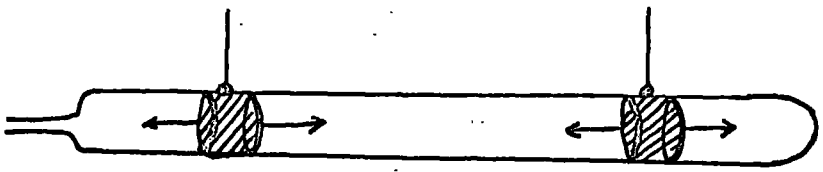

FIG. 4.4. LONG TUBE : SLEEVE ELECTRODES.

shown in Fig(4.3) by soldering a circular copper disc to a ring of copper tube and then by trimming the profile. A pair of such discs were next made into a robust capacitor (suitable also for voltage measurements) by mounting as shown.

4.5 Electrodes (both internal and external) for the Discharge System.

The details of the mounting of the internal and external electrodes used are described below:

(A) Long cylindrical tubes

(i) external electrodes: Close fitting sleeve electrodes of about 1 cm width were used so that their separation could be easily altered Fig.(4.4)

(ii) internal electrodes: At first hollow cylindrical electrodes Fig.(4.5a) of brass were used. These were mounted by the QVF bolted flange couplings and 'O'-rings. The mounting was not found to be satisfactory at first in respect of vacuum. Moreover, after some time of running of the discharge through the tube, these electrodes deteriorated due to sputtering effects. Further, in order to compare results with those in the flat cavities, where plane parallel electrodes were to be used*(see over),

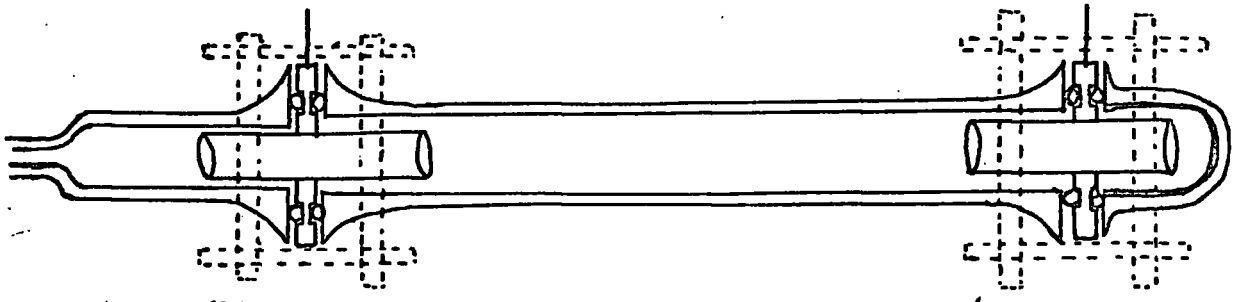

FIG. 4.5 (a) : LONG TUBE : INTERNAL ELECTRODES (HOLLOW CYLINDERS).

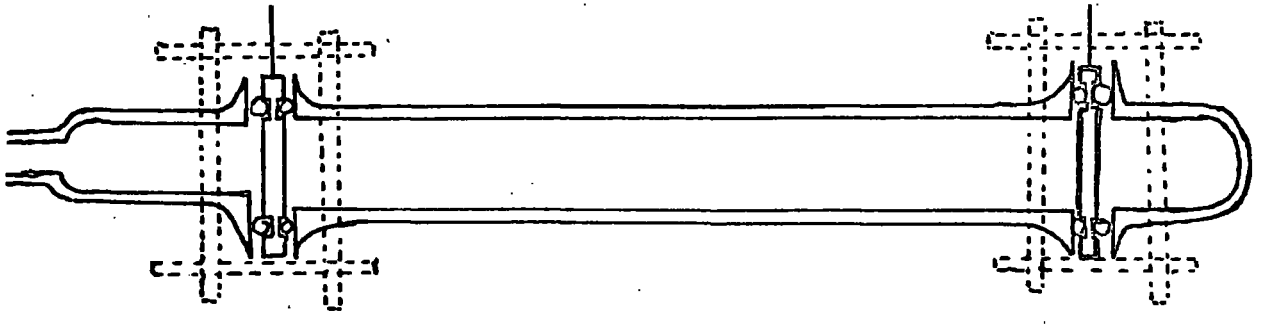

FIG. 4.5(b): LONG TUBE: INTERNAL ELECTRODES (SOLID DISCS).

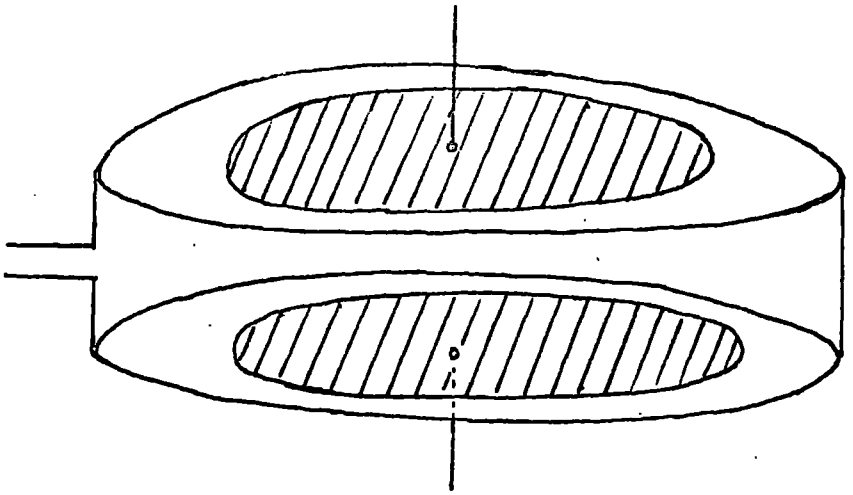

FIG. 4.6. FLAT CAVITY: EXTERNAL DISC ELECTRODES.

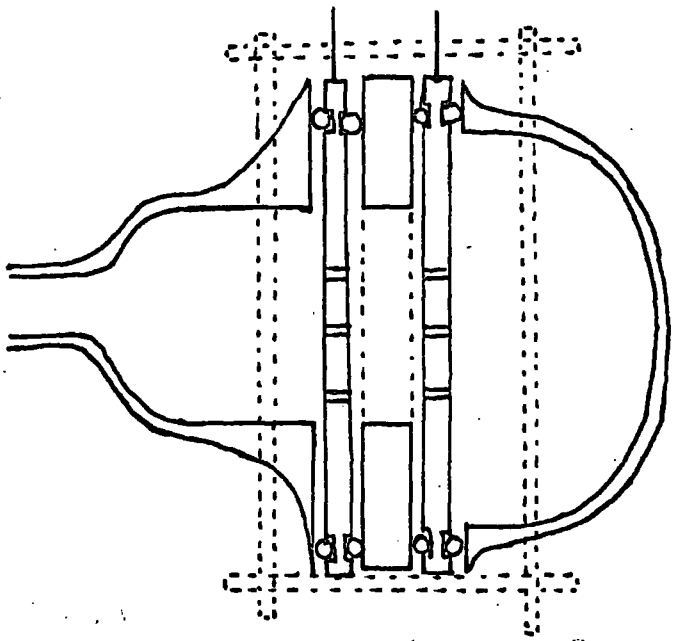

FIG. 4.7. FLAT CAVITY: INTERNAL ELECTRODES.

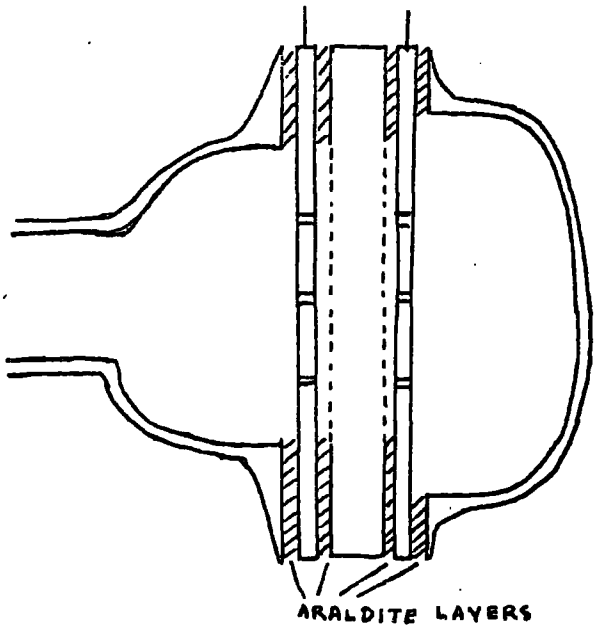

FIG. 4.8. FLAT CAVITY: INTERNAL ELECTRODES.

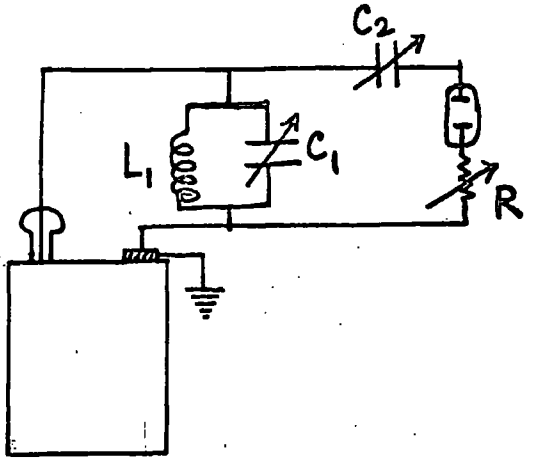

FIG. 4.9. RESISTANCE CONTROL OF CURRENT AND CAPACITIVE COUPLING.

solid circular discs of mild steel (to reduce sputtering) were employed Fig.(4.5b) instead of the hollow cylindrical ones.

(B) Flat cavities

(i) external electrodes: These were close-fitting thin circular discs of copper as shown Fig.(4.6).

(ii) internal electrodes: Circular discs of mild steel having a few small holes to let gas in were used. They were mounted in the same way as the internal electrodes in the long tubes i.e. with the help of QVF bolted flange coupling and 'O'-rings, with glass spacers of different aspect ratios in between Fig.(4.7). Bigger electrodes necessary for cavities of larger dimensions were simply araldited Fig.(4.8).

4.6 The Current Control and the Difficulties.

In the initial stages the oscillator was used at full power with the intention of employing a resistance control of the power supplied to the discharge

---

* The formula $\frac{1}{\Lambda^2} \doteq \left(\frac{\pi}{\ell}\right)^2 + \left(\frac{2.405}{r}\right)^2$ is applicable to the system which is bounded by plane parallel electrodes, the boundary condition being that the electron density is zero at either electrode.

tube. When this was attempted using variable resistor R mounted on a board, with tuning capacitors C_1 and C_2 as shown Fig.(4.9), the resistors and the board were rapidly charred by stray discharges etc. To divert the energy dissipation and to obtain a steady symmetrical discharge, various measures were adopted, e.g. (a) insertion of some dielectric load between the plates of C_1; (b) continuous flow of water through a glass box placed between them; (c) adjustment of C_1 and C_2; (d) interchanging the position of C_2 and R; (e) connecting R and C_2 in parallel; (f) replacement of the metallic rods of the framework by glass rods for reducing displacement current, etc., without any avail.

It was next decided to use the oscillator at low power by introducing a suitable resistor in its anode lead. This was tried in stages; several resistors (of high wattage) were mounted on a tufnol incline. For efficient cooling, this was placed near the blower motor of the oscillator meant for cooling of the oscillator valve, to the anode lead of which these resistors were included.

At first one 1600Ω resistor was tried. The anode

current came down to 0.8 amp from the previous 1.5 amp. The resistance was further increased in steps. Some typical observations on anode currents are noted below:

Number of resistance (in parallel) of 39 KΩ in the anode lead of the oscillator.	Anode current (amp)
5	0.30
4	0.28
3	0.25
2	0.20
1	0.10

Under conditions represented by the last two rows the oscillations stopped. With three 39KΩ in parallel, when the anode current was 0.25 amp, conditions were most stable and the previous random charring or flashing stopped altogether.

4.7 Asymmetry of the Discharge.

Though a stable discharge now occurred within the tube, it was far from symmetrical. Also, the discharge was very sensitive to the body movements; when the hand

was placed near the tube or one of the capacitance plates, the discharge could even be extinguished. Reduction of resistance in the discharge tube circuit made the discharge steady but not symmetrical. The asymmetry could possibly be ascribed to the various unknown stray capacitances inherent in the physical laying out of the circuit components.

An inductive coupling, instead of the capacitative one so far used was next tried. After preliminary tests it was found that the system worked satisfactorily with a turns ratio of 3:10, i.e. with adjustment of C_2, discharge was obtained. Nevertheless, the discharge was still asymmetrical. Variation of R, C_1 or C_2 Fig.(4.10) only varied the length of the asymmetrical discharge, which was all due to stray capacitances.

An attempt to produce uniformity of the discharge by using guard rings which would ensure uniform gradient inside the tube was also unsuccessful. The guard rings were therefore subsequently removed.

4.8. Symmetry of the Discharge.

The primary coil in the oscillator output stage was next connected to the earthed terminal rather than to the live terminal as was done heretofore. This worked

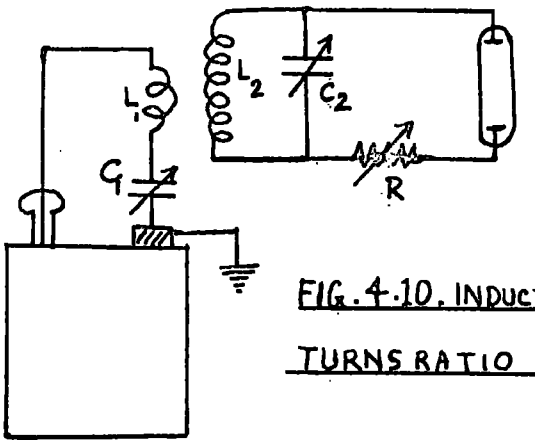

FIG. 4.10. INDUCTIVE COUPLING: TURNS RATIO 3 : 10 .

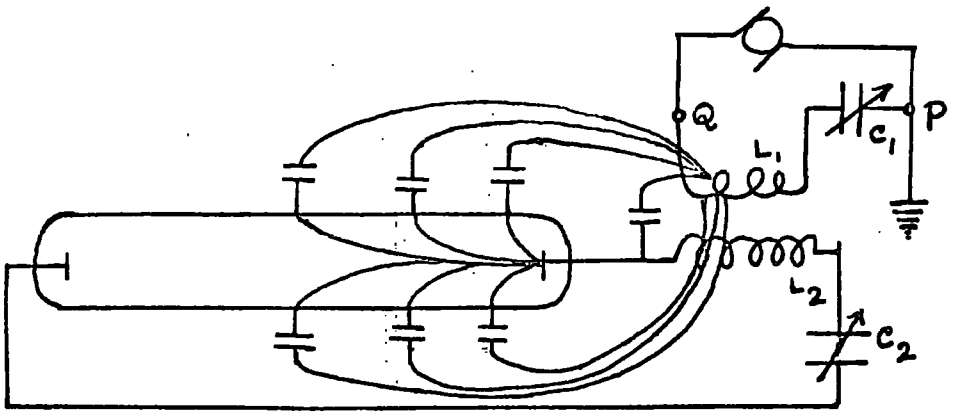

FIG. 4.11 . ILLUSTRATING ASYMMETRY OF DISCHARGE DUE TO STRAY CAPACITIVE COUPLING.

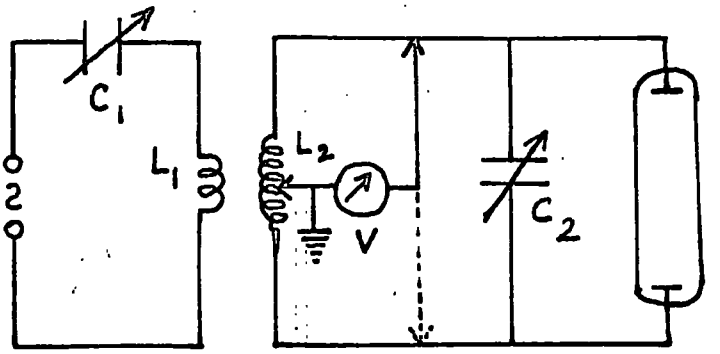

FIG. 4.12. TEST BY VACUUM TUBE VOLTMETER.

successfully and the discharge was quite symmetrical. Also, it was noted that (i) when the hand was placed near the primary coil, the symmetry or the intensity of the discharge was not affected as much as previously and that (ii) the inclination of the axis of the primary or the secondary coil with the vertical did not matter much so far as the symmetry of the discharge was concerned.

The reason why the connection of the primary coil to the earthy terminal instead of the live one produced a symmetrical discharge, could be clear from Fig. (4.11). The asymmetry of the discharge might well have been due to the stray capacitive coupling as shown; an interchange of earth connection between P and Q would much reduce this coupling. Some preliminary observations at this stage are reported in Table 4.1 on the following page:

TABLE - 4.1

Pressure mm.Hg	Effect of Position of the Controlling Knob of the Oscillator.	Distance between vertical stands of C_1 and the effect of change of this distance etc.	Distance between vertical stands of C_2 and the effect of change of this distance etc.	Nature of the discharge (intensity, colour, striations etc.)
10	about 45° clockwise from minimum coupling position.	17 cm.	15 cm.	Stationary striations at the end and moving striations at the middle of the tube; discharge symmetrical and the tube was very hot.
4	about 60° clockwise from minimum coupling position makes the striations sharper.	"	The discharge remains stable for a large variation of the distance between the plates of C_2	More intense discharge; colour changed from bluish violet to pink; striations more separated; moving striations observed; discharge symmetrical and the tube less hot.

continued on next page ...

TABLE - 4.1 continued.

Pressure mm.Hg	Effect of Position of the Controlling Knob of the Oscillator.	Distance between vertical stands of C_1 and the effect of change of this distance etc.	Distance between vertical stands of C_2 and the effect of change of this distance etc.	Nature of the discharge (intensity, colour, striations etc.)
3	about 90° clockwise from the minimum coupling position extinguishes the discharge.	Minimum distance for extinction of discharge was 16cm; maximum distance for the same was 17cm; when the distance between the plates of C_2 was fixed at 15cm, with those between C_1 being 17cm, the discharge started and stopped automatically and periodically about two to three times per second; movement of the hand near the live electrode under this condition extinguished the discharge; by a little adjustment of C_1, the discharge could again be made stable.	Distance between C_1 stands being fixed at 17 cm, the maximum distances between those of C_2, for extinction of discharge was found to be 21.5 cm and 14.5 cm respectively.	Intense discharge-violet at the ends and pinkish red at the middle; discharge less extended beyond the electrodes compared with that at .05 mm.Hg. (see below); discharge symmetrical - rotation of the primary coil influences the discharge appreciably but not that of the secondary coil.
.05	Two complete turns clockwise from the minimum coupling position extinguishes the discharge.	Maximum distance required for extinction of discharge = 31.5 cm, when the distance between the vertical stands of C_2 was fixed at 15 cm; under the same conditions, the minimum distance required for extinction of discharge = 15 cm.	With the distance between C_1 stands being fixed at 17 cm, the discharge could not be extinguished even when the C_2 plates were at the extreme ends of the board; the minimum distance for extinction, however, was found to be 12 cm.	Discharge very intense and extended much beyond the electrode on the pump side. Colour of the discharge blue at the end and pinkish at the middle - discharge symmetrical - the tube very little heated.

4.9 Measurement of Voltage.

(i) Observations with a vacuum tube voltmeter.

A commercial vacuum tube voltmeter of maximum range of 100 volts a.c. suitable for measuring h.f. voltages was tried at first. The common earthed lead of the voltmeter was connected to the centre of the secondary coil and the lead was touched momentarily with either end of the discharge tube in succession Fig.(4.12), the discharge within the tube being symmetrical and intense. Both ends showed readings much beyond the voltmeter scale. The obvious conclusion that could be drawn was that the voltage across the discharge tube was much greater than 200 volts. During this experiment the discharge tube used had an internal diameter of 1.61 cm and the distance between the internal electrodes was 10 cm; the tube contained air at a pressure of 4 mm. Hg.

It was also observed that momentary touch of the voltmeter lead with either end of the discharge tube had a large influence not only on the intensity but also on the symmetry of the discharge and in some cases, the discharge could even be extinguished.

Some further steps taken in the course of attempts to obtain a reliable voltage measurement are next outlined:

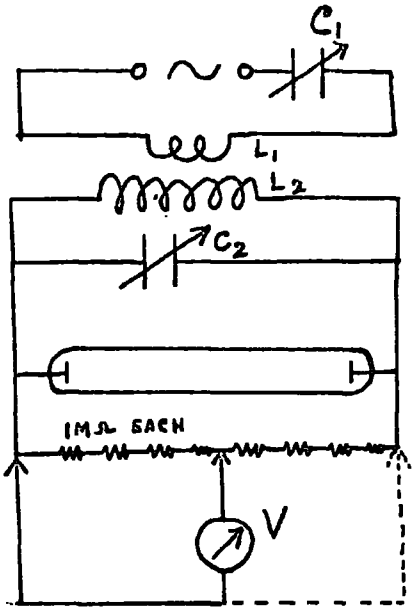

FIG. 4.13.

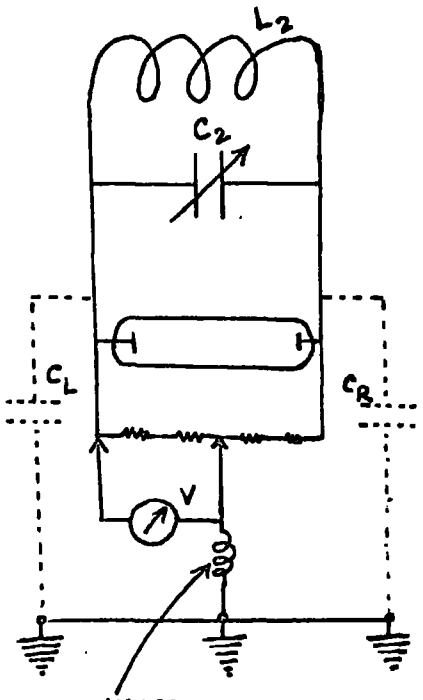

FIG. 4.14. LEAKAGE CURRENT THROUGH C_R FLOWS THROUGH C_L AND V IN PARALLEL.

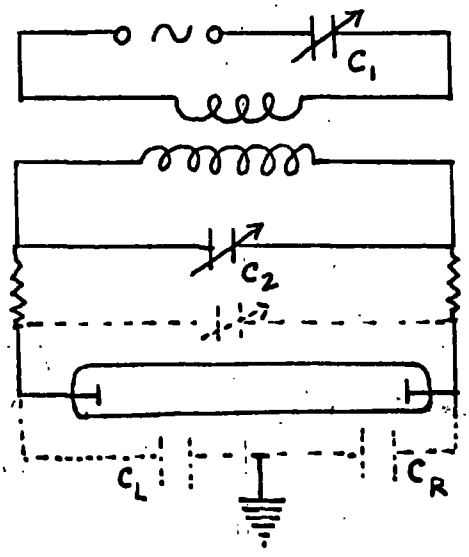

FIG. 4.15.

A total resistance of 8 MΩ in steps of 1 MΩ was connected in parallel with the discharge tube Fig.(4.13). The connection of the voltmeter was as shown, the common lead of the voltmeter being connected to the middle (geometrically speaking) of the row of resistances. The deflection of the voltmeter needle was far outside the scale, even across 1 MΩ. When only the common lead was touched with either end of the discharge tube, the other lead remaining free, sparking occurred at the contact point. With a resistance of 2 MΩ between either end and the point of contact with the common lead, the sparking ceased to occur. All of these observations are consistent with the view that the voltmeter circuit is completed by stray capacitances and that the resistances in the circuit are unimportant Fig(4.14). The effectiveness of the stray capacitances C_L and C_R was tested by inserting resistors as shown in Fig.(4.15). With 1 KΩ resistors the tube glowed at the ends only and one resistor burnt out. With 1 MΩ resistors the tube did not glow but the resistors heated up. When a capacitor was deliberately added (dotted) the effect was intensified.

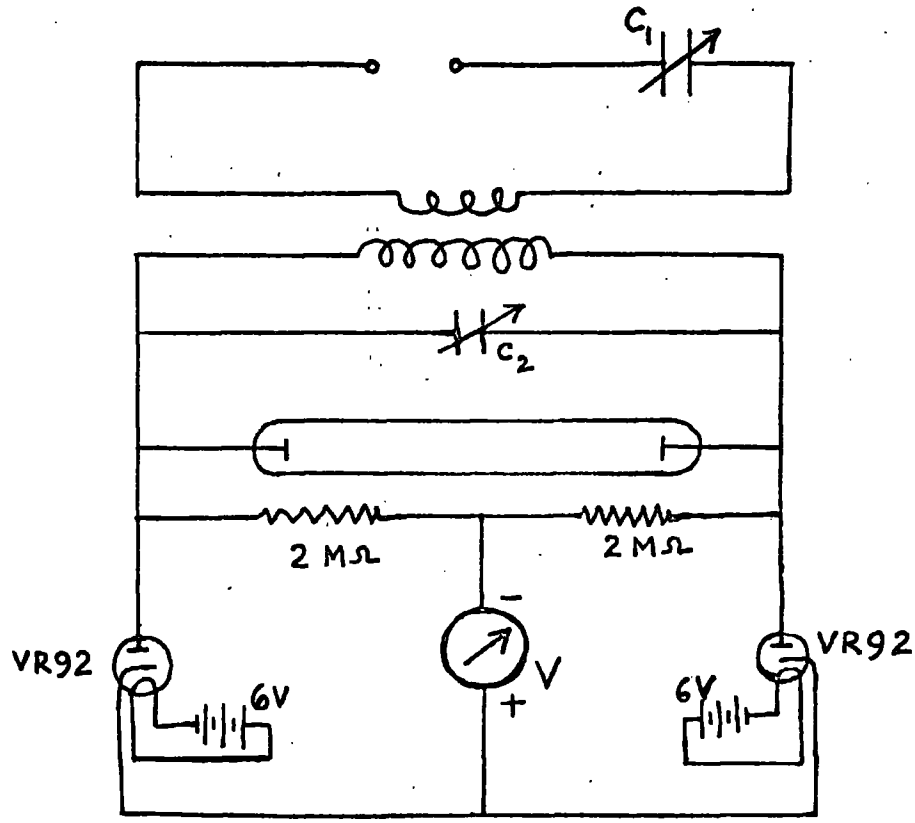

FIG. 4.16. VOLTAGE MEASUREMENT WITH SYMMETRICAL PEAK VOLTMETER (A. VON ENGEL[30])

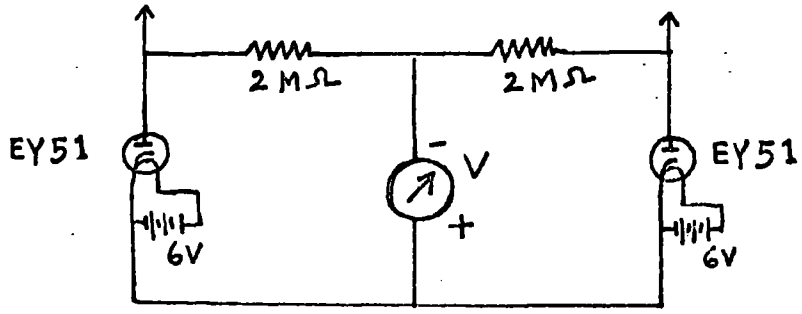

FIG. 4.17

(ii) Observations with the symmetrical peak voltmeter (Gill and von Engel, 1948).

After the failure of the commercial voltmeter, it was realised that the symmetrical peak voltmeter of Gill and von Engel[30] should be tried. The connections are shown in Fig.(4.16). In place of the VR92 diodes, solid state diodes were tried at first, with the result that one of them immediately burnt out as soon as the oscillator was switched on. With VR92 diodes connected, however, the voltage recorded, when the oscillator was switched on, was about 900 volts. Even with this large voltage, breakdown did not occur. When two 1 MΩ resistances were used instead of two 2 MΩ, the reading of the voltmeter under otherwise unaltered conditions was found to be 150 Volts. Evidently, this was not what we wanted e.g. the voltmeter should give the same reading if everything else like the pressure of the gas, the gap geometry, etc. remains unaltered. Perhaps, this could be ascribed to the self-capacities of the diodes which were not low enough. To provide high enough impedence in the diode circuit, EY 51 diodes, instead of the VR92's were used Fig.(4.17); these diodes had a self-capacity of 0.8 pf, compared to 2.1 pf of the VR92.

The magnitude of the induced voltages in the different parts of the voltmeter circuit was considerable. It was found that even when one of the filament supplies of the diodes was disconnected, the filament concerned was glowing intensely as the oscillator was switched on.

At a certain pressure, a typical reading of 500 Volts was necessary for breakdown; this reading remained the same when instead of both the diodes, either of them was in operation; further, when none of the diodes was in operation, the voltmeter reading was still 500 Volts which, however, gradually fell to zero in a time of about half a minute or so. This fact pointed to the thermal inertia of the diode filaments.

By changing the position of the control knob, the length and intensity of the glow could be changed -- the intensity being maximum for the maximum value of the potential recorded by the voltmeter.

4.10. Observations with both Voltmeter and Ammeter Connected to the Circuit.

It was next decided to look for both the ammeter and voltmeter deflections simultaneously, with some arrangement for current control through the system. The

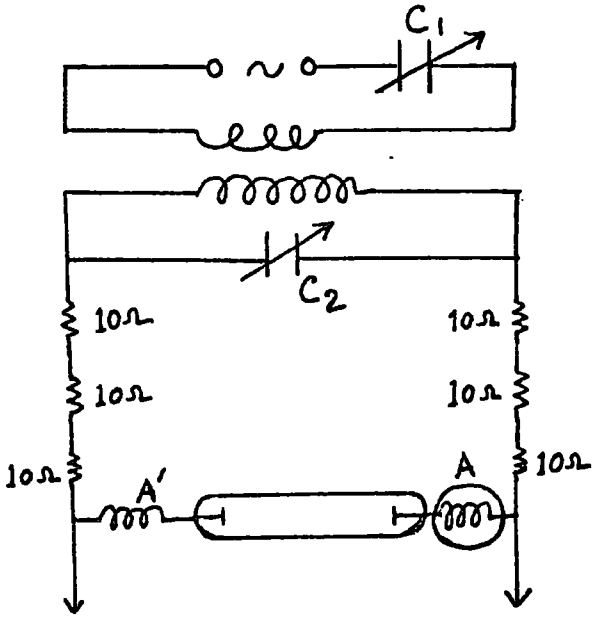

TO VOLTMETER LEADS OF FIG. 4.17.

FIG. 4.18

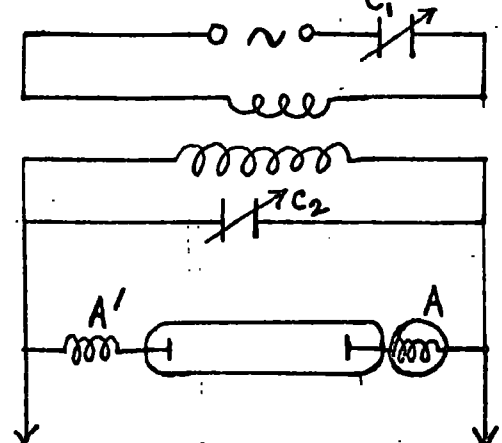

TO VOLTMETER LEADS OF FIG. 4.17.

FIG. 4.19

circuit shown in Fig.(4.18) was next tried, with a few 10Ω resistances on each side of the discharge tube for symmetry. The inclusion of these resistances was thought to be a possible device for current control. The eddy-current ammeter A was connected to the circuit and for symmetry again, a compensating coil A' of the same geometry was placed on the other side of the discharge tube.

When the oscillator was switched on, it was observed that --

(i) the ammeter gave a small deflection (a few mms. on the scale),

(ii) the voltmeter read about 500 Volts for breakdown,

(iii) the 10Ω resistances were much heated,

and (iv) the glow was confined to the ends of the discharge tube, its middle portion remaining dark.

Instead of placing these resistances in series, when they were placed in parallel with C_2, there was no breakdown, showing that the current flowed through the resistors. When, however, higher resistances were used in parallel with C_2, breakdown occurred at precisely the same voltage as before, with little heating of the resistances.

All the attempts of effecting a suitable current control brought difficulties of one kind or another. It was then decided to solve the problem by varying the position of the control knob of the oscillator. There was an apprehension that this might change the frequency of oscillation. It was, However, found with a C.R.O. that the change, if any, was inappreciable. Use of resistances in the circuit was, therefore, avoided. This simplified the circuit of Fig.(4.18) to that in Fig.(4.19).

Typical values of the voltmeter and ammeter readings at a pressure of 6.2 mm Hg in air are shown in Table 4.2 on the following page.

TABLE - 4.2: Air: p = 6.2 mm. Hg.

V volts	d mm.
90	7
170	16
240	27
260	32
320	45
340	52
430	80
500	108
530	132
560	157
600	177
630	205
680	242
710	264
730	283
760	305
770	323
790	345

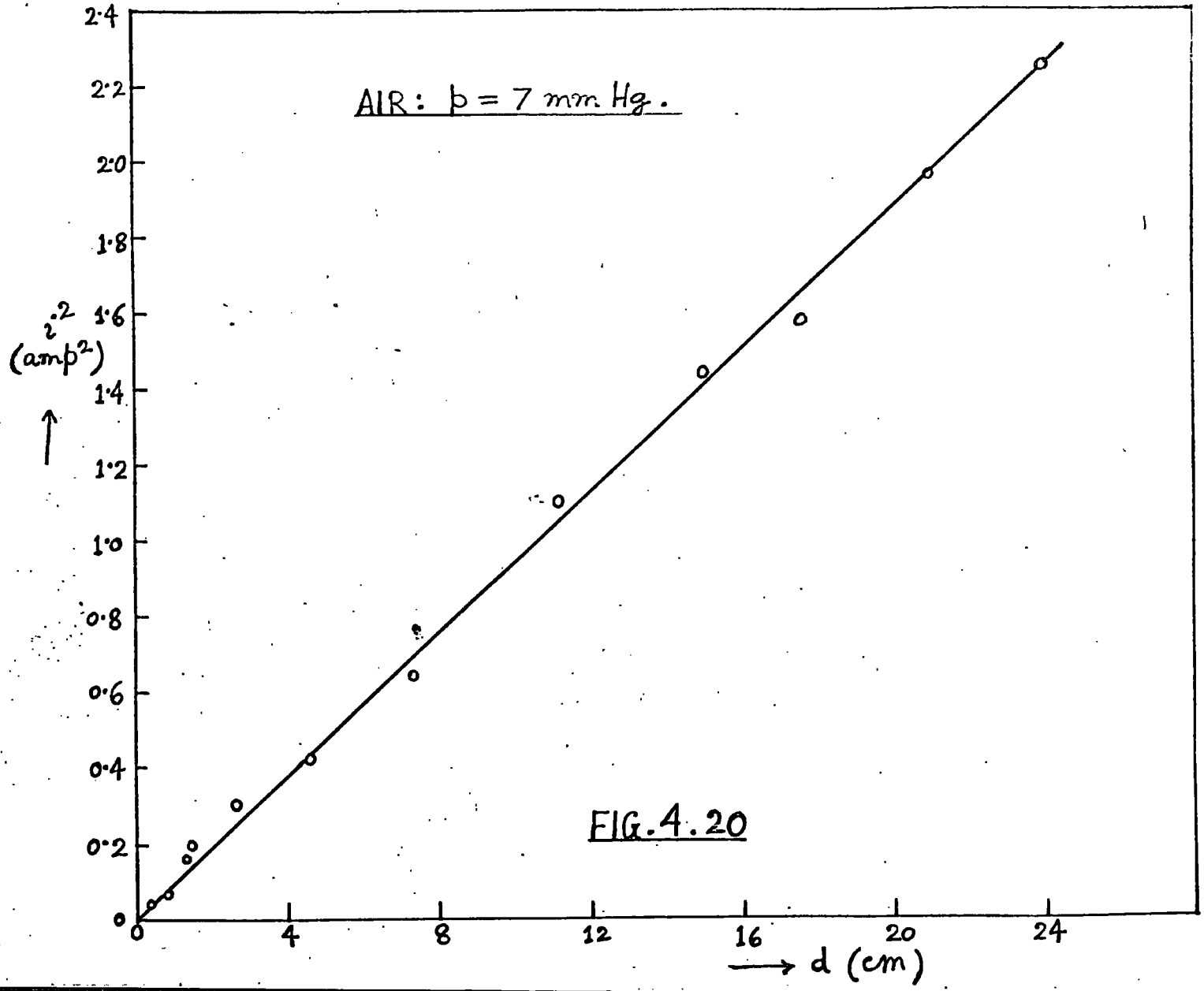
AIR : p = 7 mm Hg.
i² (amp²)
2·4
2·2
2·0
1·8
1·6
1·4
1·2
1·0
0·8
0·6
0·4
0·2
0
0
4
8
12
16
20
24
d (cm)

FIG. 4.20

Some of the primary difficulties associated with the ammeter were that there was a slight creeping of the zero of the scale and that the deflections were not very steady. Moreover, it took a long time for the spot of light to settle down. These difficulties were eliminated by introducing an oil-damping device to the ammeter.

An u.h.f. thermo-junction of rated current 250 mA was used at first to calibrate the ammeter but the thermo-junction burnt out immediately showing that the gap current was much higher. A thermo-couple type of h.f. ammeter of range 0-3 Amp. was next used for the purpose. A set of data for i and d was noted at 7 mm Hg in air. A plot of i^2 vs d gave a good straight line Fig.(4.20).

4.11 Slow Drift of the Ammeter Readings:

The drift with time of the ammeter reading was another difficulty of a more serious kind. This was apprehended to be due to the dielectric heating of the material of the discharge tube and of its assembly or of the various components inside the voltmeter or its associated circuit. Several steps were taken to eliminate this trouble (for details see Appendix I).

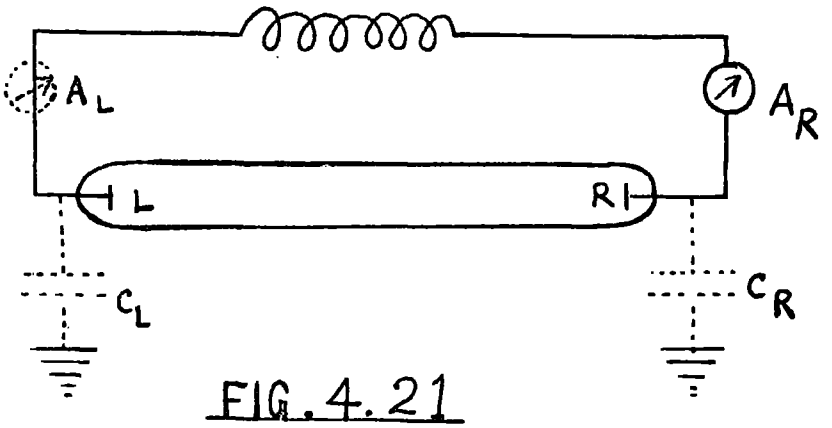

FIG. 4.21

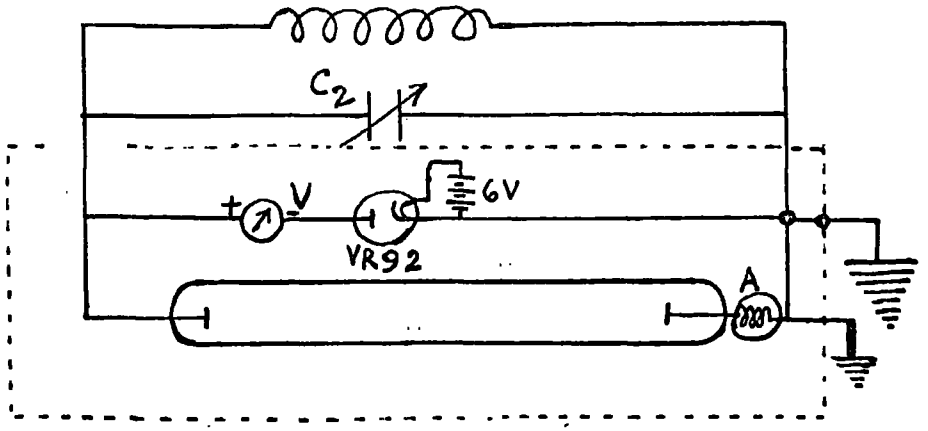

FIG. 4.22. THE ASYMMETRICAL ARRANGEMENT.

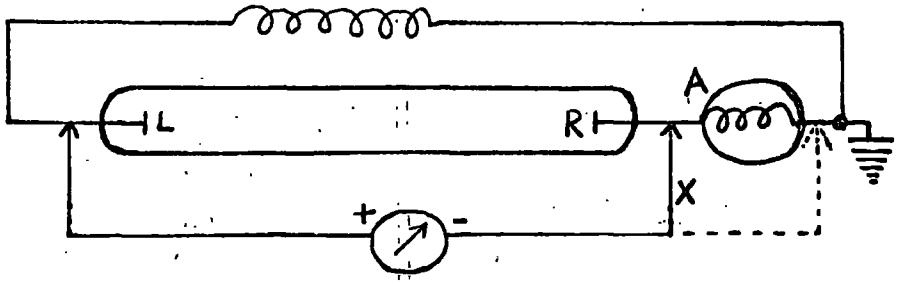

FIG. 4.23. TEST OF RELIABILITY OF DATA.

4.12. Minimisation of the Strays.

At 17 Mc/s stray capacitances are great sources of trouble, especially those from the electrodes to the earth (C_L and C_R, Fig.(4.21).

Details of the steps taken to deal with the difficulties introduced by these strays are given in Appendix II, but some general observations are made below:

The current through C_L and C_R can flow through the gas in the tube (the capacitors merely represent the electrostatic field from the electrodes to the earth). Thus, if point R is connected to earth, there will be a brighter glow of the tube at the L end than at R and vice versa. An ammeter at A_L will indicate the current to the electrode R plus the current through C_L.

In order to overcome these difficulties due to the strays C_L and C_R in obtaining true value of the current through the tube, one can apply either of the two following possibilities:

1. To use a symmetrical system and reduce C_L and C_R as far as possible by attention to design, or
2. To use a system with one end, (R say), earthed so that the current through C_R is zero. A low impedance

ammeter at A_R will then indicate the true current through the tube.

Both possibilities were tried experimentally. For simplicity, however, it was decided to use the second system for the present experiments.

4.13 Asymmetrical Arrangement of the Discharge System.

Decision to use the asymmetrical system implied certain modifications in the circuit arrangements. Fig.(4.22). These are listed below:

(i) position of ammeter:

This must be at the earthy end of the discharge tube so that it indicates the true value of the current through the tube.

(ii) single-ended voltmeter:

In order to conform to the asymmetrical system, the symmetrical peak voltmeter was modified into the form shown in Fig(4.22) having a single diode rectifier in the circuit.

(iii) screening:

An effective screening of the discharge system was an important requirement so as to give a definite and

small stray capacitance. To achieve this, an earthed metal box (shown dotted in Fig.(4.22) completely surrounding the earthy end of the discharge tube was erected.

(iv) live end of the secondary coil:

Care was taken so that the live end of the secondary coil was not too close to the earthed metal box, as this would increase the leakage of current to earth thereby reducing current through the tube.

(v) mechanical disposition of condenser, ammeter and voltmeter:

Questions like the best position of C_2, the ammeter and voltmeter etc. were all decided by trial and error so as to satisfy the condition that the effects of the strays, though much reduced already, were minimum.

4.14 Reliability of the Data.

With the asymmetrical system built up satisfying all the above conditions, observations for voltage and current in the tube were carried out. In order to test whether the measurements were reliable, it was essential to find (i) the voltage drop across the ammeter coil and (ii) the current flowing through the voltmeter. The following

tests were made:

Connection of the voltmeter lead at the ammeter end (lead X, Fig(4.23) between electrode R and A or between A and earth did not produce any noticeable change in the voltmeter reading, thus showing that (i) e.g. voltage drop across the ammeter coil was negligible. Again, withdrawal of both the voltmeter leads from the electrodes L and R did not influence the deflection of A to any appreciable extent, showing that (ii) e.g. current flowing through the voltmeter was also negligible.

4.15 Some Qualitative Observations on the Glow as a Function of Pressure.

In addition to the quantitative studies reported so far, some observations of the qualitative kind are worth reporting here. It was found that for a certain applied voltage, as the pressure was gradually reduced from a high value, (i) the gap broke down with glows confined to the ends, the centre region of the tube remaining dark; (ii) with further reduction of pressure, the glow extended throughout the tube so that the whole gap was of uniform intensity; (iii) with pressure further down, the glow detatched itself from the ends and was gradually concentrated at the centre; the appearance of

the glow at this stage was cylindrical with tapered ends; (iv) at this position, voltage increased with increase in current; (v) the pump was kept running; the central tapered glow remained steady even upto the lowest pressure attained (≈.005 mm Hg); (vi) after switching off the oscillator, (the pump still running) and waiting for a minute or so for the tube to cool down, when the oscillator was switched on again, the glow obtained filled the whole tube, at precisely the same pressure as before i.e. .005 mm Hg. When in this condition, the controlling knob of the oscillator was only slightly disturbed, the uniform glow throughout the tube reverted to the previously observed central tapered glow again. It was further observed that (vii)when the glow extended throughout the tube, the voltage recorded was quite low, whereas when the glow abruptly changed over to the tapered central one, the voltage went up abruptly too. All the above observations from (i) - (vii) were repeatedly verified.

4.16 Change of Pressure within the System due to the Probable Release of Occluded Gases with the Running of the Discharge.

It was noted that when the tube was kept glowing for some time, the pressure went up considerably, probably

due to the heating of the discharge tube and the consequent release of the occluded gases in the material of the vessel. The tube was, therefore, degassed by running the discharge for a considerable time with the pump switched on.

4.17. Observations with External Electrodes.

In order to concentrate on the electrical side, preliminary measurements were made with external sleeve electrodes.

Neon was filled into the system. When the oscillator was switched on, beautiful and complex striations appeared at breakdown of the gas. The striations in the h.f. electrodeless discharge have not been extensively studied before; their origin also is not at all clear. Some time, therefore, was spent in studying these striations in air, H_2 and Ne, by means of their photographs obtained under varying conditions of pressure, gap length and exciting voltage. These will be described and discussed in the next Chapter.

The rest of the history of the work is the study of the current-voltage relations in the discharge with both internal and external electrodes, in both long

cylindrical and flat cylindrical cavities of various lengths and diameters and at various pressures. As the deflection of the eddy-current ammeter was not large, the previous copper disc of 1 cm diameter was replaced by one of a 2 cm diameter, whereby the sensitivity of the ammeter increased about 4 times; the ammeter had to be re-calibrated and all the above observations were taken with this one.

The results of the experiments follow in Chapters V-IX.

CHAPTER - V

MOVING AND STATIONARY STRIATIONS IN THE HIGH-FREQUENCY DISCHARGE

5.1 Introduction.

The occurrence of striations, both moving and stationary, in a positive column is a phenomenon which is well-known for a long time. Nevertheless, the mechanism of their formation is far from being clearly understood. The explanations that are found in the literature are mostly of the qualitative nature; there are also available some empirical relations, which hardly satisfy all the experimental facts, nor is it possible from these empirical relations to predict the number and the nature of the striations under given experimental conditions.

Moving and stationary striations have also been observed in relatively recent years in the h.f. discharge in gases with both internal and external electrodes. These are far more complex in appearance than in the d.c. discharge. In addition to the usually observed single striations, it is known that "double striations" (31) also occur under particular conditions of discharge. It

would be a mistake if it is assumed that the formation of the h.f. striations can be explained in the same way as the d.c. striations, as the two types of discharge are fundamentally different. Before presenting our observations on the h.f. striations, a brief description of some of the observations of previous workers is given below:

At a frequency of 0.1 Mc/s in hydrogen, some observations on "double striations" were reported by Richards (31). These consisted of, as it were, two striations placed back to back; the colour of their edges was found to be pink rather than the usual blue. With increase in gap separation, the number of double striations increased.

Placing the hand near one end of the tube had a rectifying effect, as it reduced the intensity of the glow near the hand and striations lost their double appearance. It was suggested that they were of the same nature as the more frequently observed single striations, the two sets, as it were, belonging to the two d.c. discharges in opposite directions, with their sharp convex surfaces turned towards the corresponding cathode. The distance between the two members of a double striation,

it was suggested, could possibly be regarded as the distance the positive ions would describe in a half-cycle of the applied field.

Mention of the formation of h.f. striations in helium for certain ranges of gap current and pressure was also made by Townsend and Jones (13) in 1931. They found that at pressures greater than 20 mm Hg, increase of current beyond 10 mA encourages the formation of striations; below 10 mA, the column is uniform. At pressures less than 13 mm Hg, no striations could be found between 1 and 15 mA. In this respect, Townsend states, the h.f. discharge differs from the d.c. discharge, as in the latter, striations are obtained at pressures less than about 2 mm Hg.

Peka'rek and Krejci (32) have attempted to give a possible explanation of the nature of standing striations in an h.f. discharge. They have suggested that if at some point within the tube, the electron concentration is lowered, the plasma conductivity decreases with consequent local increase of the amplitude of the field. This, in turn locally raises the electron temperature. An increase in electron temperature gives rise to two

phenomena: (i) an increase in the ionisation probability and (ii) diffusion of electrons outwards from that place due to temperature gradient into neighbouring regions of higher concentration and hence in the opposite direction to the normal concentration gradient. Thus, (i) increases the electron concentration and balances the original cause, while (ii) helps the original cause. If (ii) predominates, a periodic structure would result.

Very recently, Nakata et al (33) have reported some observations on stationary striations in h.f. discharge in argon. Their experiments were conducted in cylindrical tubes of diameters between 5.8 and 18 mm and pressure range of 0.07 to 8 mm Hg: it was found that the spatial interval between the striations (the so-called "wavelength")

(a) is proportional to the gap length,

(b) increases linearly with the radius of the discharge tube,

(c) decreases exponentially as the gas pressure increases,

(d) is independent of the frequency of the h.f. source over a range of 5Mc to 53 Mc,

(e) increases as the h.f. power increases, and

(f) when a d.c. field is superposed on the h.f. field, striations move towards the cathode with a velocity proportional to the d.c. current.

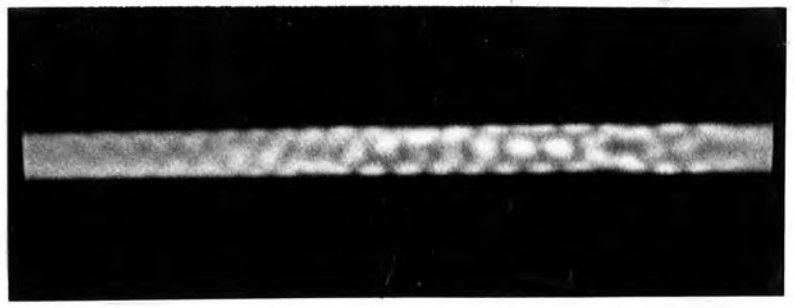

$d = 15$ cms

$V_0 = 510$ VOLTS ; $p = 9 \cdot 5$ mm Hg

FIG. 5.5.

$d = 15$ cms

$V_0 = 530$ VOLTS ; $p = 12$ mm Hg.

FIG. 5.6.

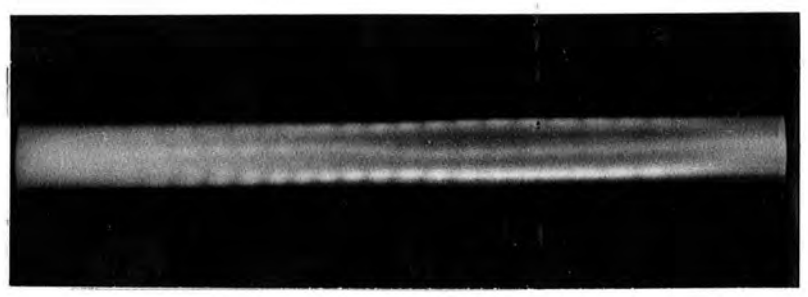

$d = 13$ cms

$V_0 = 600$ VOLTS ; $p = 10$ mm Hg.

FIG. 5.7

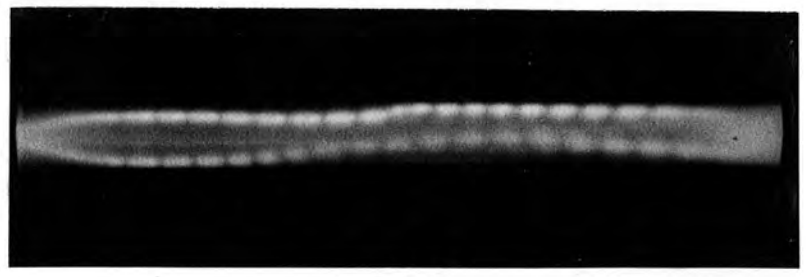

$d = 13$ cms.

$V_0 = 550$ VOLTS ; $p = 10$ mm Hg.

FIG. 5.8.

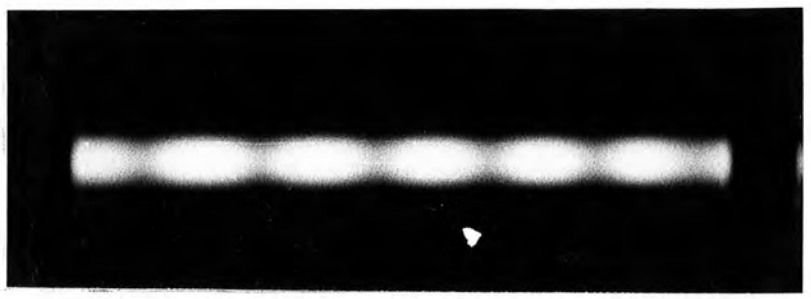

d = 13 cms

V_0 = 520 VOLTS ; p = 0·8 mm Hg.

FIG. 5.1.

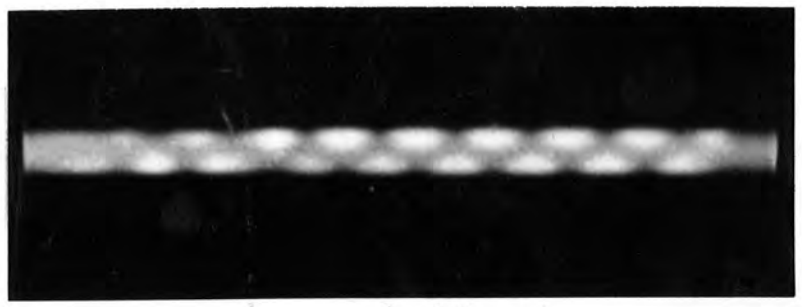

d = 15 cms

V_0 = 510 VOLTS ; p = 2·5 mm Hg.

FIG. 5.2.

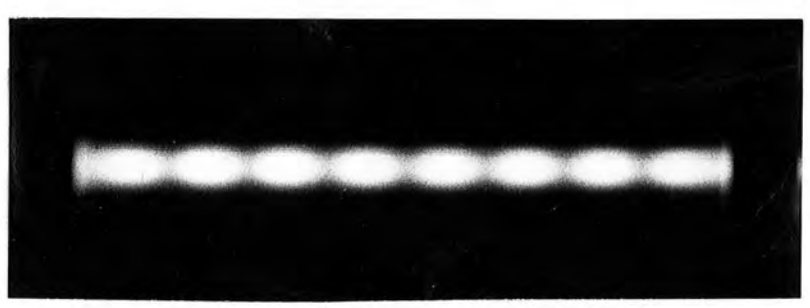

d = 13 cms

V_0 = 480 VOLTS ; p = 6 mm Hg.

FIG. 5.3

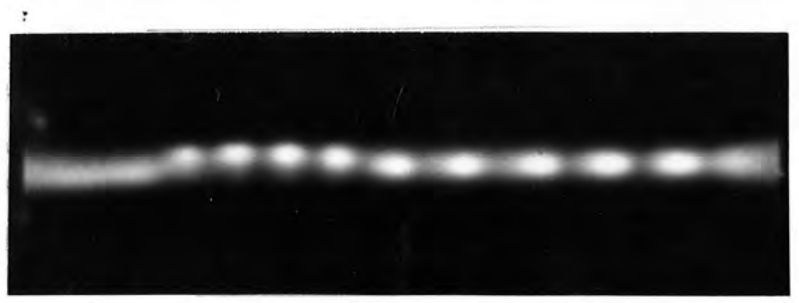

d = 13 cms.

V_0 = 270 VOLTS ; p = 7·5 mm Hg.

FIG. 5.4.

No theoretical analysis of the phenomena has been made.

5.2 Present Observations on Striations.

During the present experiments, striations were observed in neon first in the case of electrodeless discharge in a tube of internal diameter 1.28 cm and external diameter of 1.55 cm:; the distance between the external sleeve electrodes was about 13 cm. The appearance of the striations in neon was highly complex. They were photographed under varying conditions of gas pressure, gap length and the exciting voltage and some typical ones are shown in Figs. (5.1)-(5.8).

By varying the pressure, the moving striations could be made stationary. Their number then could be counted. Table 5.1 on the following page shows how the number of the striations changed with the gap separation, gap voltage etc.

TABLE - 5.1: Observations in neon

Voltmeter reading (for nearly the same intensity of the striations).	Distance between electrodes cm	Pressure mm. Hg	Number of Striations
540	15.3	0.7	6
570	11.7	"	5
590	8.4	"	3
610	6.5	"	2
775	19.6	0.25	7
540	17.8	"	7
530	14.5	"	6
780	10.8	"	4
800	7.0	"	2
445	7.0	3.7	3
440	8.0	"	4
440	9.0	"	4
430	10.4	"	5
435	12.0	"	6
425*	14.0*	"*	7*
660	14	5.5	8
650	18.2	"	10
630	22	"	16
665	11	"	6
690	7.5	"	4
680	6	"	3

Under the conditions represented by the row of data marked with an asterisk in Table 5.1, a very interesting phenomenon was observed which is described below:

It was found that the voltage could be adjusted for each spacing between the electrodes, so as to obtain maximum illumination and distinct striations having sharp boundaries. When this was done, it was noted that the value of 425 Volts suddenly changed to 590 Volts which was the maximum value recorded by the voltmeter under the given conditions. However, this value changed to 720 Volts after some time. As the discharge was run for some time more, it was noted that the number of striations increased from 7 to 8 and then to 9; also, the striations which were stationary before, began to move along the discharge tube; rather, a sort of wave motion was observed to be superposed on the stationary striations*. It was further observed that the boundaries between striations which were previously sharp, when the

---

* While the striations between the electrodes were stationary, those beyond the electrodes at the earthy end of the discharge tube were moving slowly into the gap; this eventually looked like a general superposition of the moving striations over the stationary ones existing between the electrodes.

discharge started, became diffuse with time and the voltage across the tube dropped from 720 to 640 Volts. These facts were repeatedly observed. Thus, summarising the above, one can tabulate as follows:

TABLE - 5.2: Neon

p = 3.7 mm. Hg; d = 14 cm.

Observations just after starting of the discharge		
Voltmeter reading volts	Number of striations	Appearance of the discharge
425 → 590 → 720	7	boundaries between striations sharp.

Observations after about a minute from the start		
Voltmeter reading volts	Number of striations	Appearance of the discharge
640	9	boundaries between striations diffuse.

5.3 General Description of Striations in Neon.

At a pressure of 9 mm Hg and 300 Volts gap voltage, the striations were bead-like in appearance, moving in opposite directions sometimes, sometimes in the same direction, sometimes stationary, sometimes one row joined by two rows, this pattern again being wavy; bead-like striations also extended beyond either electrode; columnar striations and a host of other patterns were obtained which were oscillating and moving.

By changing the voltage, the direction of propagation of striations could be changed; there was an indication that a critical value of voltage, under otherwise unaltered conditions, existed at which it appeared to be possible to make them stationary; at other times, due to their speed of motion, it was difficult to count their number. There was a certain voltage range for a given pressure and a certain pressure range for a given voltage in which the striations appeared.

Movement of the striations in whatever form and mode, and their appearance and disappearance -- all seemed to be periodic -- with a period varying from about a second to a few seconds depending upon the

pressure and the operating voltage.

5.4 Search for Striations in Air.

In air, the entire pressure range of 0.01 to 6.8 mm Hg in which the discharge occurred, search was carried out to observe striations. No striations were observed at all. With immersed electrodes, however, striations were obtained within a pressure range of 1.2 and 10 mm Hg; some of them were very much fluctuating in character and were found to be parallel to the axis of the discharge tube and resting, as it were, on the surface of each cylindrical electrode on the gap side. Some striations were also observed within and outside the gap.

5.5 Search for Striations in Hydrogen.

In the electrodeless case, no striations could be found in the entire pressure range of 1.5 to 7.5 mm, in which the discharge occurred. With immersed electrodes, moving striations were obtained at a pressure of 6.5 mm Hg and around this value. The appearance of these striations was disc like and these were mainly confined near the live electrode.

CHAPTER - VI

OBSERVATIONS ON THE CURRENT-VOLTAGE RELATIONS IN LONG CYLINDRICAL TUBES IN THE ELECTRODELESS CASE.

6.1 Introduction.

With the asymmetrical arrangement of the experimental set-up as described in Chapter IV, observations were carried out in air. H_2 and Ne in cylindrical tubes fitted with external electrodes Fig.(4.4). In this chapter, the results of such observations will be reported. The use of the external electrodes necessitated an accurate determination of the voltage drop between the external electrodes and the inner surface of the tubes. This, in turn, meant an evaluation of the capacitances between the electrodes and the interior of the tubes.

6.2 Determination of the Tube Capacitance.

The circuit employed for this is shown in Fig.(6.1). S is a signal generator capable of delivering an output power of 3 W across the high output terminals AB. L_1 is a coil of a few turns of copper wire connected across

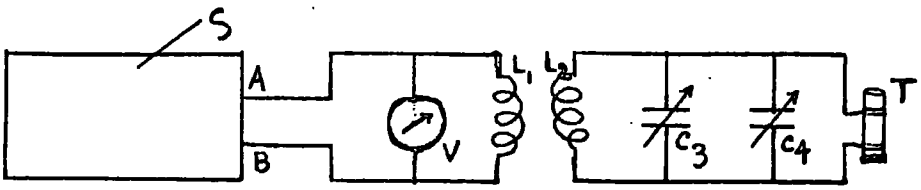

FIG.6.1. CIRCUIT FOR MEASUREMENT OF CAPACITANCE OF TUBES.

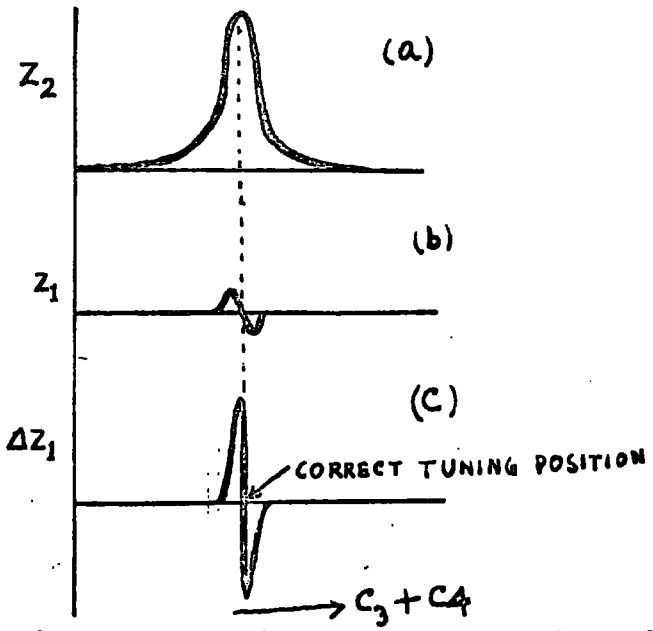

FIG.6.2. ILLUSTRATING THE CORRECT TUNING POSITION.

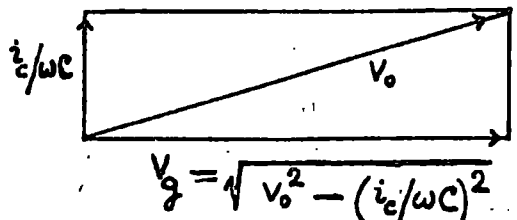

FIG.6.3. SHOWING PHASE QUADRATURE BETWEEN V_g AND $i_c/\omega C$.

AB and serves as the primary, the voltage across the primary being measured by a vacuum tube voltmeter V. The secondary also consists of another copper coil L_2 of similar dimensions. C_3 and C_4 are two condensers, one big and the other small, for rough and fine adjustments respectively. Across the secondary at the farthest end is connected the tube sample T, the capacitance of which is to be determined.

T was a portion of exactly the same tube as was used in the actual experiment and it was mounted vertically with its bottom end closed with a piece of cork. Further, it was fitted with the same external electrodes as were actually used for the experimental tube. When the tube was empty, the bigger condenser C_3 was adjusted to a suitable value so as to obtain a sharp change in the constant reading of V. This is illustrated in Fig.(6.2); in Fig.(6.2a) is shown the variation of the secondary impedence Z_2, in (b) that of the primary impedence Z_1, and in (c) that of the transferred impedence ΔZ_1 to the primary, with the total capacitance in the secondary circuit $C_3 + C_4$. In the correct tuning position (shown in Fig(6.2c)) there is a sharp change in the

constant voltage reading. This position could be very accurately determined by varying the finer condenser C_4. The tube was next filled with Hg and the above procedure was repeated to obtain the correct tuning position again, without altering C_3 (as the change in capacitance of the tube was in fact small, adjustment of the finer condenser C_4 was only necessary to obtain the second tuning position). The difference of the two readings of C_4 gave the value of the tube capacitance. The experiment was repeated several times for each tube. A typical set of condenser readings is given in Table 6.1 on the following page. A few such sets of readings were taken for each tube. The mean capacitances of the tubes are given in the last column of the table.

TABLE - 6.1: Condenser readings for correct tuning position

Tubes of various diameters Int.diam=D_1 cms. Ext.diam=D_2 cms.	Condenser readings (dvns)		Difference dvns	Mean Capacitance of tube in μμf
	without Hg	with Hg		
D_1 = .525 D_2 = .800	2.60 2.60 2.60 — 2.60	9.15 9.17 9.16 — 9.16	6.56	2.20
D_1 = .930 D_2 = 1.200	3.65 3.67 3.66 — 3.66	12.82 12.85 12.82 — 12.83	9.17	3.09
D_1 = 1.280 D_2 = 1.550	3.13 3.13 3.13 — 3.13	13.50 13.50 13.50 — 13.50	10.37	3.69
D_1 = 1.455 D_2 = 1.800	2.95 2.97 2.97 — 2.96	18.60 18.64 18.62 — 18.62	15.66	5.21
D_1 = 1.640 D_2 = 2.020	3.96 3.97 4.04 — 3.99	21.13 21.12 21.12 — 21.12	17.13	5.98

6.3 Correction for the Voltage Drop in the Tube

The voltage drop across the capacitance C of the tube is $i_c/\omega C$, where i_c is the h.f. current of angular frequency ω flowing through the gap. i_c was obtained from the deflections of the eddy-current ammeter which was previously calibrated by a vacuum thermo-junction. In order to eliminate displacement current, it was found possible to adjust C_1 and C_2 Fig.(4.22) so that there was no deflection of the ammeter until there was breakdown of the gap. At breakdown, the ammeter showed a large deflection which then corresponded entirely to the conduction current in the gap.

Assuming that this voltage drop $i_c/\omega C$ and the drop V_g in the gas are in phase quadrature Fig.(6.3), the observed voltage V_o was corrected for V_g according to the relation

$$V_g = \sqrt{V_o^2 - \left(i_c/\omega C\right)^2} \qquad (6.1)$$

By continuously varying the position of the control knob of the oscillator, the gap current and hence the gap voltage were continuously varied.

6.4 Experimental Results.

(a) Observations in air.

Results in air are graphically represented by Figs.(6.4 - 6.6) at three values of pressure, namely, 4, 2.5 and 1.5 mm. Hg respectively.

(b) Observations in hydrogen.

In Figs.(6.7 - 6.9) are given values of V_g vs i_c in hydrogen at 9, 6 and 3.2 mm. Hg. respectively.

(c) Observations in neon.

Similarly, Figs.(6.10 - 6.12) represent results in neon at pressures of 13, 10 and 6.5 mm. Hg. respectively.

6.5 Discussion of Results.

From a study of the curves it is evident that ----

(i) the current-voltage characteristics are positive and nearly linear for lower currents. They flatten out slightly on the higher current side where there is an indication that they can even go negative in particular cases. (Fig.(6.8)).

(ii) the effect of gap current on gap voltage becomes less for higher gap separations. In some cases, the

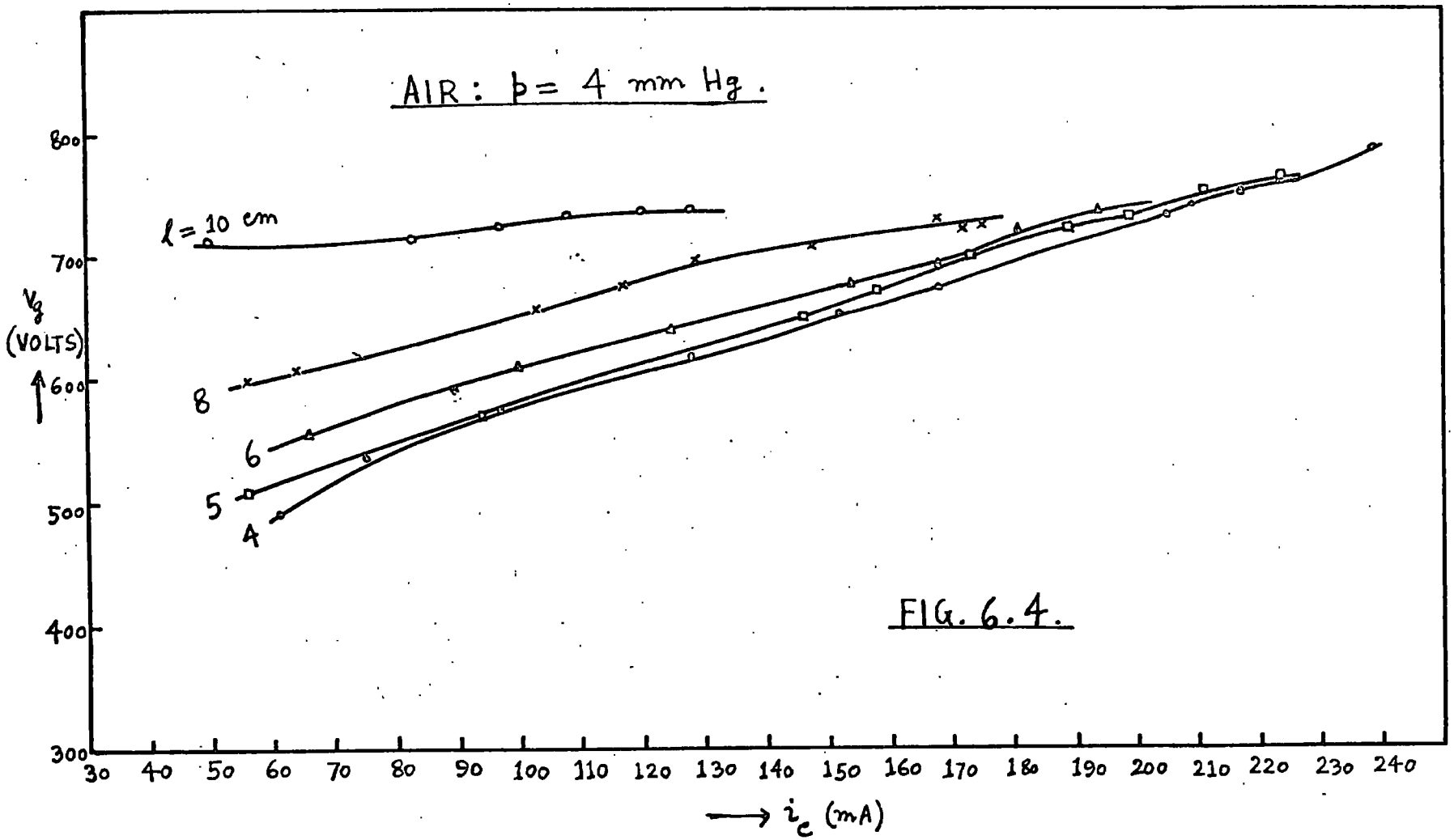
AIR : p = 4 mm Hg.
800
700
600
500
400
300
V_g (VOLTS)
l = 10 cm
8
6
5
4
30 40 50 60 70 80 90 100 110 120 130 140 150 160 170 180 190 200 210 220 230 240
i_e (mA)

FIG. 6.4.

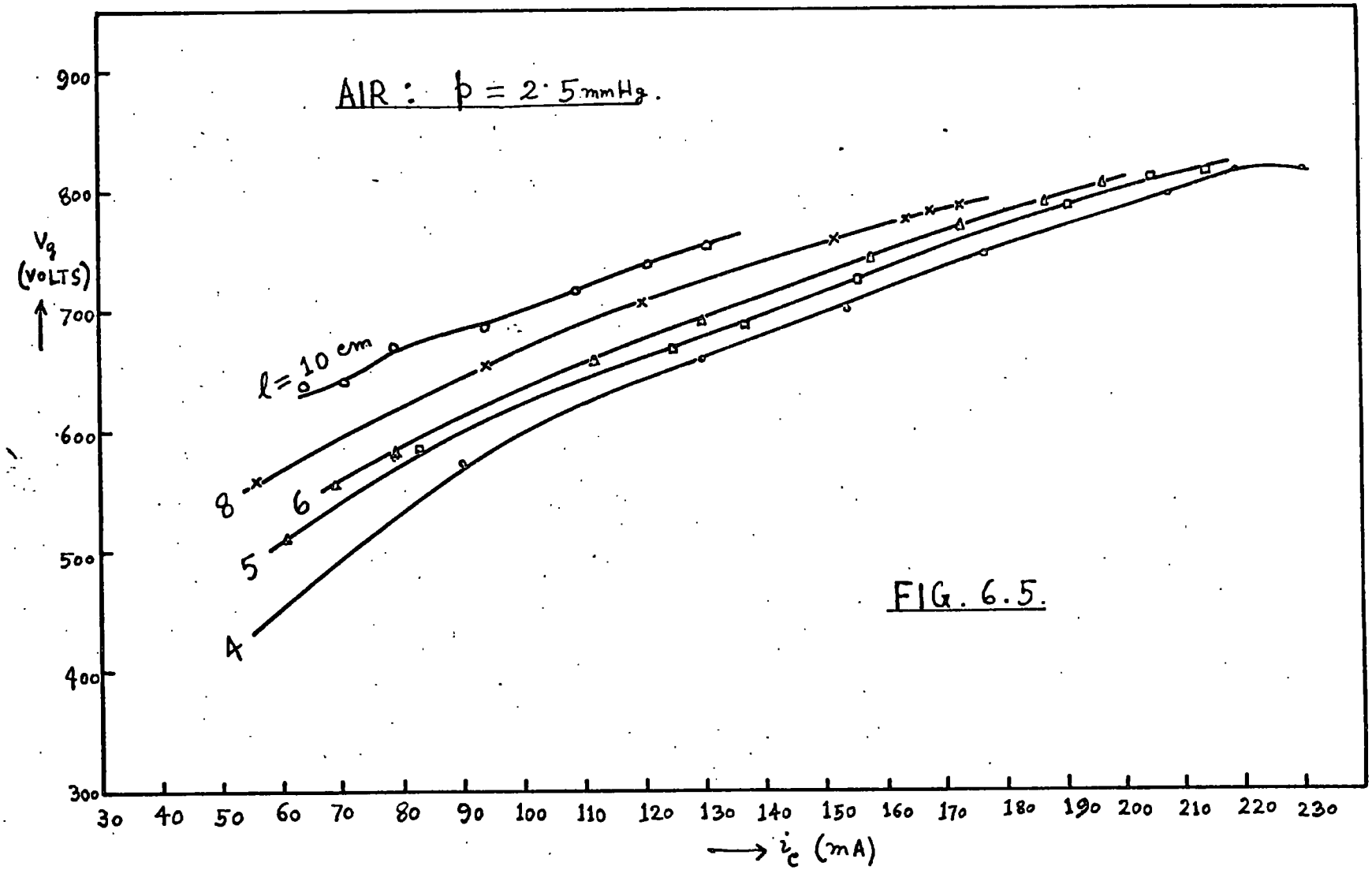
AIR : p = 2·5 mmHg.
900
800
700
600
500
400
300
V_g (VOLTS)
ℓ = 10 cm
8
6
5
4
30 40 50 60 70 80 90 100 110 120 130 140 150 160 170 180 190 200 210 220 230
i_c (mA)

FIG. 6.5.

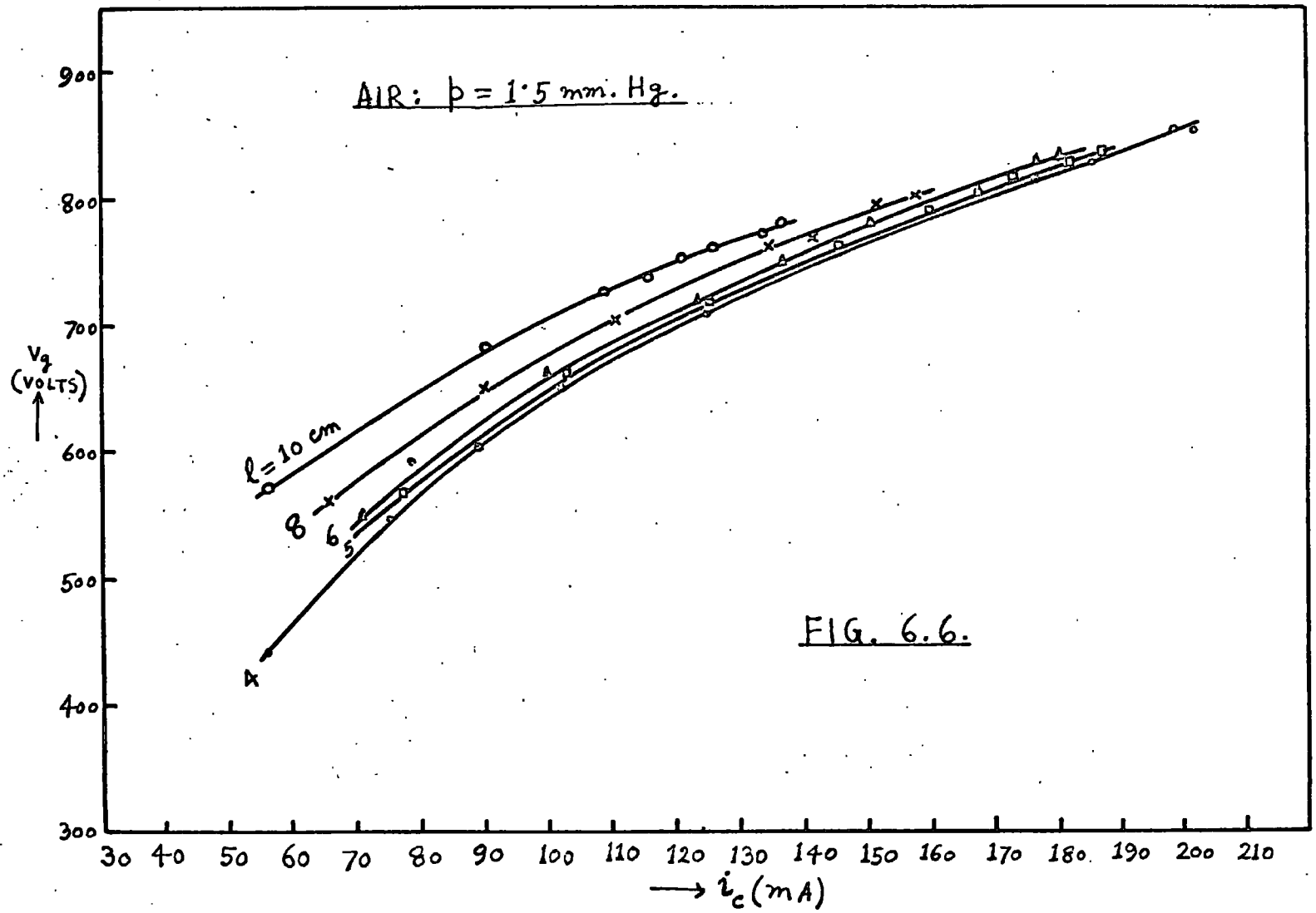
AIR: p = 1·5 mm. Hg.
900
800
700
600
500
400
300
V_g (VOLTS)
ℓ = 10 cm
8
6
5
A
30 40 50 60 70 80 90 100 110 120 130 140 150 160 170 180 190 200 210
i_c (mA)

FIG. 6.6.

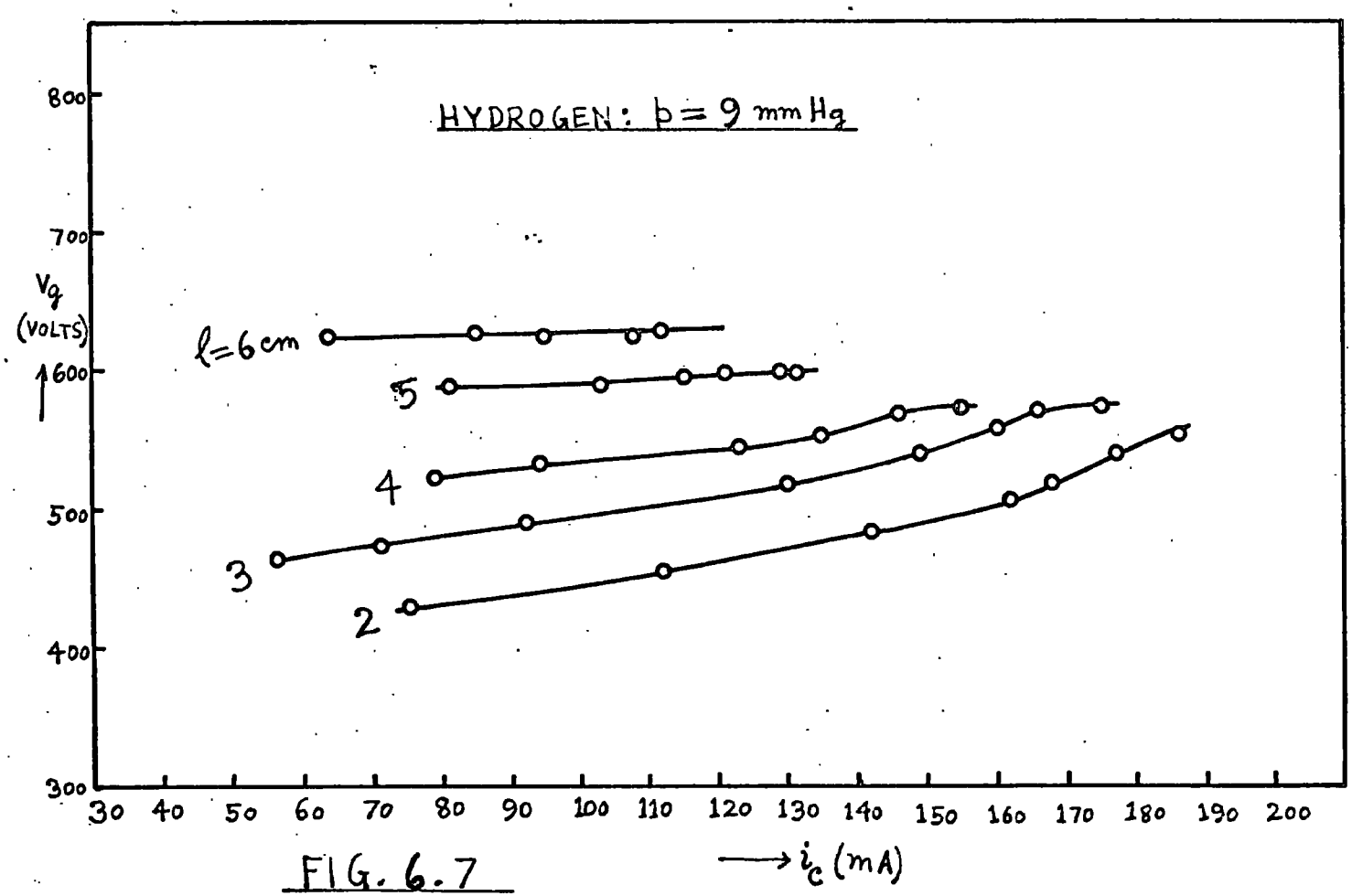
HYDROGEN: b = 9 mm Hg
800
700
V_g (VOLTS)
600
500
400
300
ℓ=6cm
5
4
3
2
30 40 50 60 70 80 90 100 110 120 130 140 150 160 170 180 190 200
i_c (mA)

FIG. 6.7

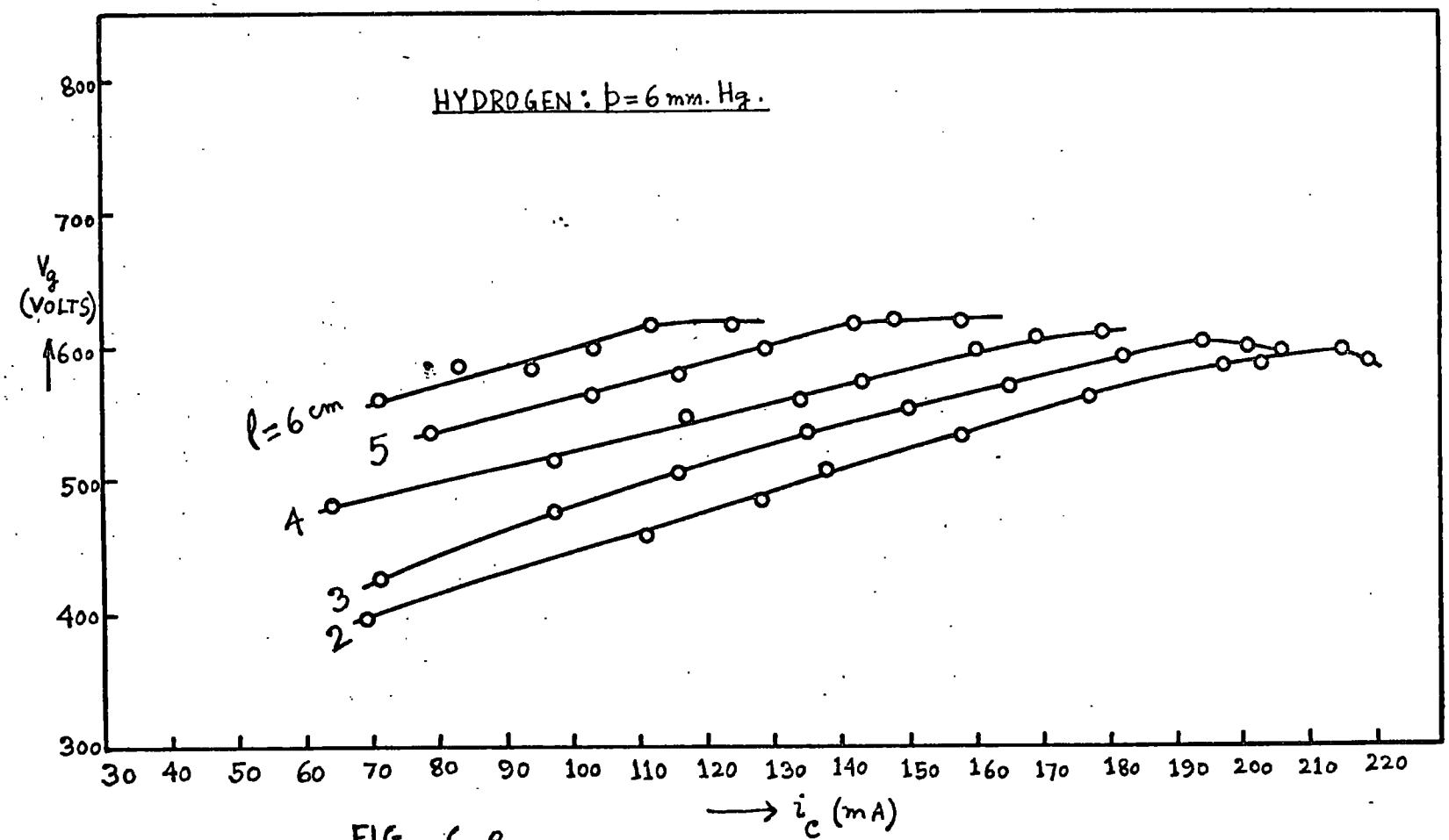
HYDROGEN : p = 6 mm. Hg.
800
700
V_g (VOLTS)
600
500
400
300
l = 6 cm
5
4
3
2
30 40 50 60 70 80 90 100 110 120 130 140 150 160 170 180 190 200 210 220
i_c (mA)

FIG. 6.8.

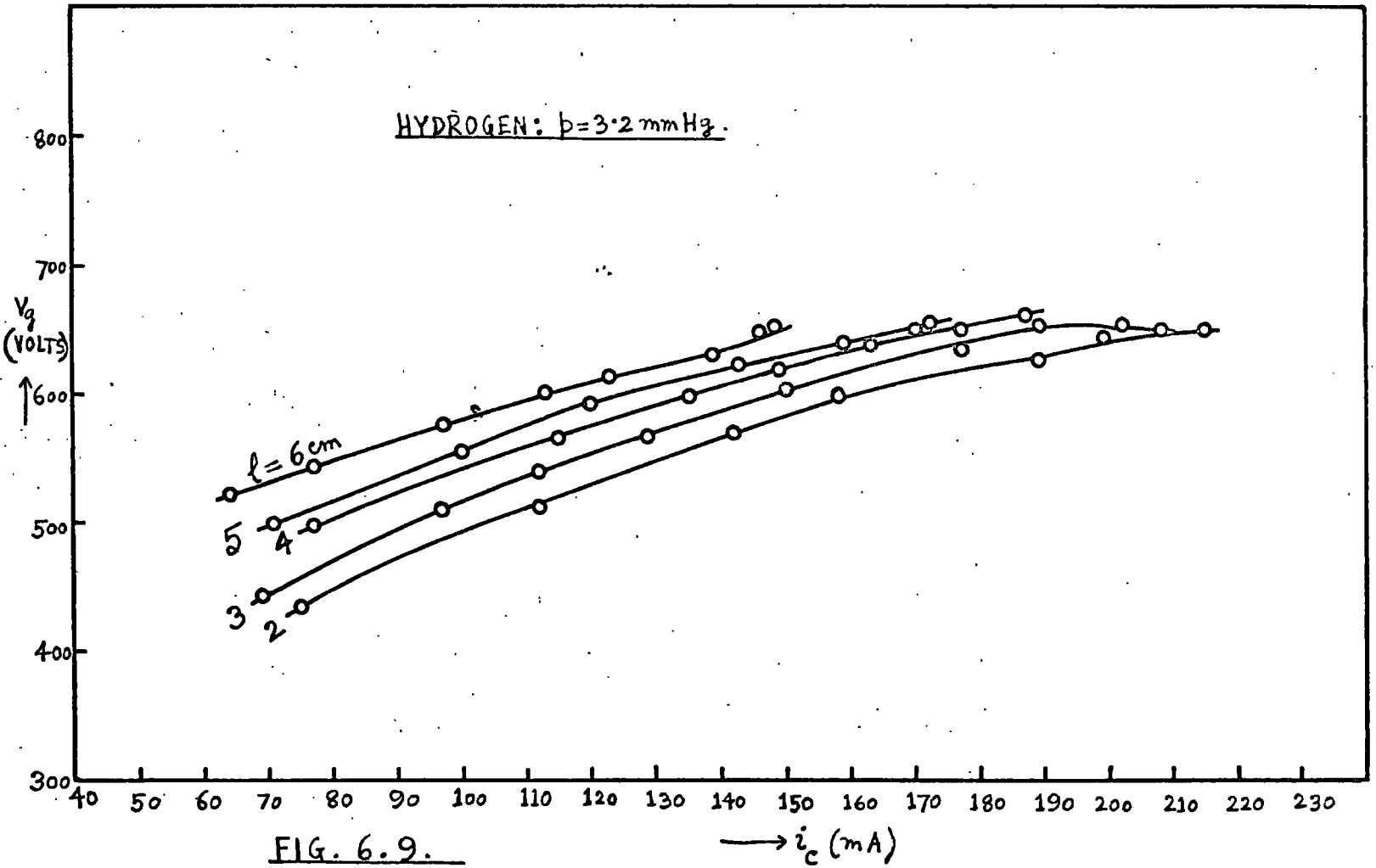
HYDROGEN: p=3·2 mm Hg.
800
700
V_g (VOLTS)
600
500
400
300
ℓ = 6 cm
5
4
3
2
40
50
60
70
80
90
100
110
120
130
140
150
160
170
180
190
200
210
220
230
i_c (mA)

FIG. 6.9.

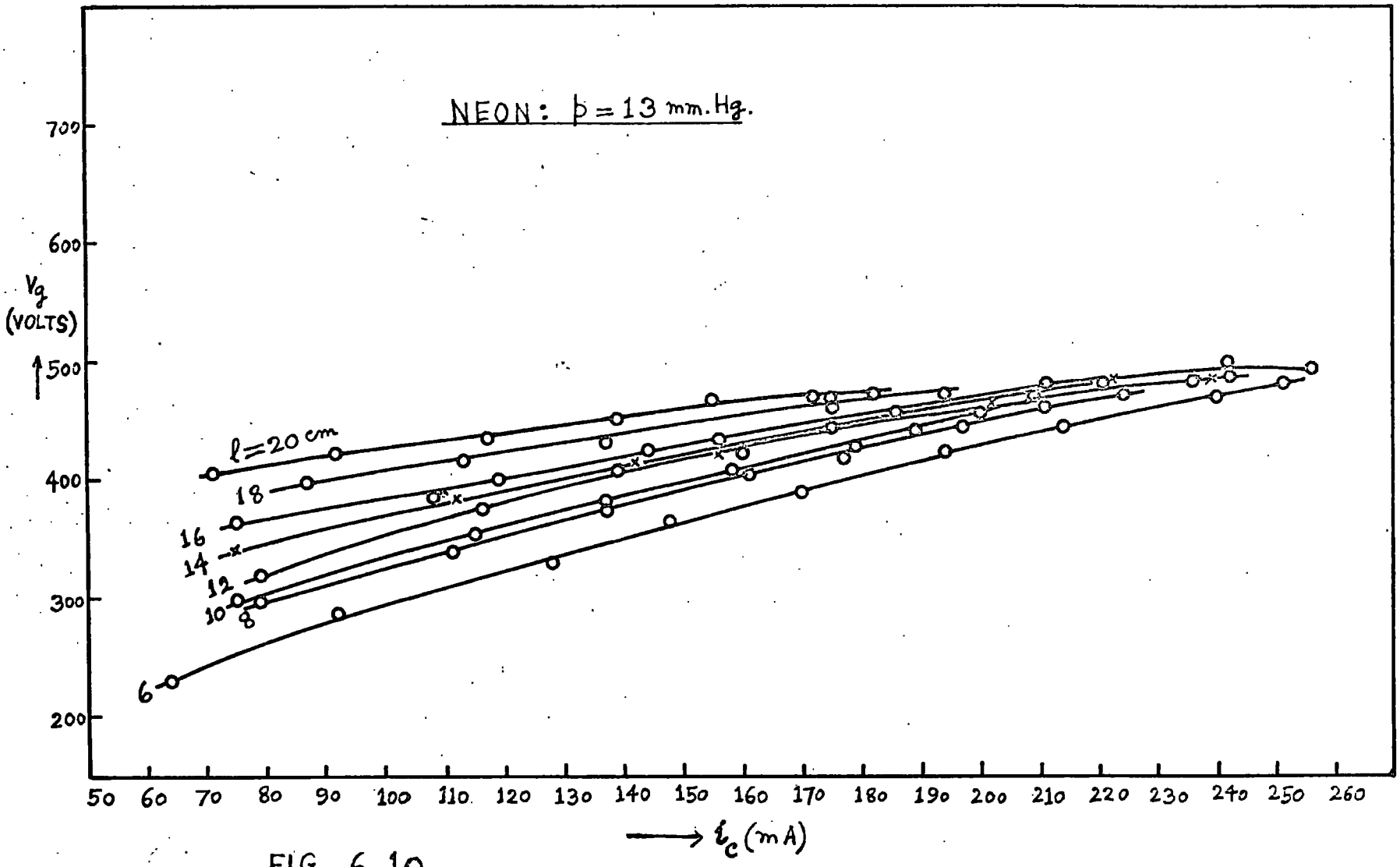
NEON: p = 13 mm. Hg.
700
600
V_g (VOLTS)
500
400
300
200
l = 20 cm
18
16
14
12
10
8
6
50 60 70 80 90 100 110 120 130 140 150 160 170 180 190 200 210 220 230 240 250 260
i_c (mA)

FIG. 6.10

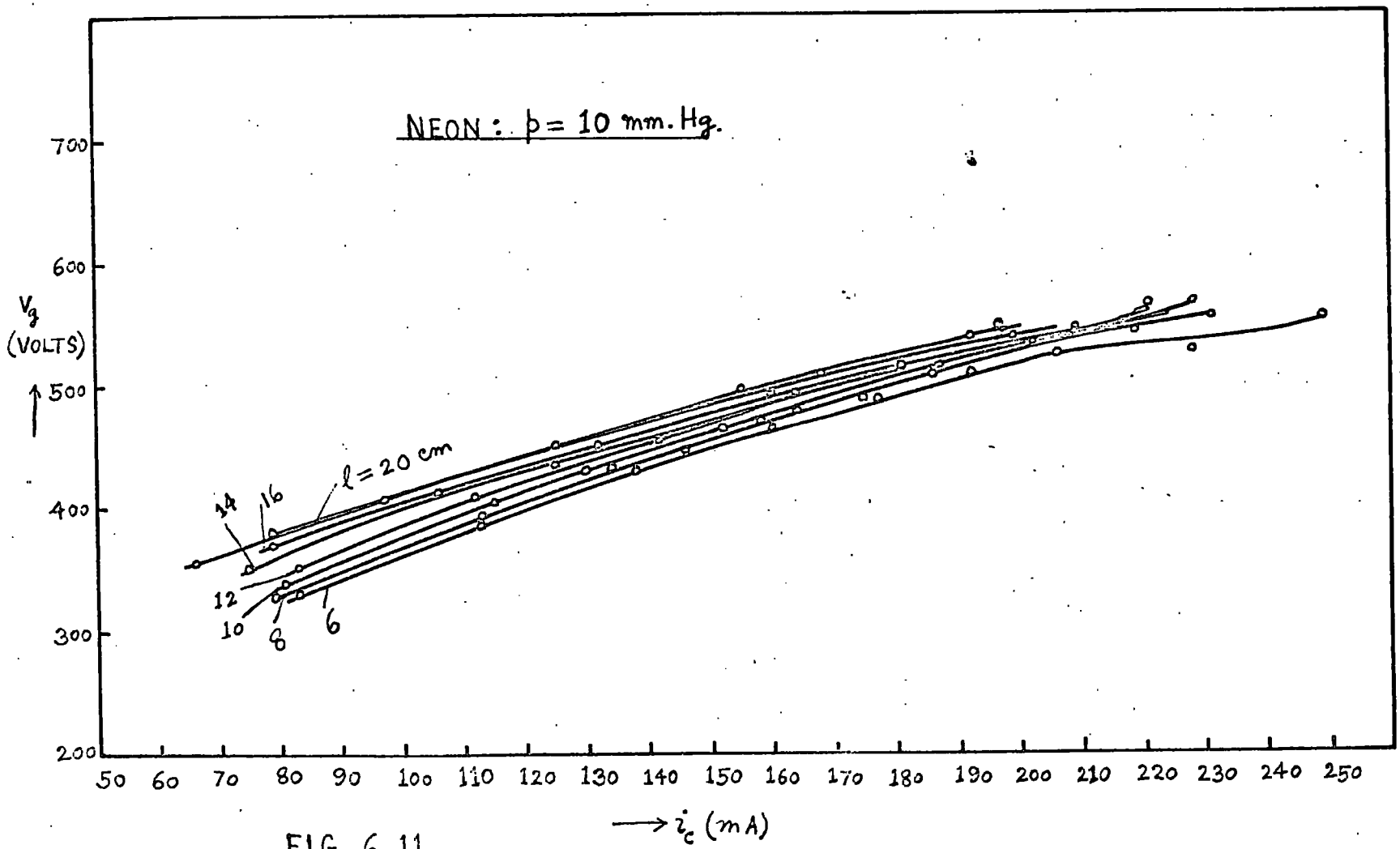
NEON : p = 10 mm. Hg.
700
600
500
400
300
200
V_g
(VOLTS)
50 60 70 80 90 100 110 120 130 140 150 160 170 180 190 200 210 220 230 240 250
$\rightarrow i_c$ (mA)
l = 20 cm
14
16
12
10
8
6

FIG. 6.11

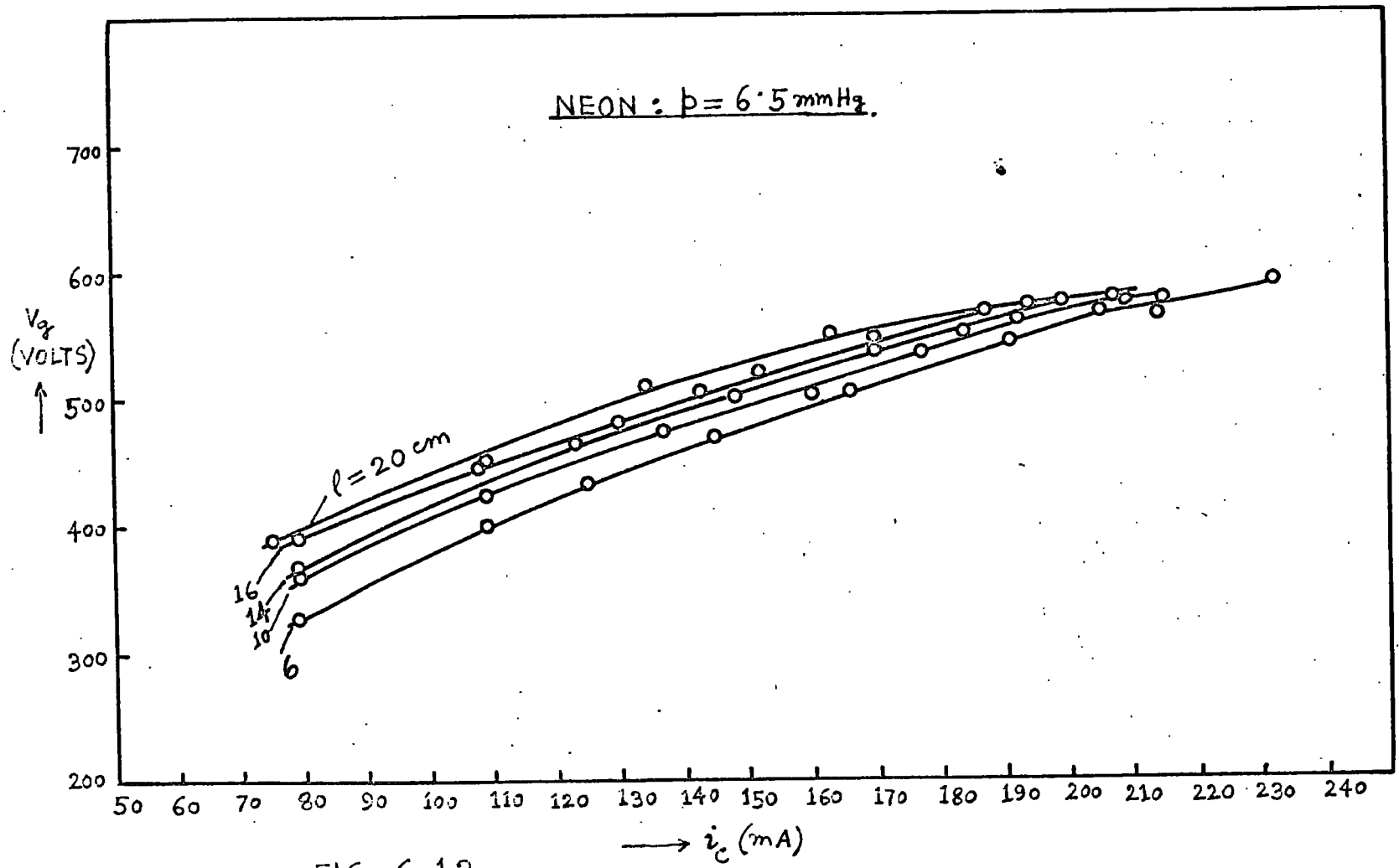
NEON : p = 6·5 mm Hg.
700
600
500
400
300
200
V_g (VOLTS)
ℓ = 20 cm
16
14
10
6
50 60 70 80 90 100 110 120 130 140 150 160 170 180 190 200 210 220 230 240
i_c (mA)

FIG. 6.12.

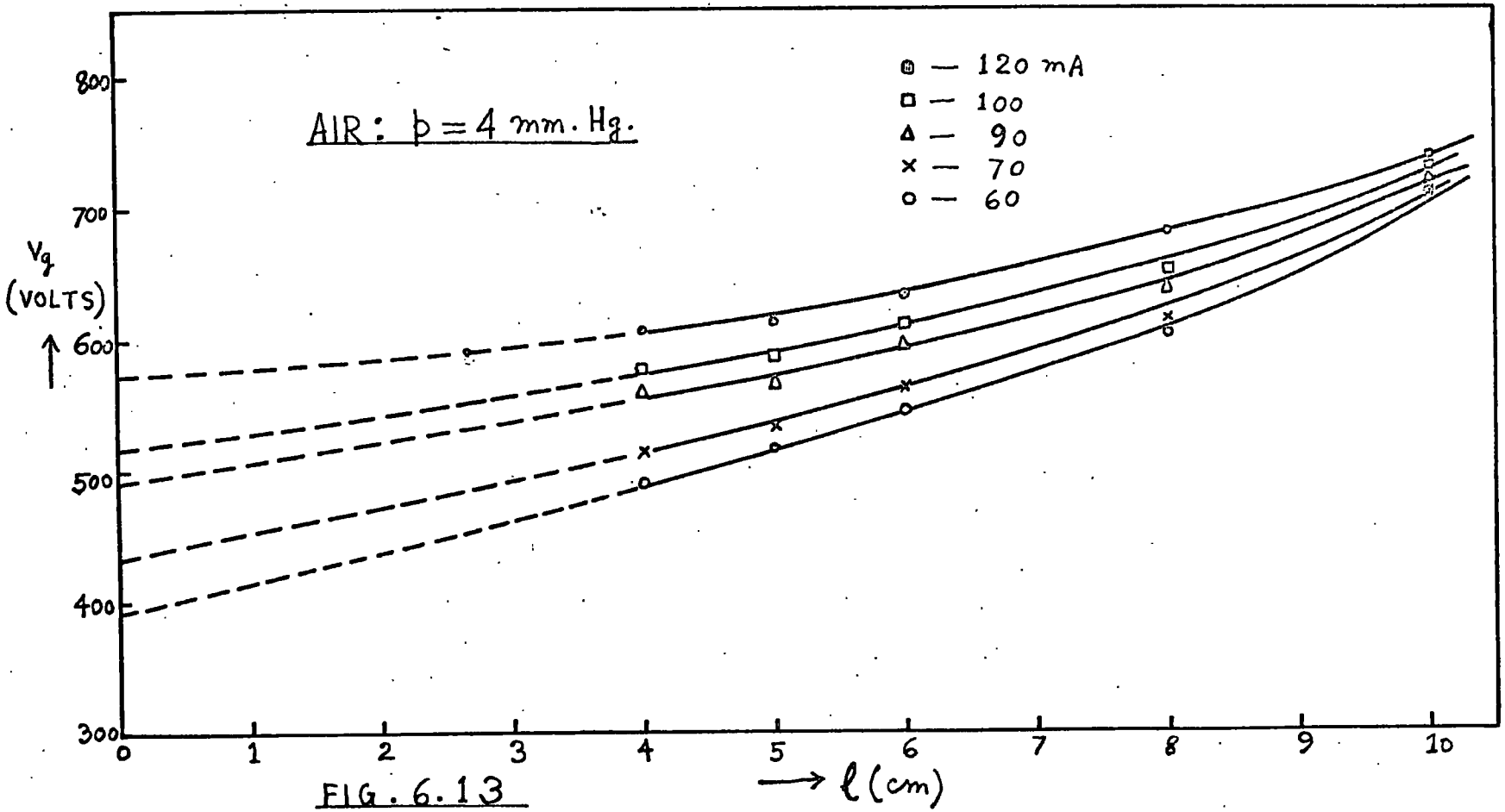
AIR : p = 4 mm. Hg.
⊙ — 120 mA
□ — 100
△ — 90
× — 70
○ — 60
V_g (VOLTS)
800
700
600
500
400
300
0
1
2
3
4
5
6
7
8
9
10
ℓ (cm)

FIG. 6.13

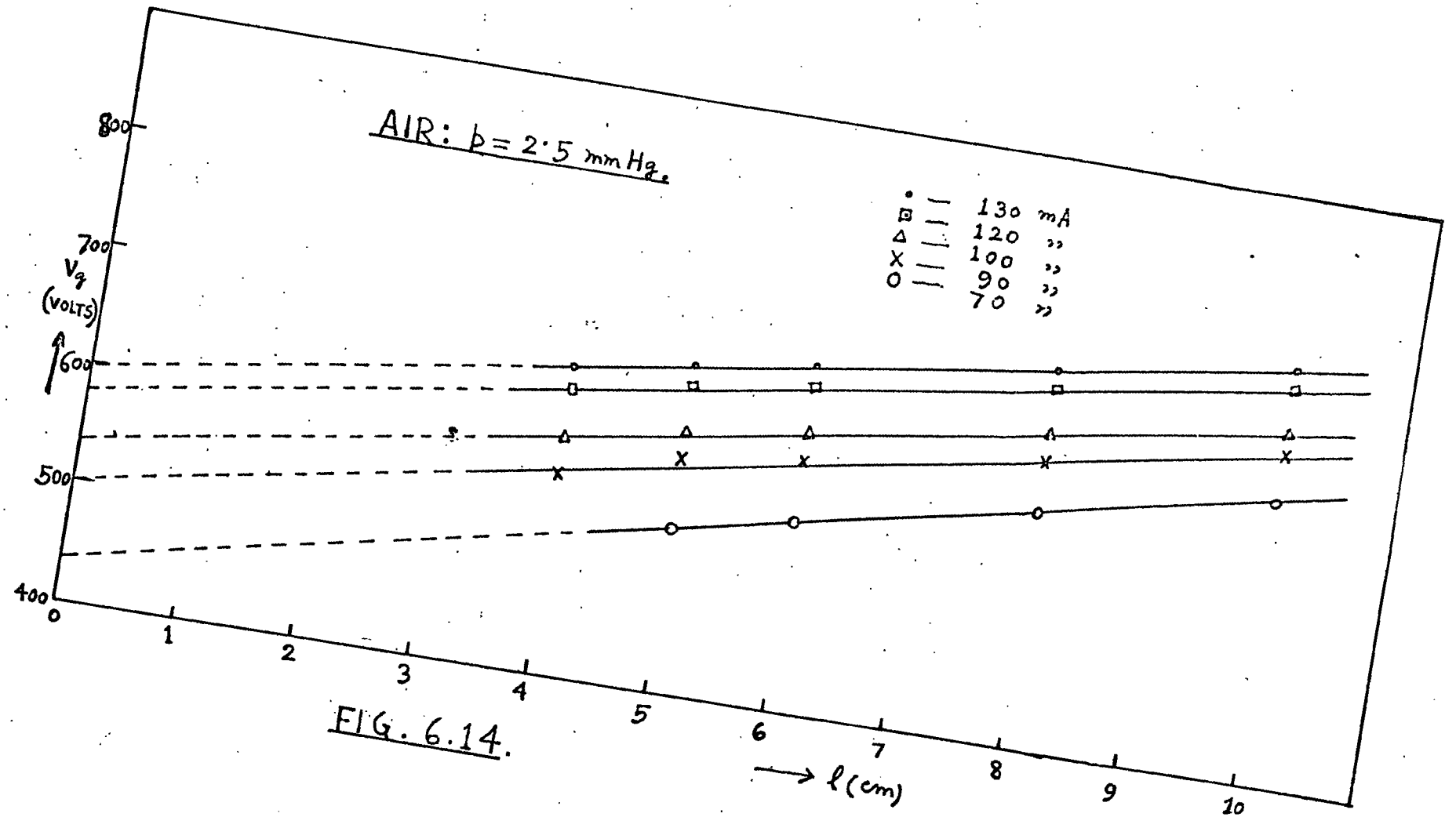
AIR: p = 2·5 mm Hg.
• — 130 mA
□ — 120 ,,
△ — 100 ,,
X — 90 ,,
O — 70 ,,
800
700
V_g (VOLTS)
600
500
400
0
1
2
3
4
5
6
7
8
9
10
→ l (cm)

FIG. 6.14.

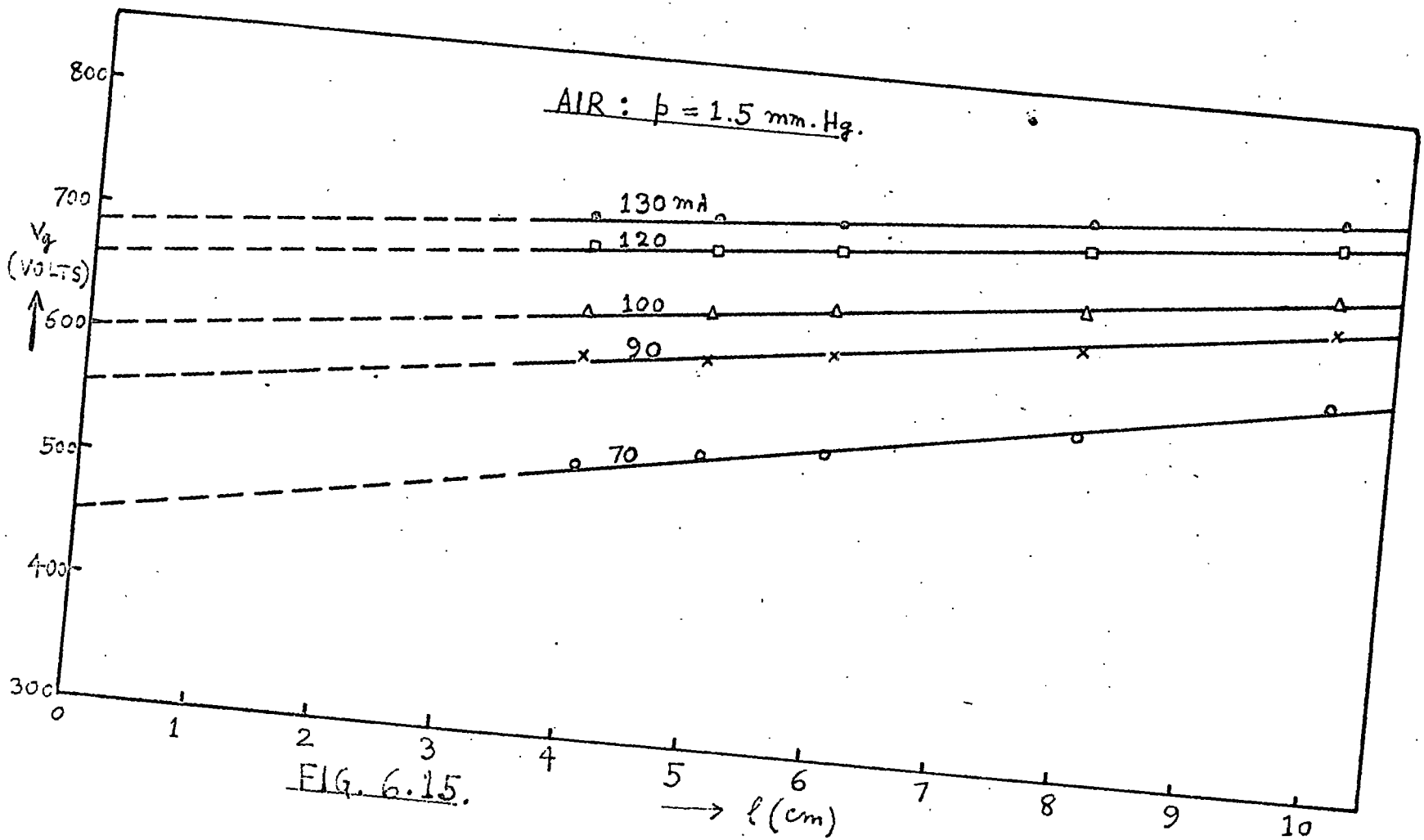
AIR : p = 1.5 mm. Hg.
130 mA
120
100
90
70
800
700
600
500
400
300
V_g (VOLTS)
0
1
2
3
4
5
6
7
8
9
10
ℓ (cm)

FIG. 6.15.

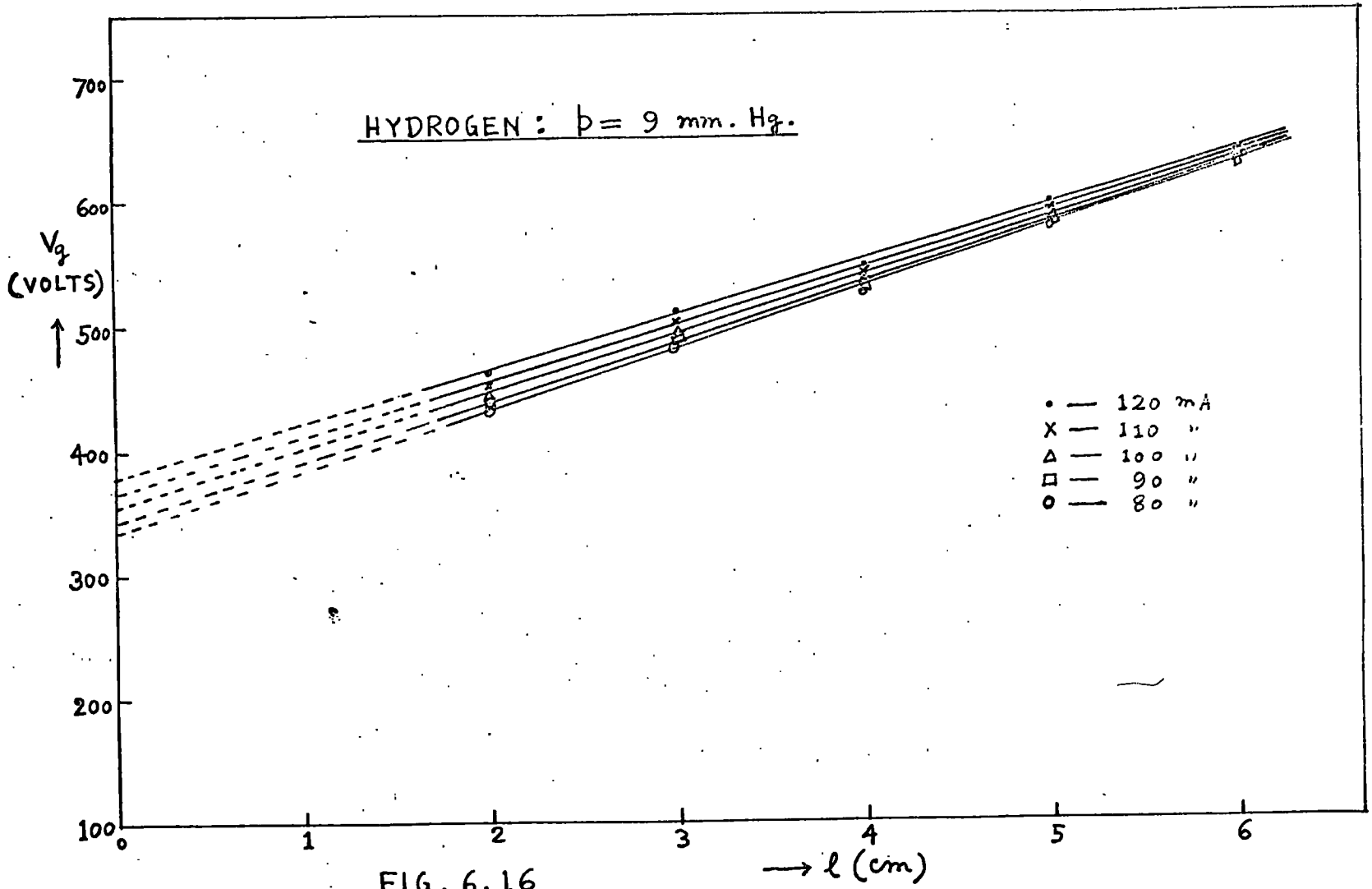
HYDROGEN : p = 9 mm. Hg.
V_q (VOLTS)
700
600
500
400
300
200
100
0
1
2
3
4
5
6
l (cm)
• — 120 mA
X — 110 "
Δ — 100 "
□ — 90 "
o — 80 "

FIG. 6.16

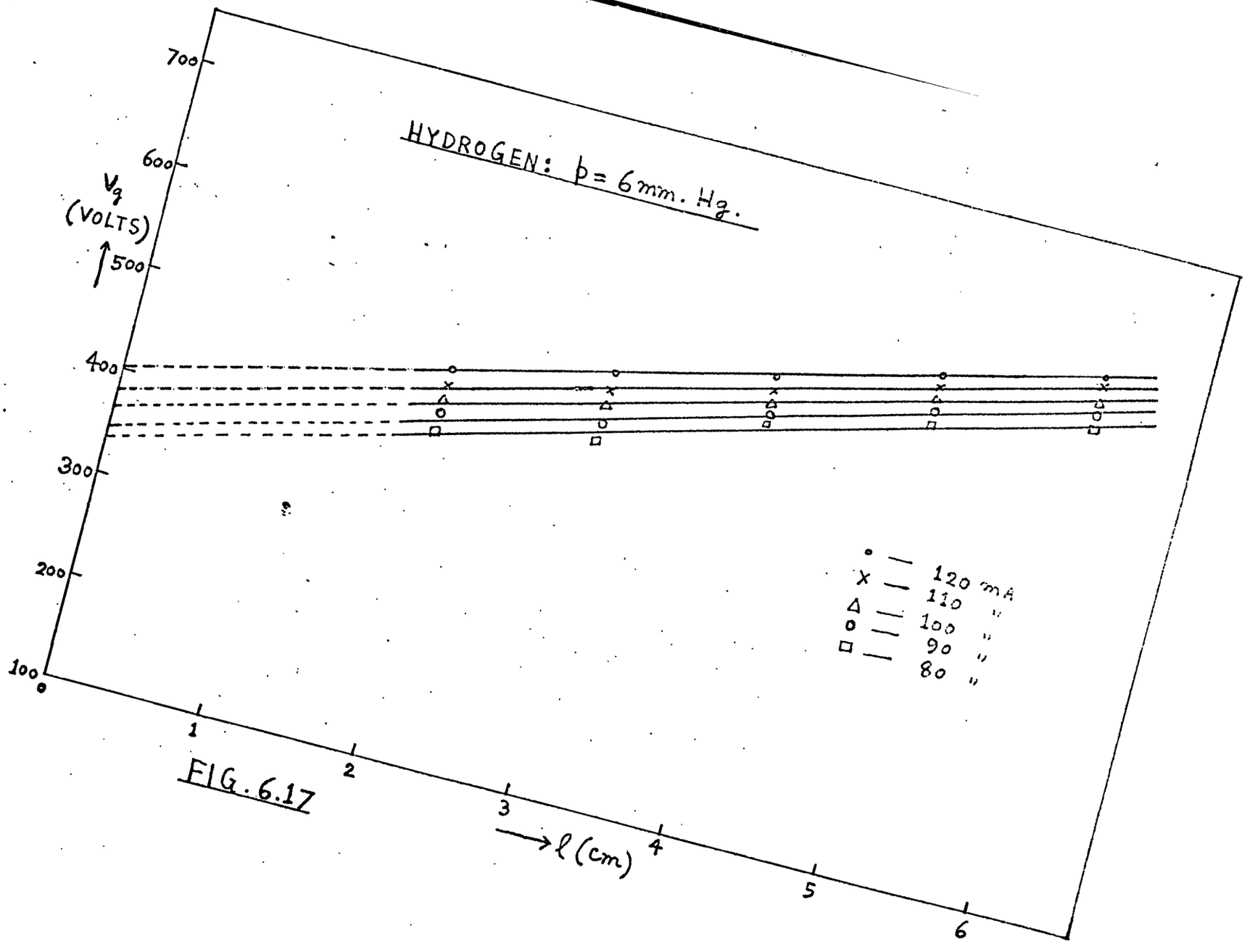
HYDROGEN: p = 6 mm. Hg.
V_q (VOLTS)
700
600
500
400
300
200
100
1
2
3
4
5
6
l (cm)
• — 120 mA
× — 110 "
Δ — 100 "
o — 90 "
□ — 80 "

FIG. 6.17

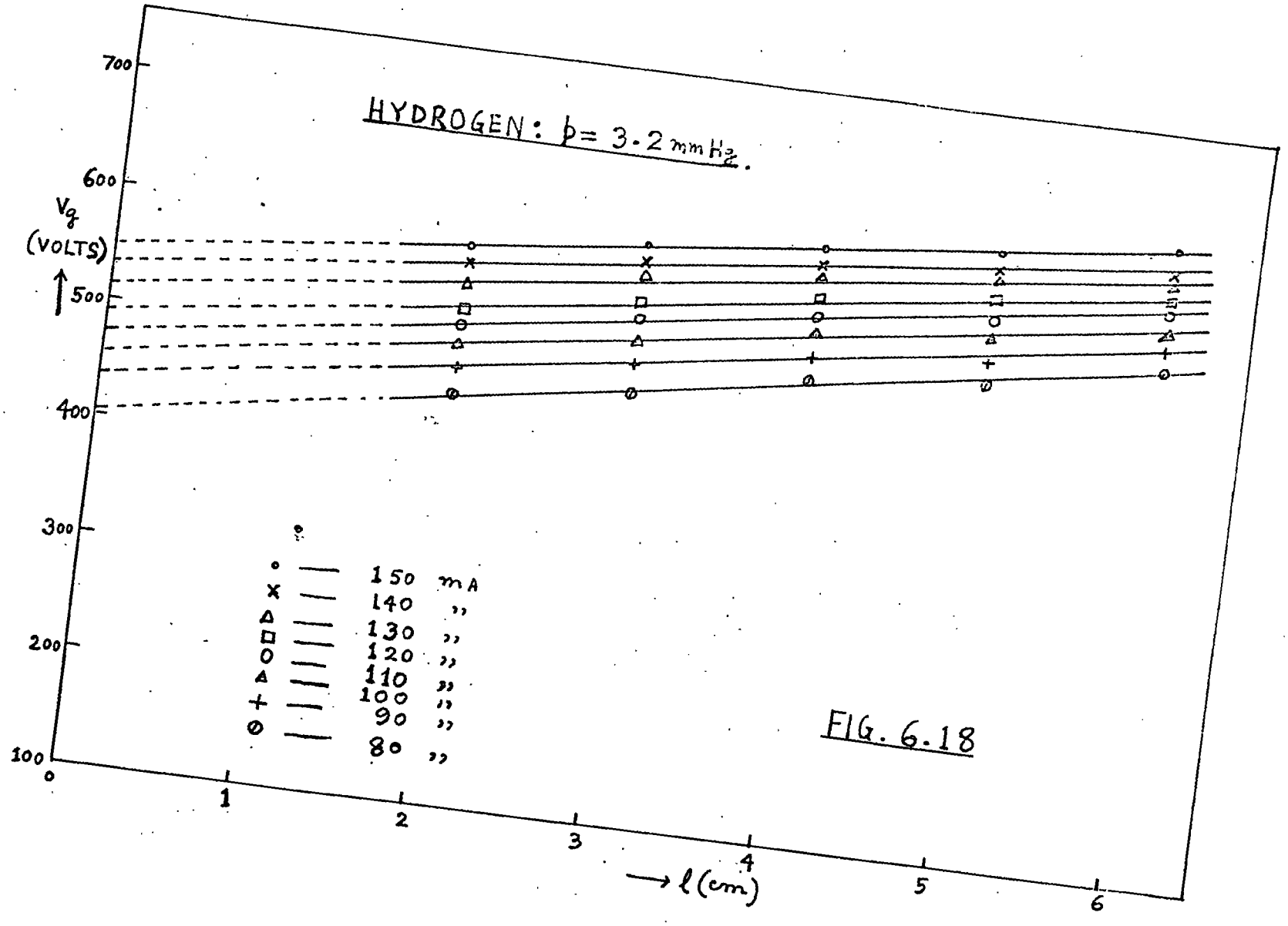
HYDROGEN: $p = 3.2$ mm H_g.
V_g (VOLTS)
700
600
500
400
300
200
100
0
1
2
3
4
5
6
$\rightarrow l$ (cm)
150 mA
140 ,,
130 ,,
120 ,,
110 ,,
100 ,,
90 ,,
80 ,,

FIG. 6.18

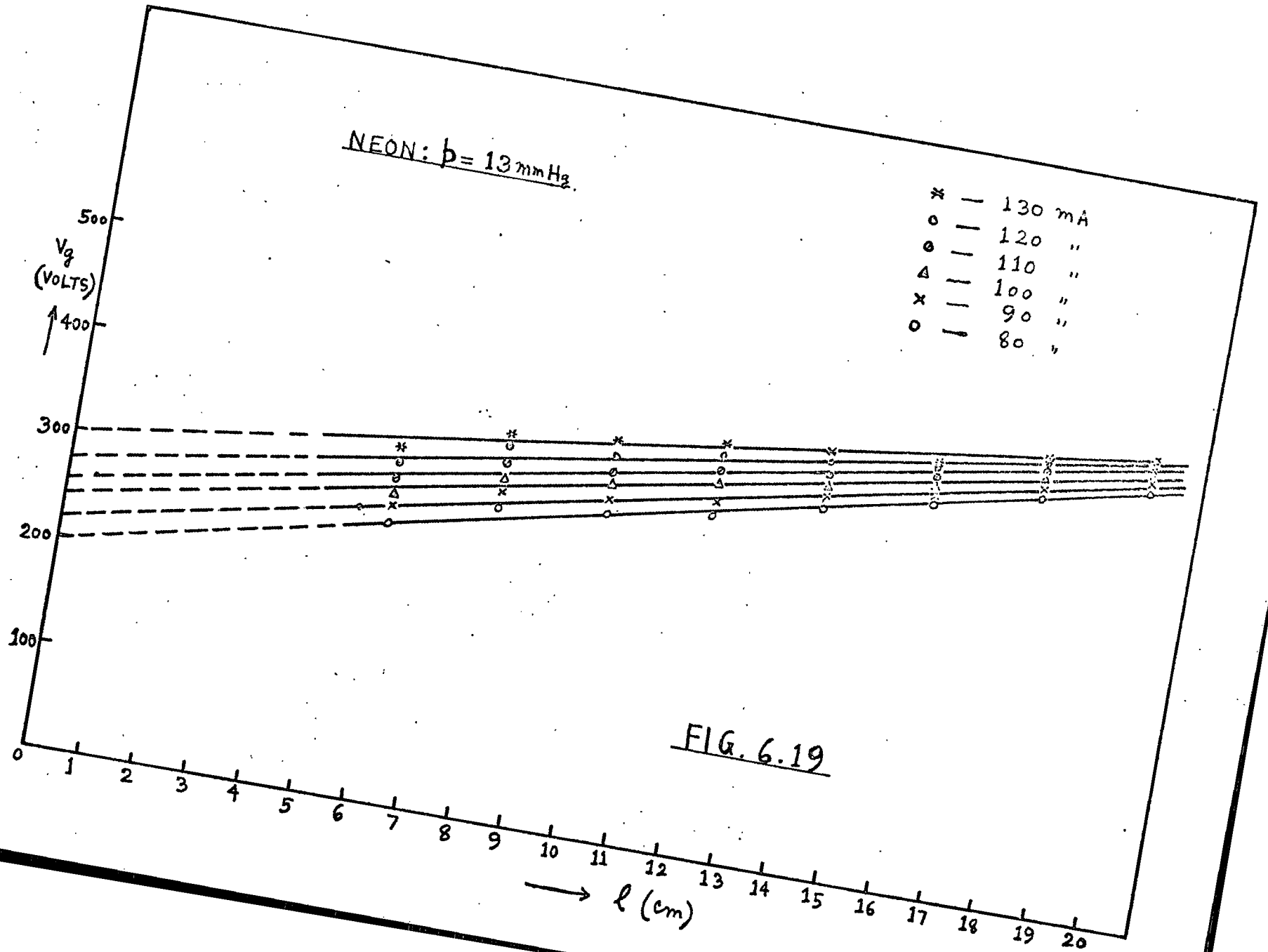
NEON: $p = 13$ mm Hg.
* — 130 mA
o — 120 "
⊙ — 110 "
Δ — 100 "
× — 90 "
o — 80 "
V_g (VOLTS)
500
400
300
200
100
0
1
2
3
4
5
6
7
8
9
10
11
12
13
14
15
16
17
18
19
20
ℓ (cm)

FIG. 6.19

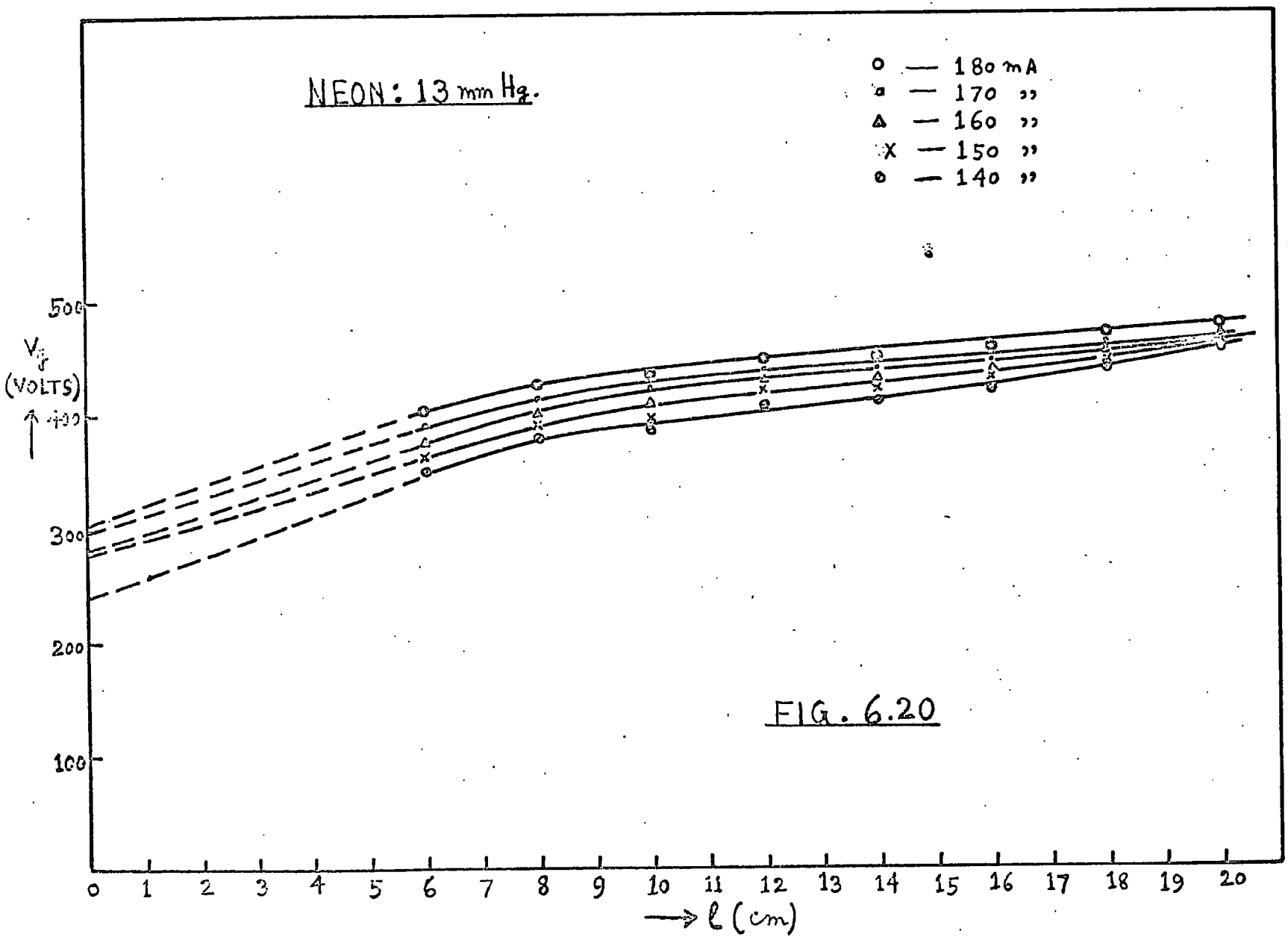
NEON: 13 mm Hg.
o — 180 mA
□ — 170 ,,
Δ — 160 ,,
X — 150 ,,
o — 140 ,,
500
V_s (VOLTS)
400
300
200
100
0 1 2 3 4 5 6 7 8 9 10 11 12 13 14 15 16 17 18 19 20
→ ℓ (cm)

FIG. 6.20

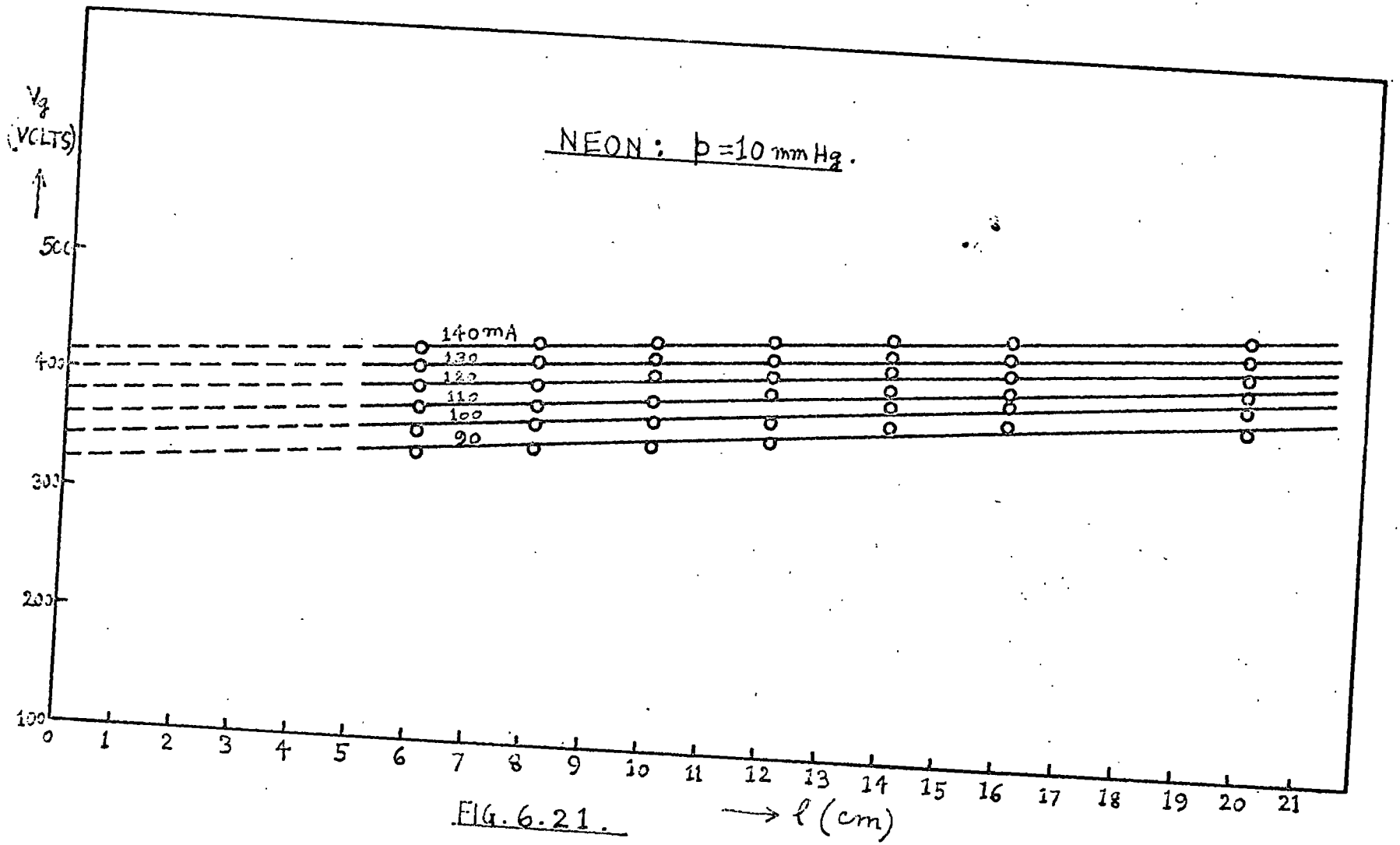
NEON : p = 10 mm Hg.
V_g (VOLTS)
500
400
300
200
100
140 mA
130
120
110
100
90
0 1 2 3 4 5 6 7 8 9 10 11 12 13 14 15 16 17 18 19 20 21
→ ℓ (cm)

FIG. 6.21.

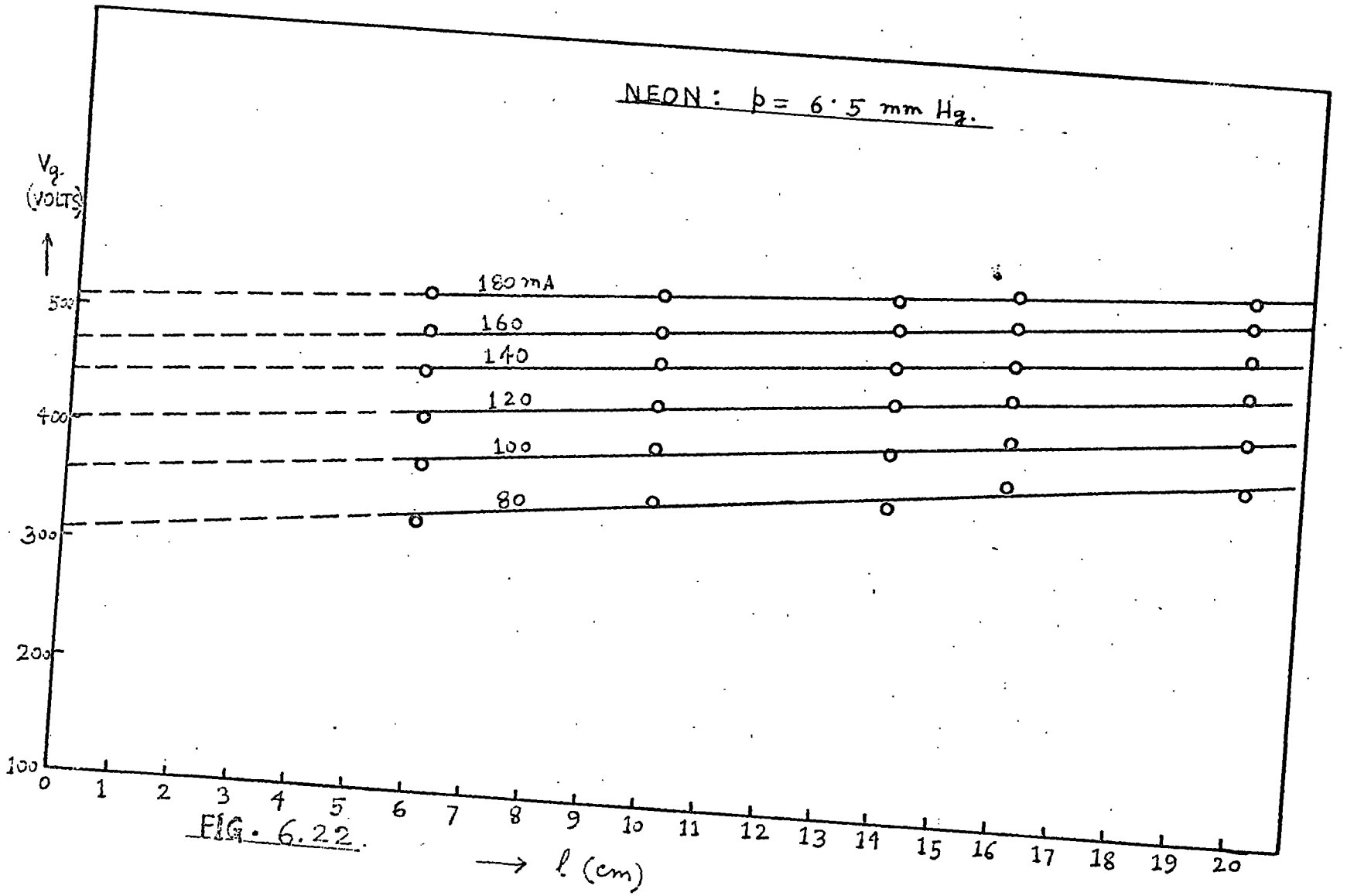
NEON : p = 6·5 mm Hg.
V_g (VOLTS)
180 mA
160
140
120
100
80
500
400
300
200
100
0 1 2 3 4 5 6 7 8 9 10 11 12 13 14 15 16 17 18 19 20
l (cm)

FIG. 6.22.

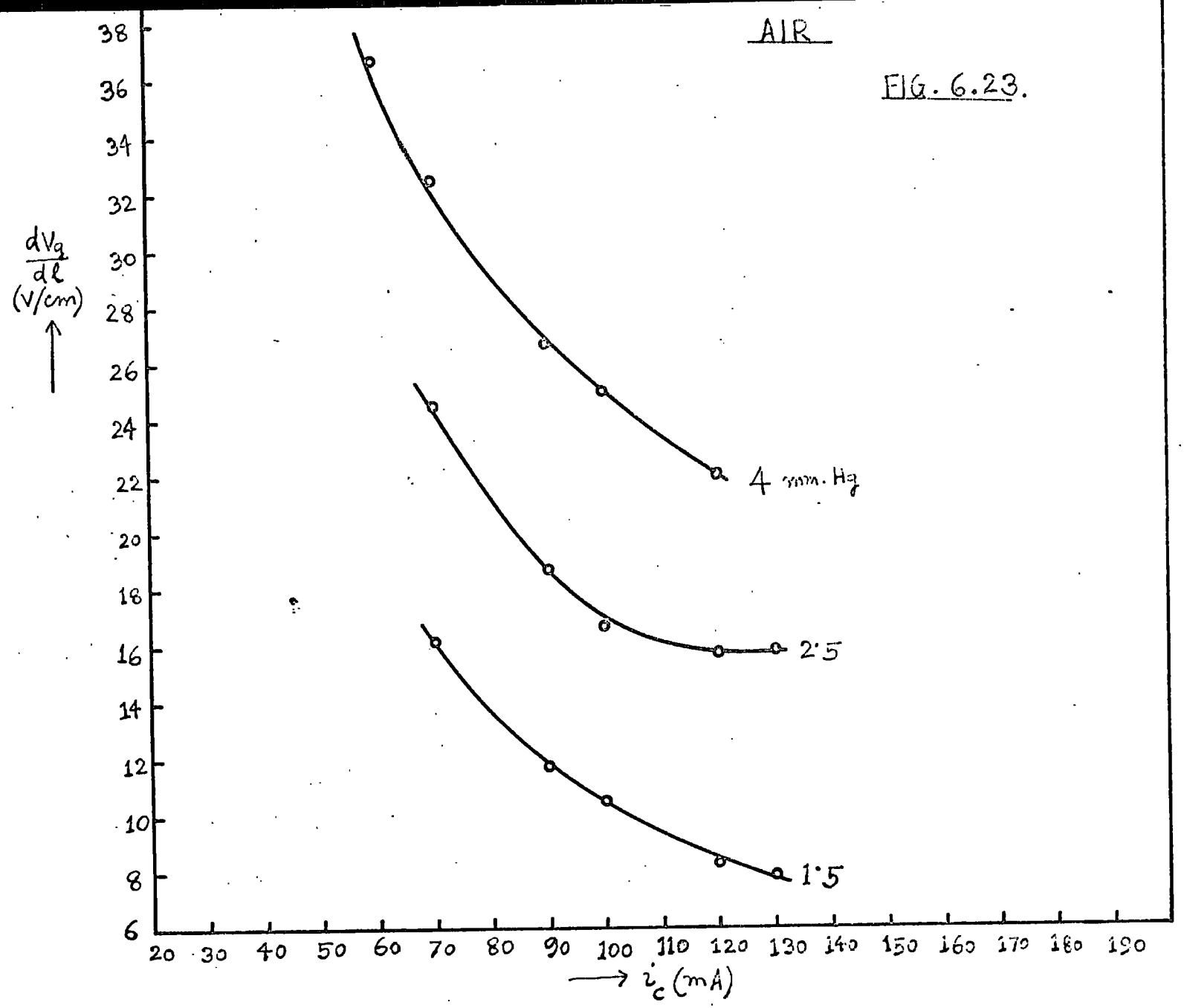
AIR
FIG. 6.23.
$\frac{dV_g}{dl}$ (V/cm)
38
36
34
32
30
28
26
24
22
20
18
16
14
12
10
8
6
4 mm. Hg
2·5
1·5
20 30 40 50 60 70 80 90 100 110 120 130 140 150 160 170 180 190
i_c (mA)

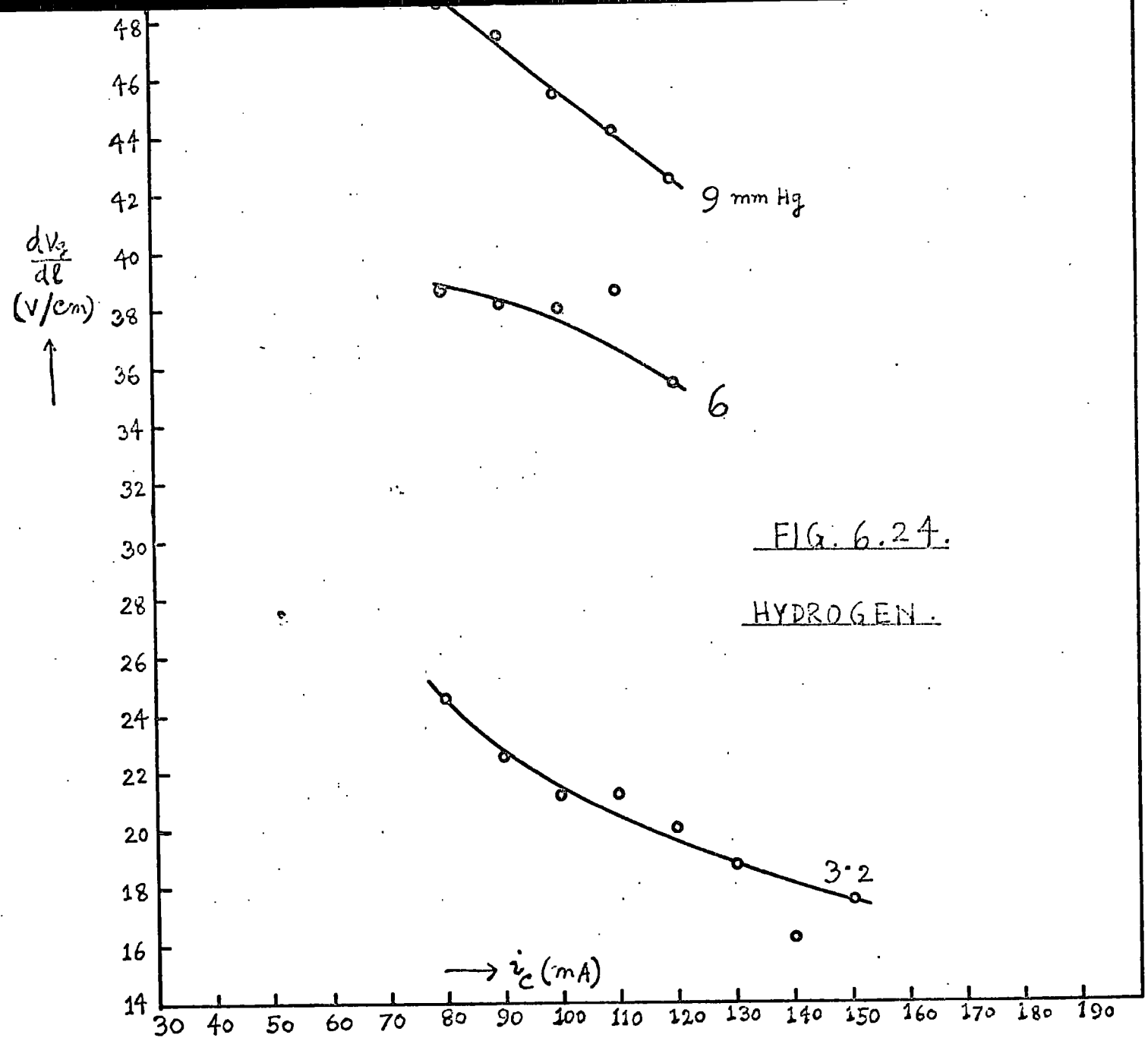

FIG. 6.24.

HYDROGEN.

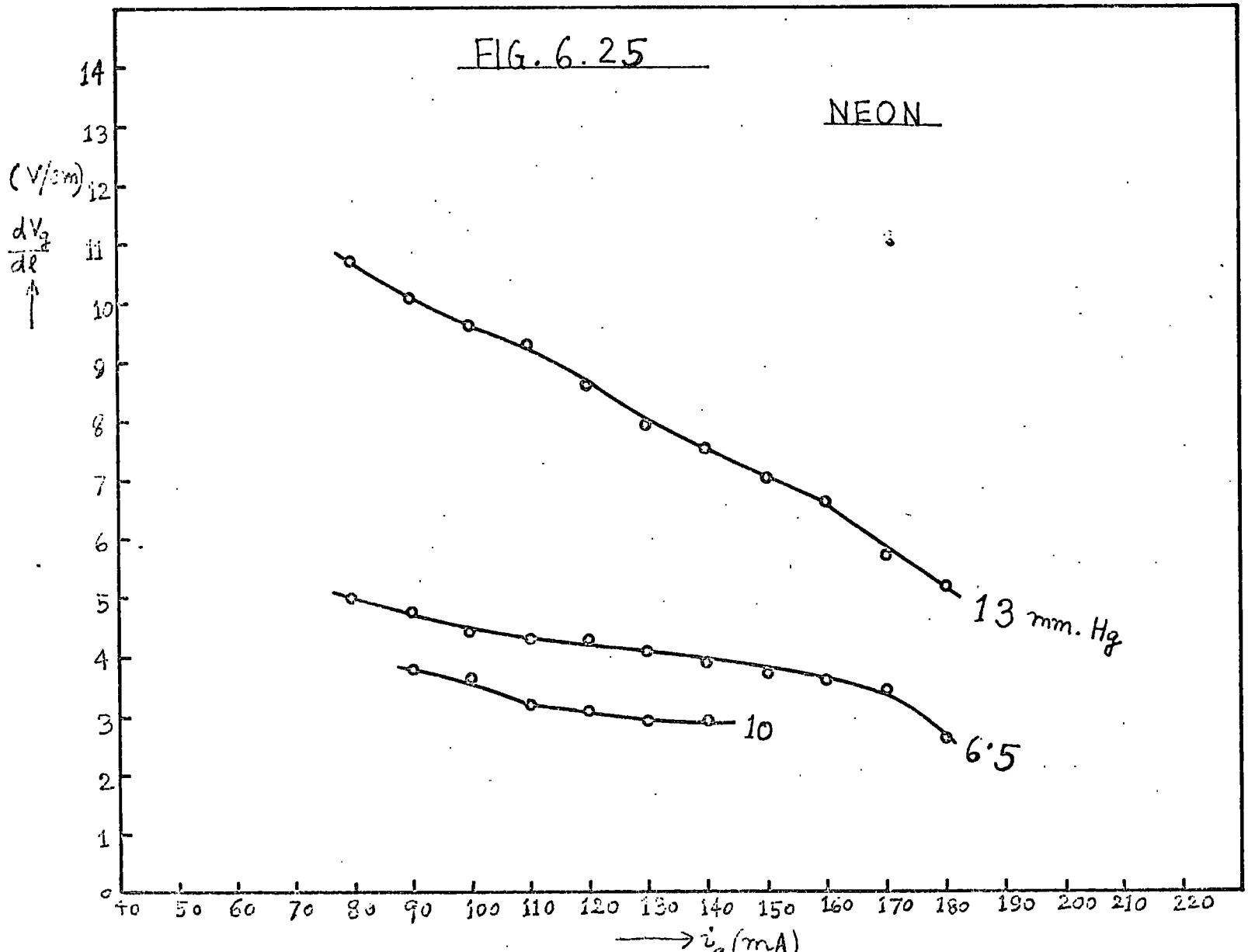
FIG. 6.25
NEON
(V/cm)
$\frac{dV_g}{dl}$
14
13
12
11
10
9
8
7
6
5
4
3
2
1
0
13 mm. Hg
10
6·5
40 50 60 70 80 90 100 110 120 130 140 150 160 170 180 190 200 210 220
i_a (mA)

characteristic is nearly parallel to the current axis (Figs.(6.4)and(6.7)).

From these curves, one can obtain V_g vs ℓ for various gap currents to examine the longitudinal gradients in the gap. This has been done and the results are shown in Figs. (6.13 - 6.22). It is evident that ---

(iii) the gradient is a constant in all cases for a given current. This is in good agreement with our hypothesis as laid down in section 1.2, namely that when $\ell >> r$, one length is like any other length and in discharges where electron temperatures are the same, one should expect a constant potential gradient at a given gap current. Also, there is a very considerable voltage drop at the ends (i.e. when $\ell = 0$); this will be further discussed in Chapter X.

(iv) There is yet another fact common in all the current-voltage characteristics, i.e. that the point representing the maximum current in each curve shifts to the left for higher gap separations. This represents a situation that the oscillator stopped oscillating when the power absorbed by the circuit was excessive. For a given output power, the greater is the gap separation, the less would be the current available since, to maintain

the sustained discharge in a longer gap, higher voltage is necessary.

(v) From the V_g - ℓ curves for different currents (Figs.(6.13 - 6.22)) one can plot field vs current. Such plots (Figs.(6.23-5)) show that the field diminishes with increase in gap current.

(vi) A comparison of the voltage gradients in different gases (Figs.(6.23-5)) shows that the maintaining fields, $E_{gAir} > E_{gH_2} > E_{gNe}$, for the same current and pA; consequently, the maintaining voltages for a given gap length of the same tube have also the same relation, namely, $V_{gAir} > V_{gH_2} > V_{gNe}$.

6.6 Observations with Tubes of Different Diameters.

The results given in section 6.4 relate to a tube of internal diameter 1.64 cm. Observations were also carried out in tubes of four other internal diameters, namely, .525, .93, 1.28 and 1.455 cm. In order to avoid too much of repetition of similar results, only a few, out of many taken, are shown in Tables 6.2 - 6.5 on the following pages. Inferences (i) to (vi) of the last section are found to be true in these experiments also.

TABLE - 6.2. Internal diameter of tube = .525 cm.

gas and gas pressure p	ℓ = 7			5			3 cms.		
	V_o volts	i_c mA	V_g volts	V_o volts	i_c mA	V_g volts	V_o volts	i_c mA	V_g volts
air	515	33	496	400	33	375	455	50	403
	600	50	561	515	50	469	560	68	480
	635	57	587	620	73	537	610	80	507
p = 1.5	650	60	598	680	85	576	640	87	522
mm. Hg	670	68	605	720	98	588	720	95	596
	720	78	640	755	107	603	750	120	550
	755	87	658	765	113	596	795	135	551
	780	93	673	795	120	610	805	139	548
	795	98	678	805	123	612	820	144	546
	810	102	685	-	-	-	820	147	532
	ℓ = 5			3			2 cms.		
hydrogen	715	46	688	415	33	391	430	46	383
	780	60	737	525	46	487	520	76	408
	800	76	732	585	68	509	570	98	390
p = 7	800	91	700	605	85	486	620	124	327
mm. Hg	805	98	689	635	104	456	640	134	293
	805	89	711	655	117	427	665	146	240
	-	-	-	675	128	400	680	155	172
	-	-	-	690	134	390	680	154	186
	-	-	-	695	138	374	-	-	-
	-	-	-	695	139	367	-	-	-
	ℓ = 5			3			2 cms.		
Neon	240	57	141	250	50	133	255	46	164
	310	65	147	390	73	237	445	80	287
	355	76	172	460	85	285	510	91	332
p = 7.8	400	85	220	570	109	332	600	110	377
mm. Hg	445	91	244	635	123	360	675	128	400
	505	104	287	735	146	395	735	142	420
	585	120	293	765	158	367	780	154	425
	640	134	297	800	169	353	790	158	417
	665	140	301	-	-	-	800	160	421
	720	154	306	-	-	-	-	-	-
	765	165	299	-	-	-	-	-	-
	785	171	258	-	-	-	-	-	-
	795	177	246	-	-	-	-	-	-

TABLE - 6.3: Internal diameter of tube = .93 cm.

gas and gas pressure p	ℓ = 7			5			3 cms.		
	V_o volts	i_c mA	V_g volts	V_o volts	i_c mA	V_g volts	V_o volts	i_c mA	V_g volts
air	685	50	668	525	50	503	410	50	381
	755	76	719	630	73	590	555	76	505
	780	89	732	685	87	633	620	93	553
p = 3.5	800	96	746	715	100	648	675	113	582
mm. Hg	820	107	753	750	117	661	725	130	609
	830	110	760	780	125	682	760	143	625
	825	105	761	800	134	690	780	153	628
	-	-	-	815	138	700	815	165	644
	-	-	-	825	142	704	840	177	648
	-	-	-	-	-	-	845	179	649
	-	-	-	-	-	-	865	183	664
	ℓ = 5			3			2 cms.		
hydrogen	715	46	701	500	57	469	395	46	370
	805	71	776	585	85	526	525	85	458
p = 9.5	820	91	773	635	112	537	530	98	440
mm. Hg	820	95	768	675	135	538	615	128	478
	820	85	779	690	143	537	630	153	427
	-	-	-	705	146	549	655	165	424
	-	-	-	-	-	-	670	170	430
	-	-	-	-	-	-	675	173	427
	-	-	-	-	-	-	675	169	441
	ℓ = 7			5			3 cms.		
Neon	300	60	239	275	60	206	260	65	170
	370	80	280	405	93	292	410	110	239
	425	93	319	505	131	313	495	139	262
p = 12	505	120	351	570	151	341	605	179	271
mm. Hg	600	151	389	640	179	342	660	198	277
	665	179	387	710	205	346	715	218	277
	705	197	377	745	218	347	760	237	252
	730	205	385	745	221	328	-	-	-

TABLE - 6.4: Internal diameter of tube = 1.28 cm.

gas and gas pressure p	ℓ = 5			3			2 cms.		
	V_o volts	i_c mA	V_g volts	V_o volts	i_c mA	V_g volts	V_o volts	i_c mA	V_g volts
air	600	42	591	450	38	440	370	42	355
	665	53	651	510	46	496	400	46	383
	720	63	702	565	57	546	465	53	445
p = 3	745	68	725	655	71	630	520	65	493
mm. Hg	775	76	751	700	80	670	620	78	588
	800	80	774	750	91	714	690	91	650
	805	85	776	800	100	759	750	104	702
	-	-	-	810	104	766	785	112	732
	-	-	-	-	-	-	830	120	772
	-	-	-	-	-	-	835	123	775
	ℓ = 5			3			2 cms.		
	820	50	810	575	46	563	470	38	460
hydrogen	865	60	852	670	65	649	575	60	555
83	880	65	864	720	80	691	610	76	579
p = 8	900	73	881	760	100	717	650	87	612
mm. Hg	905	78	883	805	117	749	710	109	654
	920	87	893	820	120	762	730	117	667
	-	-	-	830	124	768	770	130	696
	-	-	-	835	124	774	795	138	714
	-	-	-	-	-	-	820	146	732
	-	-	-	-	-	-	840	151	748
	-	-	-	-	-	-	850	153	756
	ℓ = 7			5			3 cms.		
	450	73	410	445	76	401	450	82	399
Neon	525	89	474	530	95	472	535	102	469
	580	100	522	610	110	543	630	121	551
p = 8	655	117	584	660	121	585	665	130	578
mm. Hg	685	121	613	735	139	645	715	142	618
	740	131	661	770	146	675	750	146	652
	805	146	715	825	158	722	810	163	697
	835	154	738	855	166	745	840	171	720
	850	158	750	-	-	-	850	172	730
	-	-	-	-	-	-	865	177	740
	-	-	-	-	-	-	880	180	753

TABLE - 6.5: Internal diameter of tube = 1.455 cm.

gas and gas pressure p	ℓ = 7			5			3 cms.		
	V_o volts	i_c mA	V_g volts	V_o volts	i_c mA	V_g volts	V_o volts	i_c mA	V_g volts
air	565	33	562	430	27	427	360	38	354
	615	46	609	525	50	517	435	53	425
	675	65	665	580	63	569	505	68	490
p = 3	710	76	697	645	82	628	565	82	546
mm. Hg	735	85	719	710	98	688	620	95	596
	755	93	736	745	110	718	715	121	681
	770	96	750	765	120	734	775	143	731
	800	102	779	780	124	747	800	153	751
	-	-	-	790	127	756	810	158	759
	-	-	-	-	-	-	815	159	763
	ℓ = 5			3			2 cms.		
	665	42	661	420	42	413	435	63	420
hydrogen	680	46	675	475	53	465	510	87	486
	700	53	694	545	68	531	555	115	515
p = 6.8	710	46	705	625	110	593	595	144	536
mm. Hg	715	63	706	630	123	590	615	151	552
	730	71	719	635	125	594	620	156	553
	730	60	722	630	117	594	620	153	556
	-	-	-	630	110	598	620	146	562
	-	-	-	630	107	600	615	138	563
	-	-	-	610	93	587	-	-	-
	ℓ = 7			5			3 cms.		
	380	117	317	395	124	326	430	146	341
Neon	400	134	319	405	128	333	450	155	353
	435	139	356	430	136	354	470	162	369
p = 9	445	146	360	450	146	366	480	166	376
mm. Hg	475	156	384	470	155	378	490	172	380
	500	163	405	490	162	394	510	174	403
	-	-	-	510	165	415	520	177	412
	-	-	-	510	167	412	520	179	408

CHAPTER - VII

OBSERVATIONS ON THE CURRENT-VOLTAGE RELATIONS IN THE FLAT CAVITIES IN THE ELECTRODELESS CASE.

7.1 Introduction.

As in the case of long cylindrical tubes, observations were taken on the current-voltage relations in flat cavities, i.e. in systems of which the width was much smaller than the diameter. The external electrodes used in this case were a pair of thin copper discs with a short copper wire soldered to their centre at right angles to the surface for electrical connection. They were mounted as shown in Fig. 4.6. As in the long cylindrical system, the experimental gases were air, hydrogen and neon.

7.2 Determination of the Capacitance of the Cavity in relation to Electrodes of Different Areas.

The circuit employed for determining the capacitance of the cavity was the same as shown in Fig(6.1), using the same procedure as before, namely, obtaining the two sharp tuning positions of the fine condenser C_4 when the cavity was empty and when it was filled up with Hg. The difference of the two readings gives the cavity

capacitance. The values thus found for various electrode areas are shown in Table 7.1 below.

TABLE - 7.1: Capacitances of external disc electrodes.

Area of the electrode (cm^2)	Capacitance ($\mu\mu f$)
1.19	0.99
2.77	1.35
7.64	5.42
18.39	12.77

7.3 Correction for the Voltage Drop in the Cavity.

As in the case of long cylindrical tubes, the observed voltage V_o was corrected for the gap voltage V_g by assuming phase quadrature between $i_c/\omega C$ and V_g, i.e. by assuming Eq.(6.1).

The displacement current was reduced to a negligible amount in comparison to the conduction current by adjustment of the connecting leads to the cavity as well as of C_1 and C_2 Fig.(4.22).

7.4 Experimental Results.

(a) Observations in air.

Results in air are graphically shown in Figs.(7.1 - 7.3) at pressures of 4.5, 2.8 and 1 mm. Hg. respectively, for a few electrode areas.

(b) Observations in hydrogen.

Similarly in Fig.(7.4) are given values of V_g vs i_c at 5 mm. Hg. for the same electrode areas.

(c) Observations in neon.

Results of similar observations in neon are represented graphically in Figs.(7.5 and 7.6), at 5 and 4 mm. Hg. respectively.

7.5 Discussion of Results.

From a study of the curves it is evident that ---

(i) the current-voltage characteristics are positive and nearly linear with a tendency of flattening out at higher currents. It may be recalled that the same was found to be true in the case of long cylindrical tubes.

(ii) the rate of rise of voltage with current is much faster with lower electrode areas.

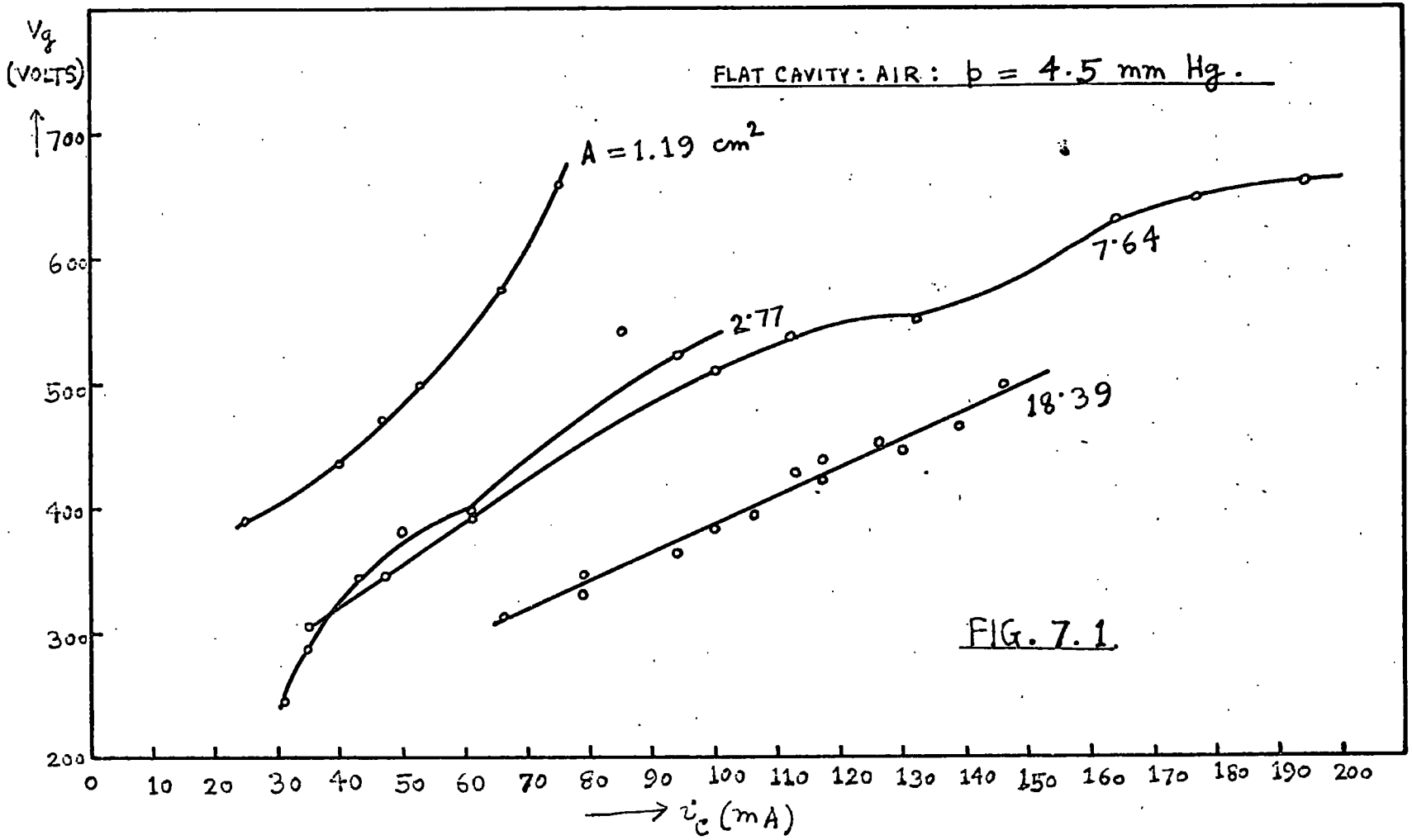
Vg
(VOLTS)
FLAT CAVITY : AIR : p = 4.5 mm Hg.
A = 1.19 cm²
7·64
2·77
18·39
700
600
500
400
300
200
0
10
20
30
40
50
60
70
80
90
100
110
120
130
140
150
160
170
180
190
200
ic (mA)

FIG. 7.1

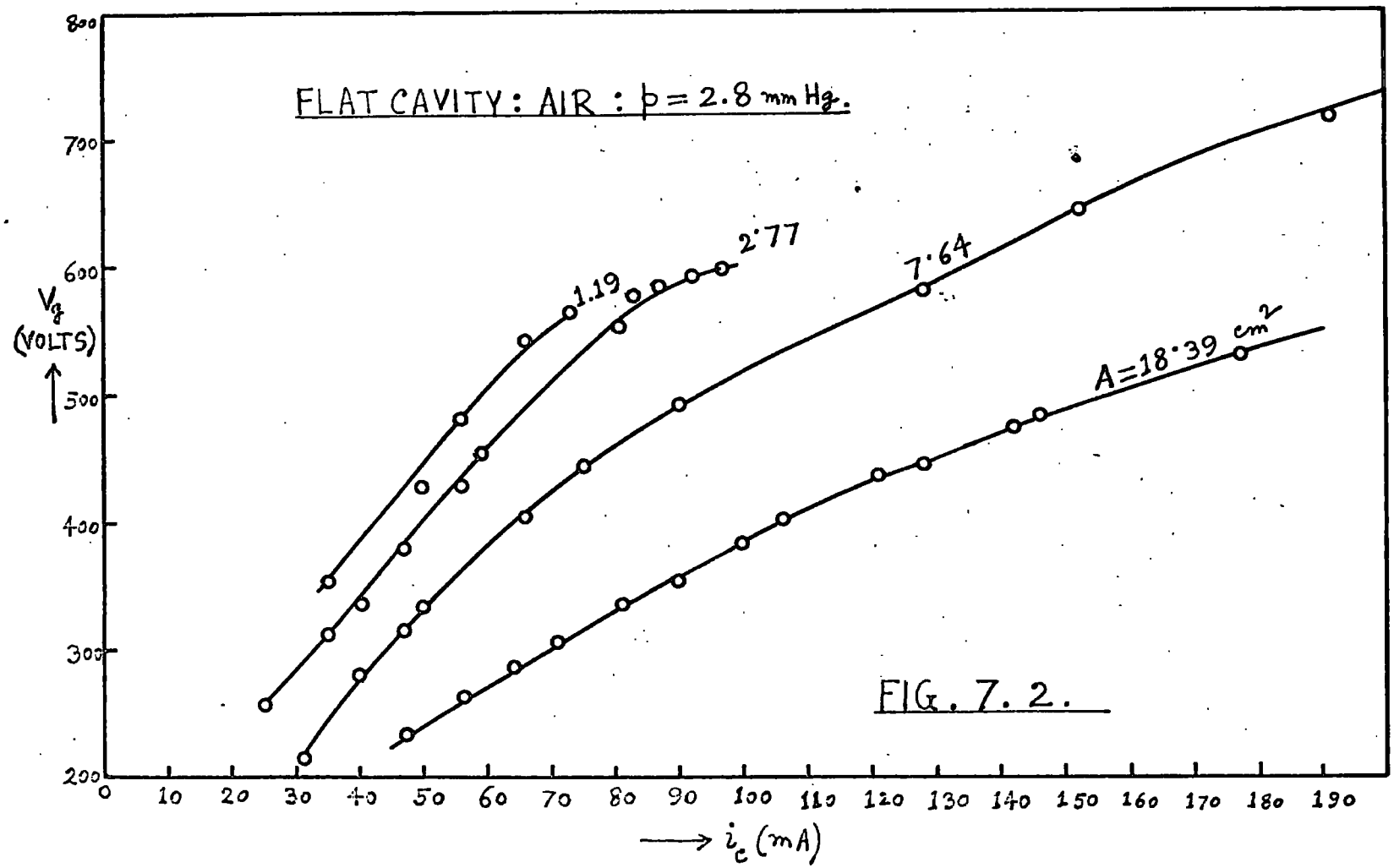
FLAT CAVITY : AIR : p = 2.8 mm Hg.
1.19
2·77
7·64
A=18·39 cm²
V_g (VOLTS)
i_c (mA)
800
700
600
500
400
300
200
0
10
20
30
40
50
60
70
80
90
100
110
120
130
140
150
160
170
180
190

FIG. 7. 2.

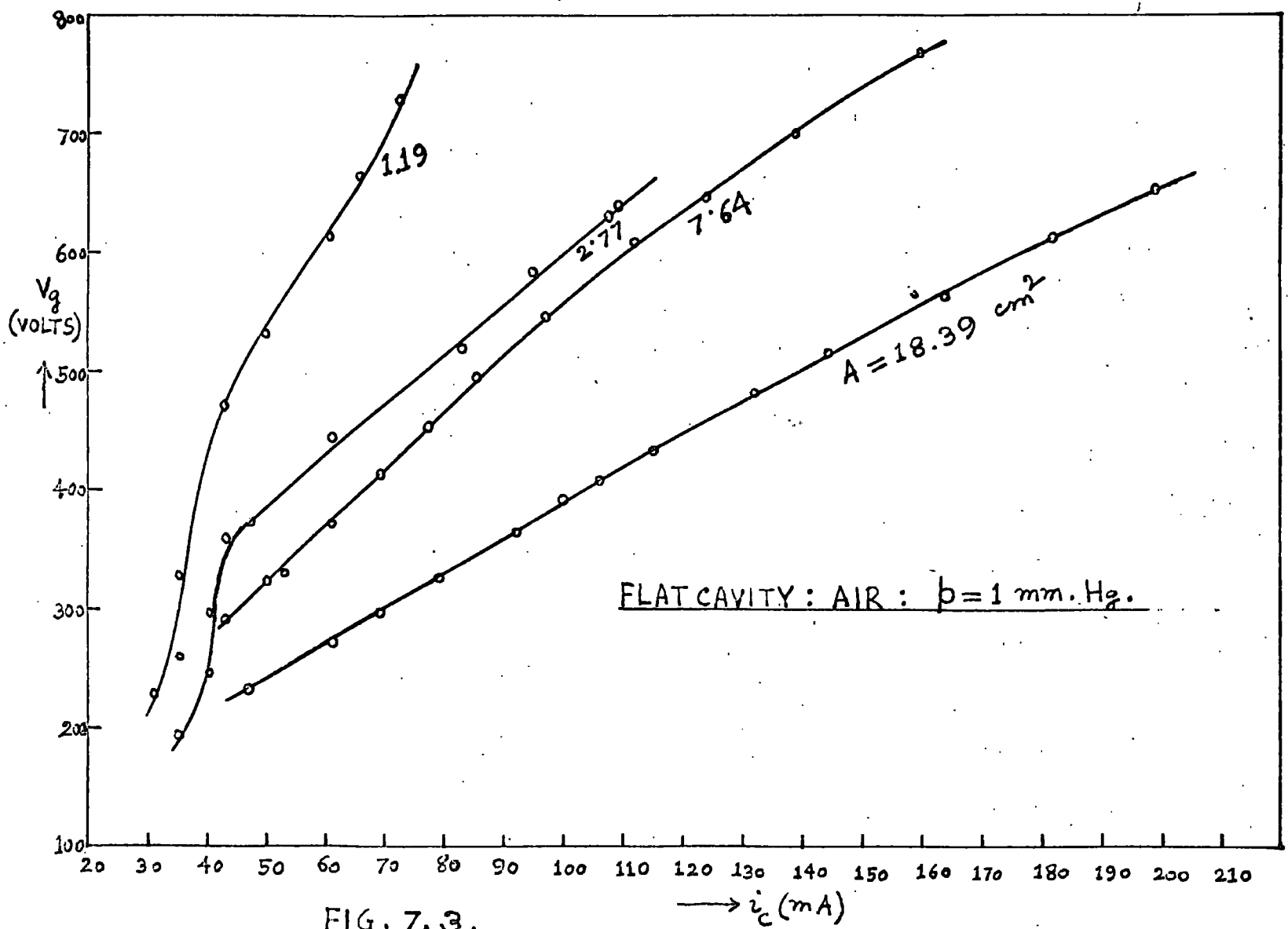
800
700
600
500
400
300
200
100
V_g (VOLTS)
1·19
2·77
7·64
A = 18.39 cm²
FLAT CAVITY : AIR : b = 1 mm. Hg.
20 30 40 50 60 70 80 90 100 110 120 130 140 150 160 170 180 190 200 210
i_c (mA)

FIG. 7.3.

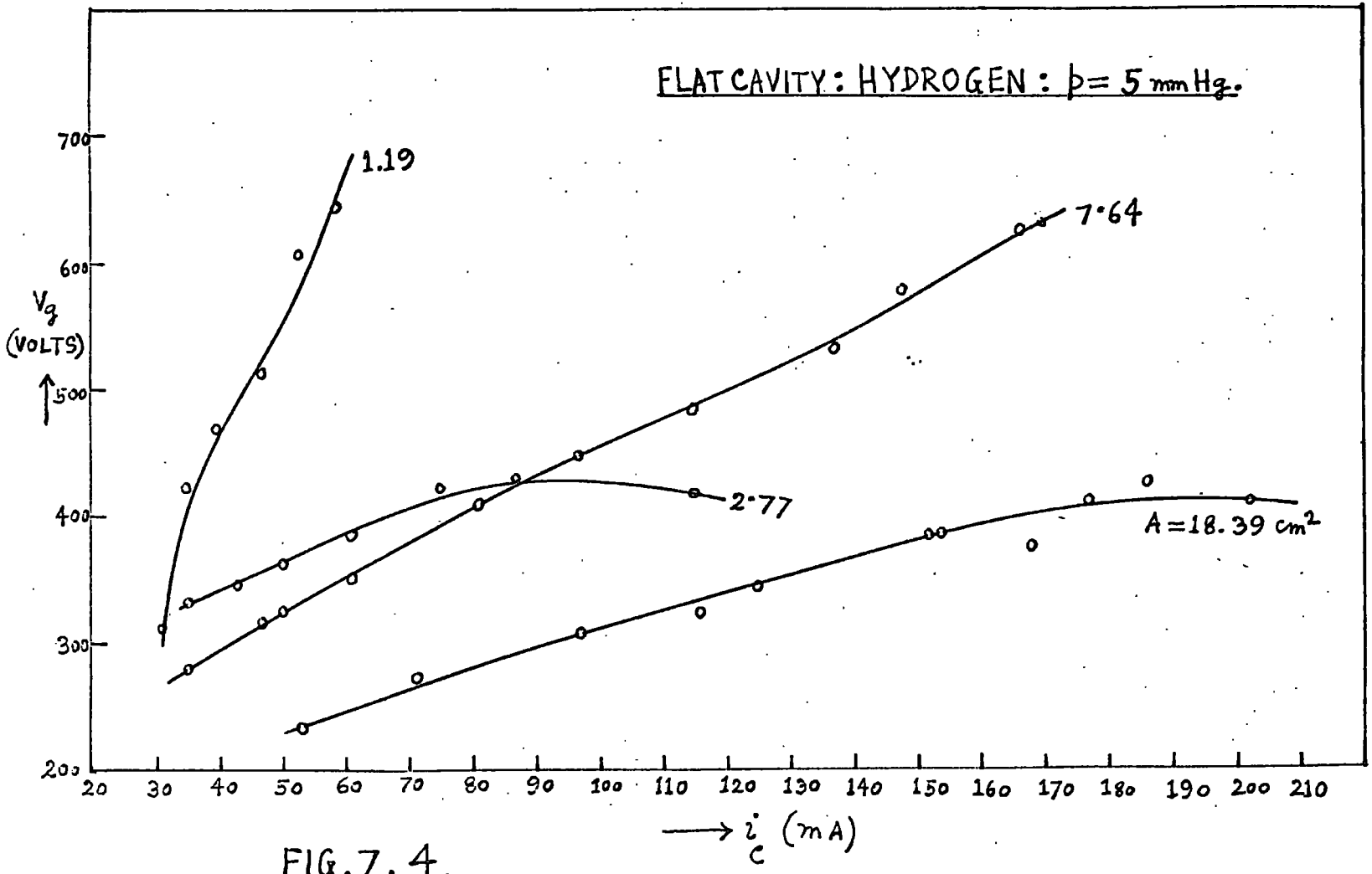
FLAT CAVITY : HYDROGEN : p = 5 mm Hg.
1.19
7·64
2·77
A = 18.39 cm²
V_g (VOLTS)
700
600
500
400
300
200
20 30 40 50 60 70 80 90 100 110 120 130 140 150 160 170 180 190 200 210
i_c (mA)

FIG. 7.4.

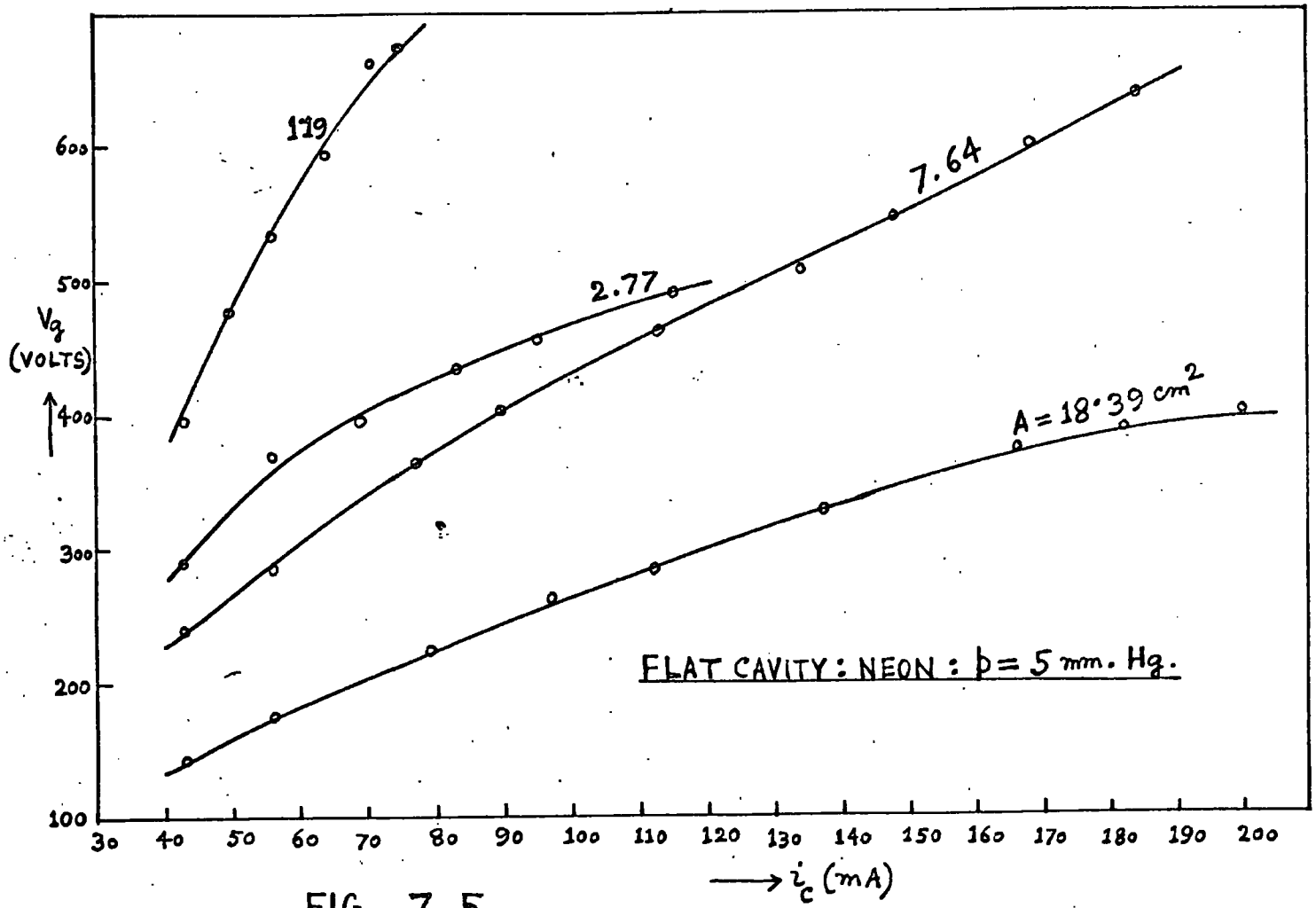
1.19
2.77
7.64
A = 18·39 cm²
FLAT CAVITY : NEON : p = 5 mm. Hg.
Vg (VOLTS)
ic (mA)
100
200
300
400
500
600
30
40
50
60
70
80
90
100
110
120
130
140
150
160
170
180
190
200

FIG. 7.5.

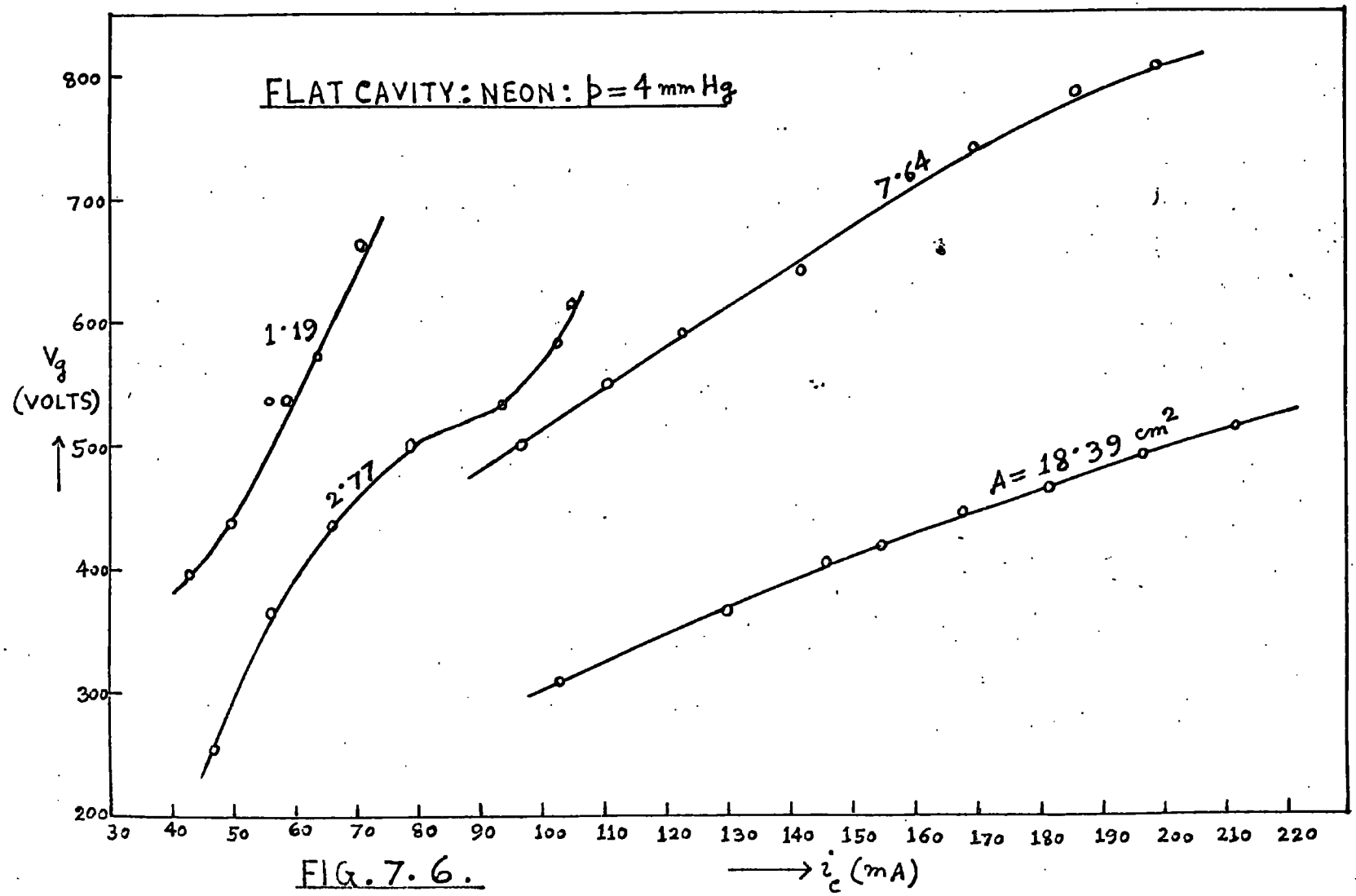
FLAT CAVITY: NEON: p = 4 mm Hg
800
700
600
500
400
300
200
V_g (VOLTS)
1·19
2·77
7·64
A = 18·39 cm²
30 40 50 60 70 80 90 100 110 120 130 140 150 160 170 180 190 200 210 220
i_c (mA)

FIG. 7.6.

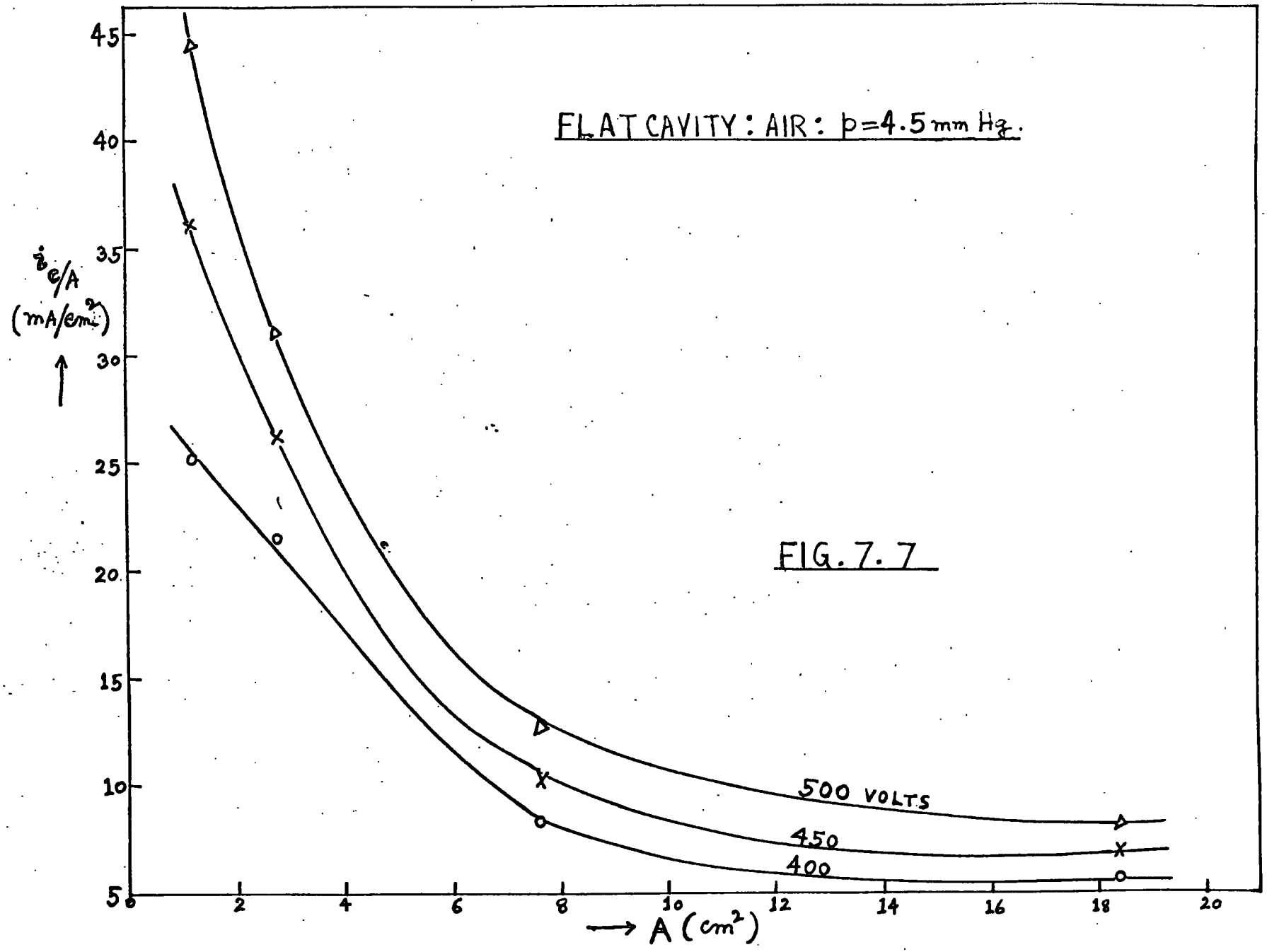
FLAT CAVITY : AIR : p=4.5 mm Hg.
$i_{e/A}$ (mA/cm²)
45
40
35
30
25
20
15
10
5
2
4
6
8
10
12
14
16
18
20
A (cm²)
500 VOLTS
450
400

FIG. 7.7

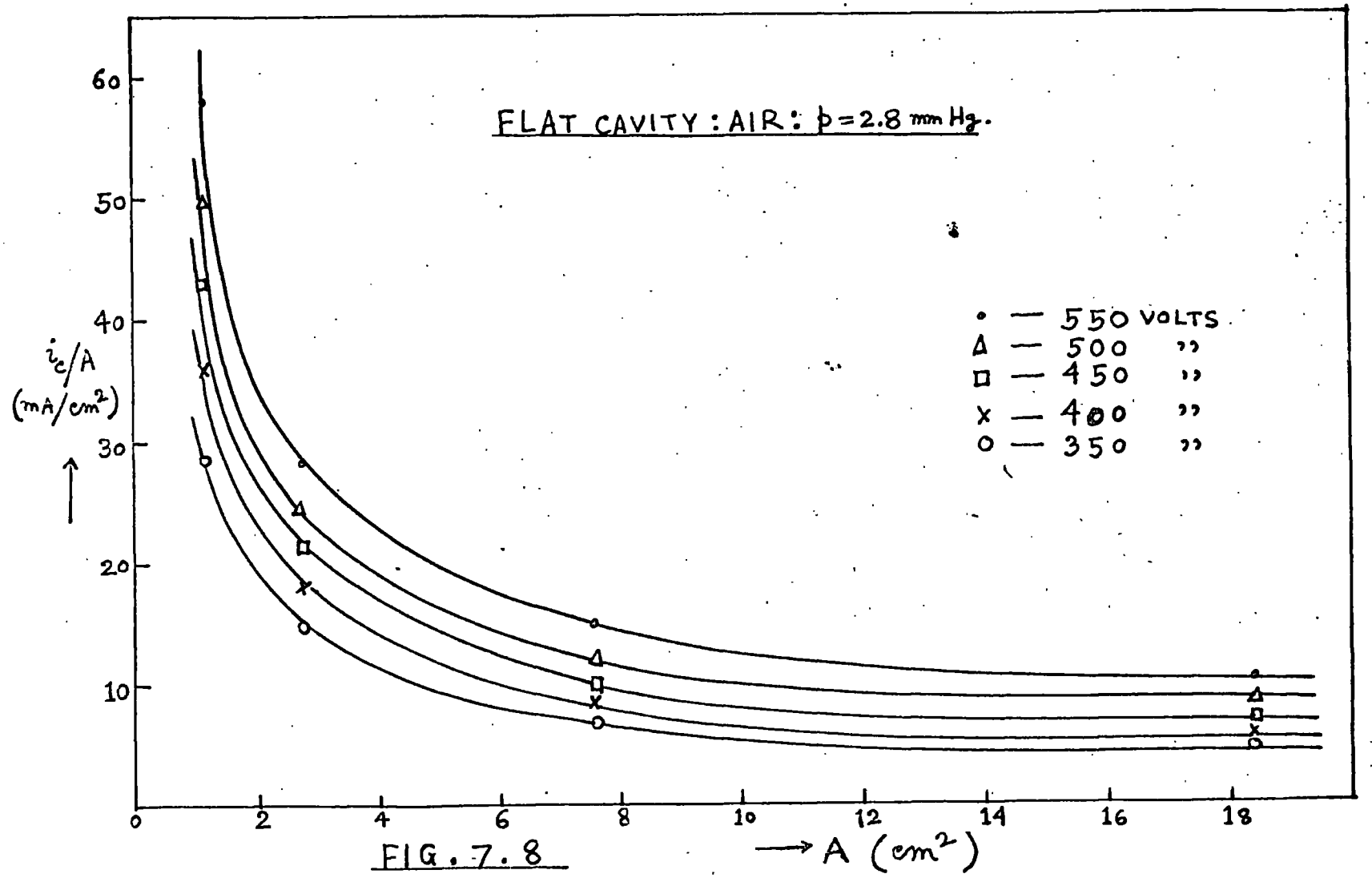
FLAT CAVITY : AIR : p = 2.8 mm Hg.
• — 550 VOLTS
Δ — 500 "
□ — 450 "
× — 400 "
○ — 350 "
i_c/A (mA/cm²)
60
50
40
30
20
10
0
2
4
6
8
10
12
14
16
18
A (cm²)

FIG. 7.8

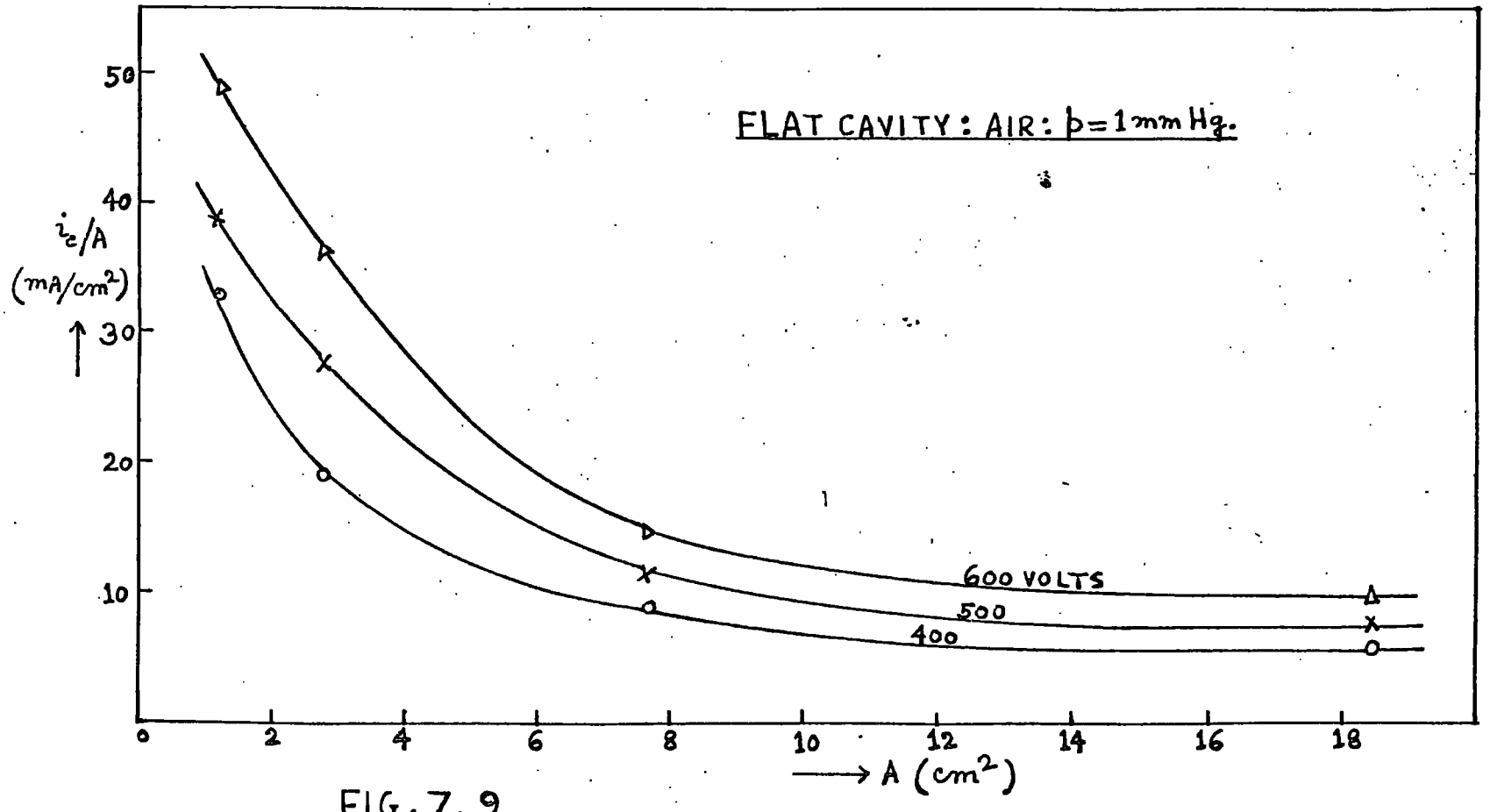
FLAT CAVITY : AIR : p = 1 mm Hg.
i_c/A
(mA/cm²)
50
40
30
20
10
0
2
4
6
8
10
12
14
16
18
600 VOLTS
500
400
A (cm²)

FIG. 7. 9.

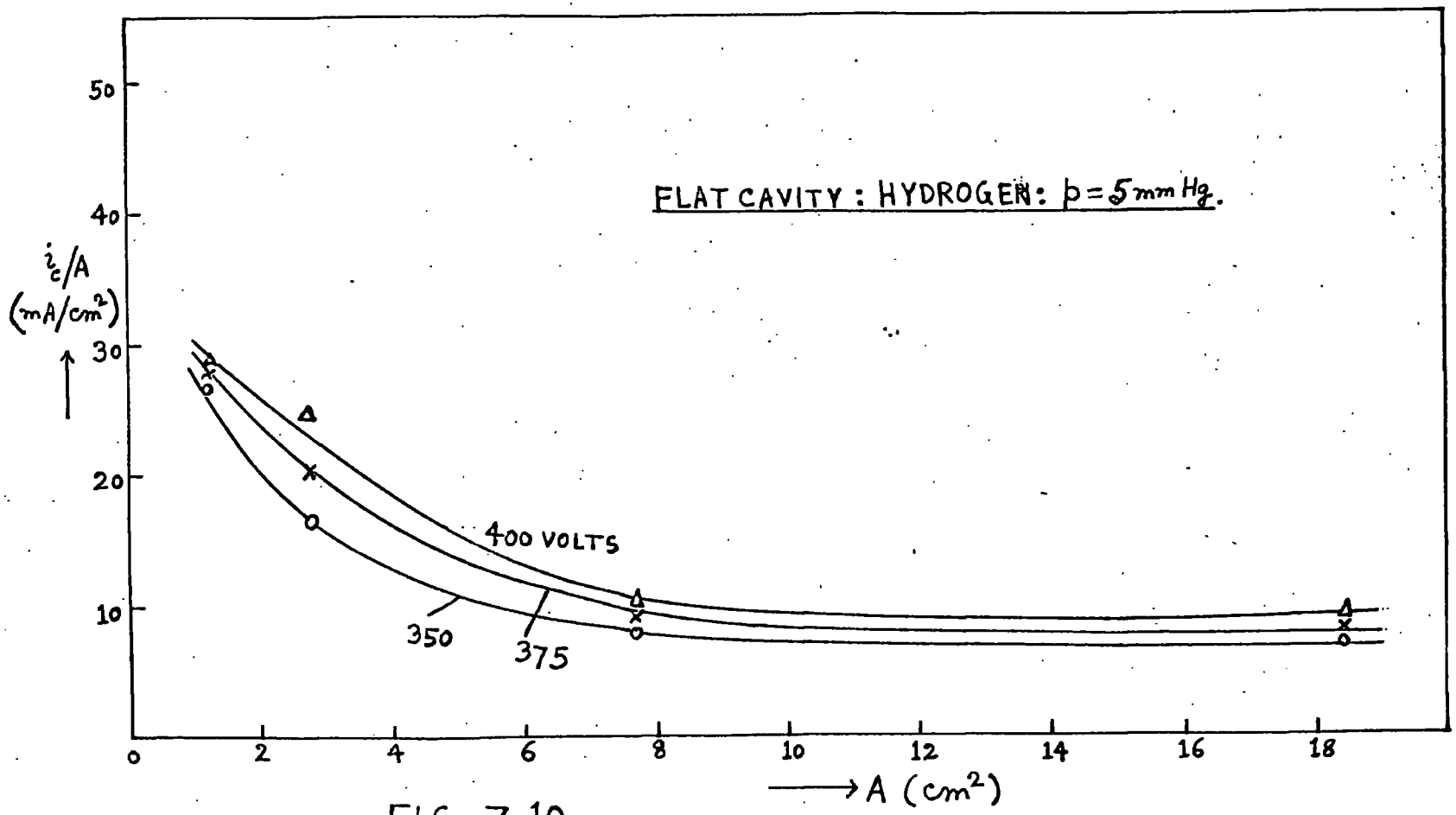
FLAT CAVITY : HYDROGEN: p = 5 mm Hg.
i_c/A (mA/cm²)
50
40
30
20
10
0
2
4
6
8
10
12
14
16
18
A (cm²)
400 VOLTS
350
375

FIG. 7.10

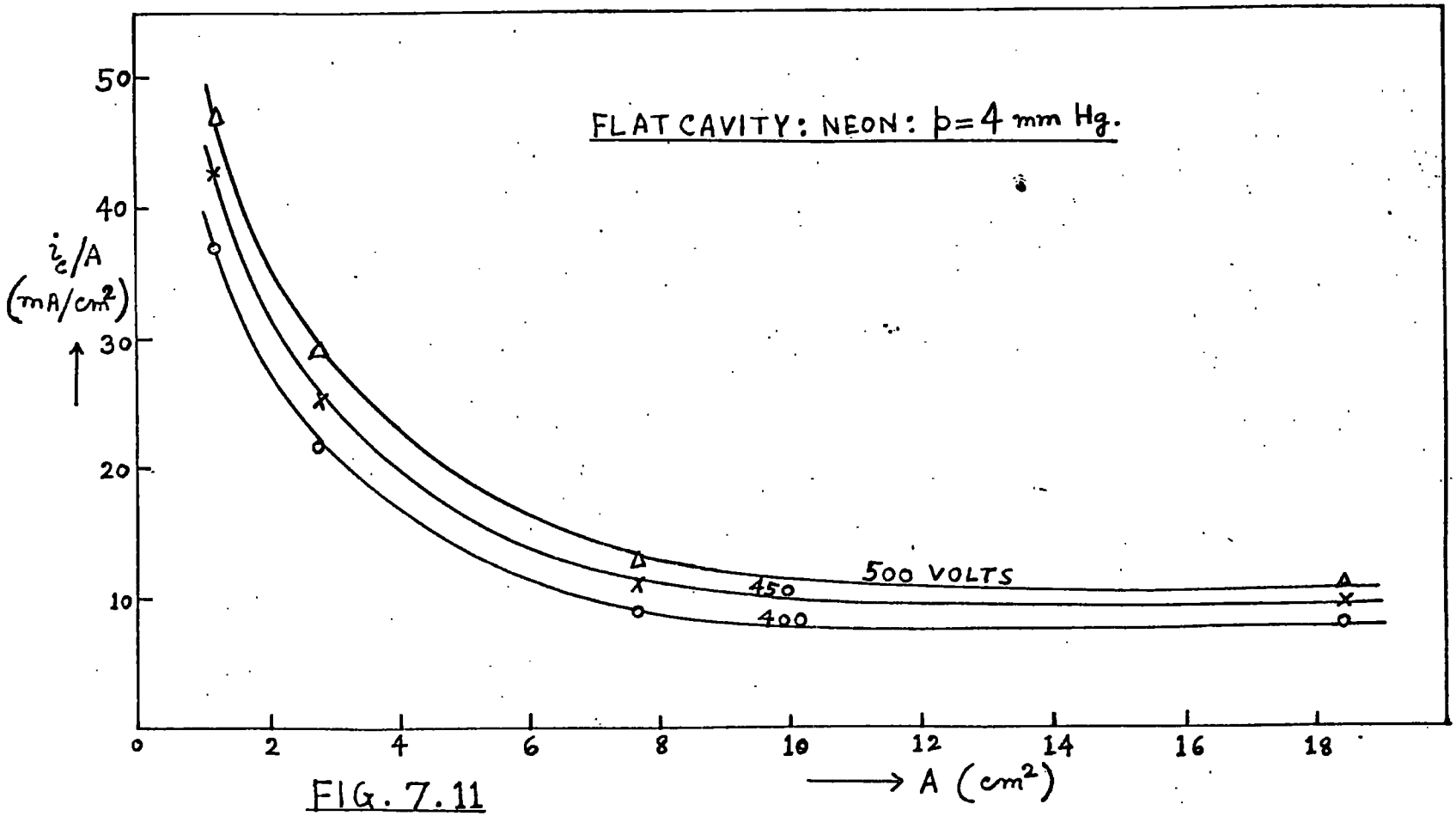
FLAT CAVITY: NEON: p=4 mm Hg.
50
40
30
20
10
i_c/A
(mA/cm^2)
500 VOLTS
450
400
0
2
4
6
8
10
12
14
16
18
A (cm^2)

FIG. 7.11

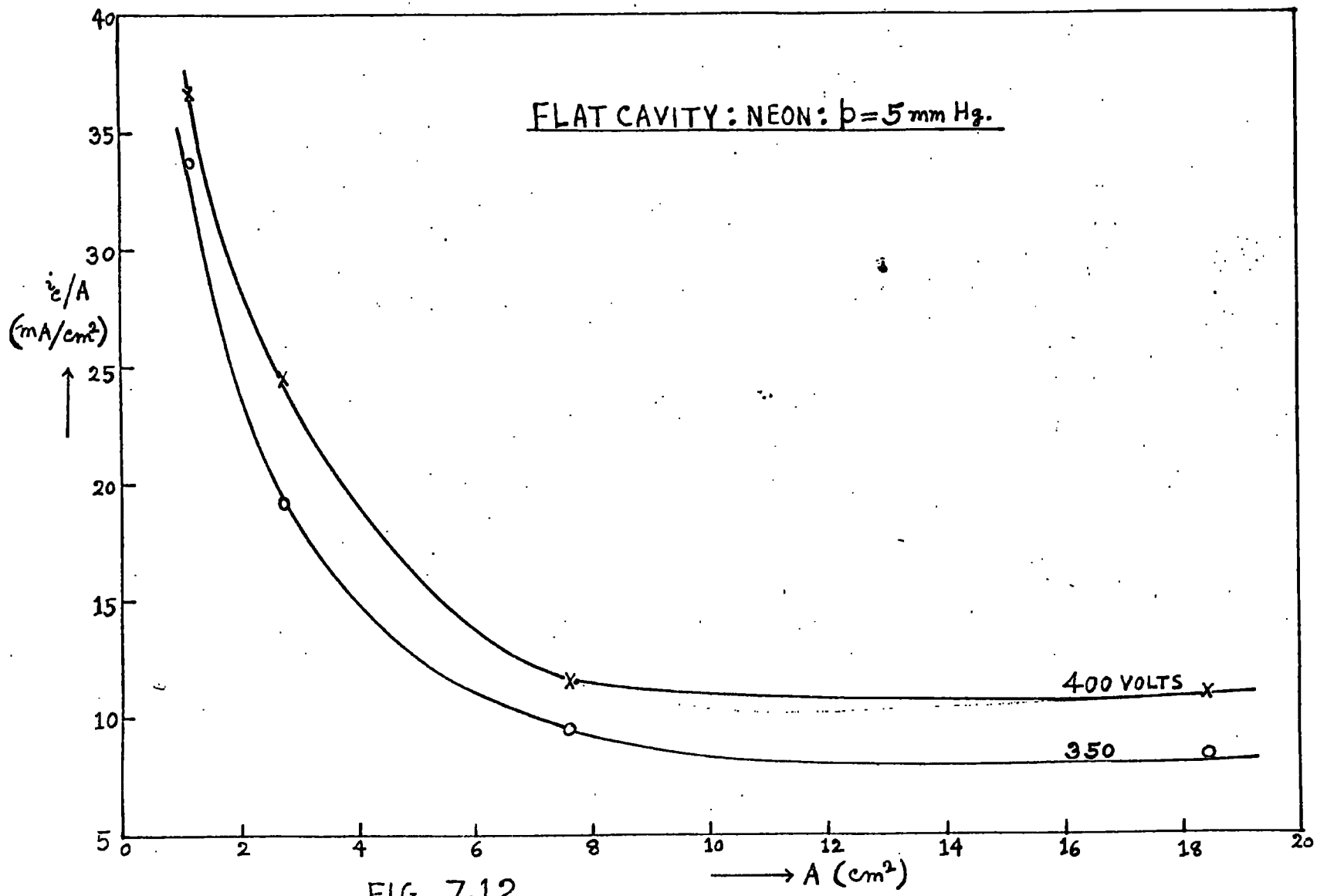
FLAT CAVITY : NEON : p = 5 mm Hg.
i_e/A (mA/cm²)
40
35
30
25
20
15
10
5
0
2
4
6
8
10
12
14
16
18
20
A (cm²)
400 VOLTS
350

FIG. 7.12.

(iii) A comparison of the maintaining voltages of different gases carrying the same current and at the same values of pΛ shows that V_g in air is greater than V_g in hydrogen and V_g in hydrogen is greater than V_g in neon (Table -7.2 below).

TABLE - 7.2: Flat Cavity: Λ=.55 cm.; A=18.39 cm^2
Values of V_g in volts.

	pΛ = 1.6 cm. mm. Hg.		pΛ = 2.75 cm. mm. Hg.	
i_c mA	air	hydrogen	hydrogen	neon
50	240	205	225	160
60	270	235	245	180
70	300	262	262	205
80	330	290	280	227
90	355	312	295	245
100	382	337	312	265
110	410	357	325	280
120	430	377	335	300
130	450	395	350	315
140	470	415	362	332
150	487	432	375	347
160	505	448	387	365
170	520	462	400	377
180	535	477	408	385
190	550	492	412	392

(iv) At a given voltage, the gap current is higher for higher electrode areas.

From these current-voltage characteristics, one can obtain various currents at a given voltage across electrode pairs of different area and hence the current densities can be calculated. If now the current densities are plotted against the area of the electrodes, one finds that ---

(v) with increase in A, the current density diminishes rapidly at first and then slowly, having a tendency to attain a constant value at higher values of A. This constant current density thus represents the "infinite"-parallel plate value.

At various constant voltages, such plots have been made. Results, graphically shown in Figs.(7.7 - 7.12), are in good agreement with our hypothesis as laid down in section 1.2, namely, that when $r >> \ell$, one area is like any other area and in discharges where electron temperatures are the same, one should expect constant current density at a given gap voltage.

(vi) For a given A, i_c/A is greater at greater gap voltage.

CHAPTER - VIII

OBSERVATIONS ON THE CURRENT-VOLTAGE RELATIONS IN LONG CYLINDRICAL TUBES FITTED WITH INTERNAL ELECTRODES.

8.1 Introduction

The results in the last two chapters for the electrodeless case were, as discussed, in very good agreement with what was expected according to the diffusion theory. This encouraged the author to carry on similar observations in tubes fitted with internal electrodes and to study how the maintaining voltage, in particular, its relation with the gap current is affected. In the following sections are described the results of such a study.

8.2. The Description of the Electrodes.

The shape of the internal electrodes was in the form of a circular disc of mild steel having circular grooves on each end face for the 'O' rings, necessary for the QVF coupling (Fig. 4.5b). A short thick copper wire was soldered to each electrode for electrical connection. Some preliminary observations were also taken, at first,

with hollow cylindrical electrodes (Fig. 4.5a). Results of such observations will be given in section 8.4.

8.3 Correction for the Displacement Current.

With the internal electrodes, no correction for the voltage drop across the tube wall was necessary, as in the electrodeless case. But, in this case it was found that there was considerable amount of deflection due to displacement current, or in other words, the ammeter showed a large deflection even when the tube did not glow. This, therefore, necessitated a correction for the displacement current. In principle, it is easy to correct for this, simply from the current-voltage characteristics for the non-glowing and glowing tube and assuming phase quadrature relation between the conduction and displacement currents (see Chap IX). This procedure, however, implies that at a given voltage, the ammeter deflection corresponding to the total current in the gap should always exceed that due to the displacement current. But, unfortunately the reverse was found.

A few typical sets of data are given in Tables 8.1 - 8.3 on the following pages.

TABLE 8.1: Air:

gap separation = 10 cm; tube diameter = 1.61 cm.

p mm. Hg.	V_g volts	i_c mA	p mm.Hg	V_g volts	i_c mA
1.3	315	117	0.5	320	112
	355	125		340	117
	362	127		360	122
	380	132		382	125
	410	137		390	127
	435	141		410	132
	450	146		428	135
	468	150		450	137
	480	152		460	141
	490	152		470	144
0.8	342	117	.01 (No glow)	355	132
	362	122		368	135
	380	127		390	139
	410	132		410	144
	432	137		430	148
	448	139		452	152
	460	141		460	154
	472	144		480	158
	480	146		490	160
	495	148		500	160

TABLE - 8.2: Hydrogen.

gap separation = 10 cm; tube diameter = 1.61 cm.

p mm. Hg	V_g volts	i_c mA	p mm. Hg	V_g volts	i_c mA
1	252	112	0.2	300	109
	292	115		320	115
	312	120		338	120
	322	122		370	125
	348	127		390	132
	370	135		420	137
	382	137		440	141
	412	144		455	146
	428	150		465	148
	440	152		475	150
	465	158		-	-
0.5	285	112	1.7 (No glow)	288	112
	320	120		340	125
	340	125		360	132
	380	132		378	135
	395	137		390	137
	412	139		408	141
	440	146		420	146
	455	148		440	150
	465	150		445	152
	-	-		455	154
	-	-		465	156
	-	-		472	158
	-	-		485	158

TABLE - 8.3: Neon

gap separation = 10 cm; tube diameter = 1.61 cm.

p mm. Hg	V_g volts	i_c mA	p mm. Hg	V_g volts	i_c mA
4.7	345	112	2.0	220	79
	385	117		260	87
	402	122		300	90
	425	125		312	94
	438	130		345	103
	450	132		390	112
	470	135		430	120
	470	137		445	122
	-	-		472	127
3.7	222	87	.01 (No glow)	222	139
	252	90		230	141
	270	94		252	115
	302	100		265	112
	345	109		282	115
	390	115		305	117
	395	117		322	122
	435	120		348	127
	452	130		360	130
	468	132		390	137
	470	132		412	144
	-	-		435	148
	-	-		468	156
	-	-		485	160
	-	-		500	162

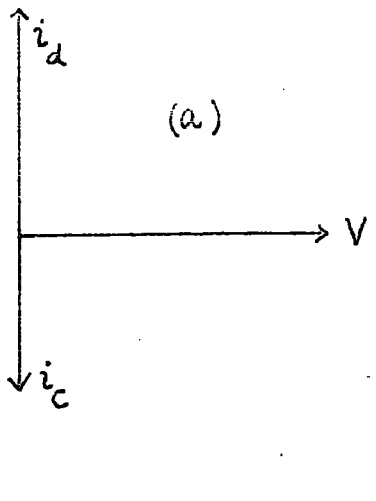

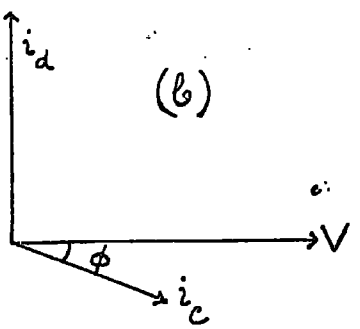

FIG. 8.1.

The difficulty of calculation of the conduction current probably lies in the assumption of the phase quadrature relation between the two currents under the given experimental conditions. The exact phase relation is not explored yet and it is being studied at the moment by another worker in this laboratory. However, a probable explanation of the above observations may be offered as in the following paragraphs:

Whatever the pressure, the displacement current i_d always leads the applied voltage V by $\pi/2$, whereas, in vacuum, the conduction current (due to electrons) lags behind by $\pi/2$ (Fig. 8.1a); at high pressure, i_c is in phase with V; in between these two extremes, i_c lags behind V by a certain phase angle ϕ (Fig. 8.1b), so that

$$i^2 = i_d^2+i_c^2-2i_c i_d \sin\phi$$

$$= i_d^2+i_c(i_c-2i_d \sin\phi) \qquad (8.1)$$

where i is the total current.

Now, ϕ is also roughly given by

$$\tan\phi = \frac{\omega}{\nu} , \qquad (8.2)$$

where ω = angular frequency of the applied field and ν is

the collision frequency.

At a pressure of the order of 1 mm.Hg, $\nu \simeq 10^9$; and $\omega \simeq 10^8$, so that $\tan\phi \simeq .1 \simeq \sin\phi$. Now if i_d is large in comparison with i_c, it is possible that the second term on the right-hand-side of Eq.(8.1) be negative; for example, if $i_d > 5i_c$, $i_c - 2i_d \sin\phi < 0$. Thus, the deflection corresponding to the total current could be less than that corresponding to the displacement current alone, as was found in our experiments.

If this explanation is correct, then two things follow:

(i) i_d should be large in comparison with i_c: Now, in experiments with long tubes, the displacement current (not necessarily passing through the tube) was quite high, or rather, the displacement current due to the strays was much higher than the displacement current through the tube and this is quite likely, as in a long tube, the electrodes are much separated.

(ii) ϕ should be large: The conditions in the experiment favour this criterion also, since in the long tube, lower pressure is necessary for breakdown; this means ν will be less and ϕ greater. Further, the greater the value of ϕ

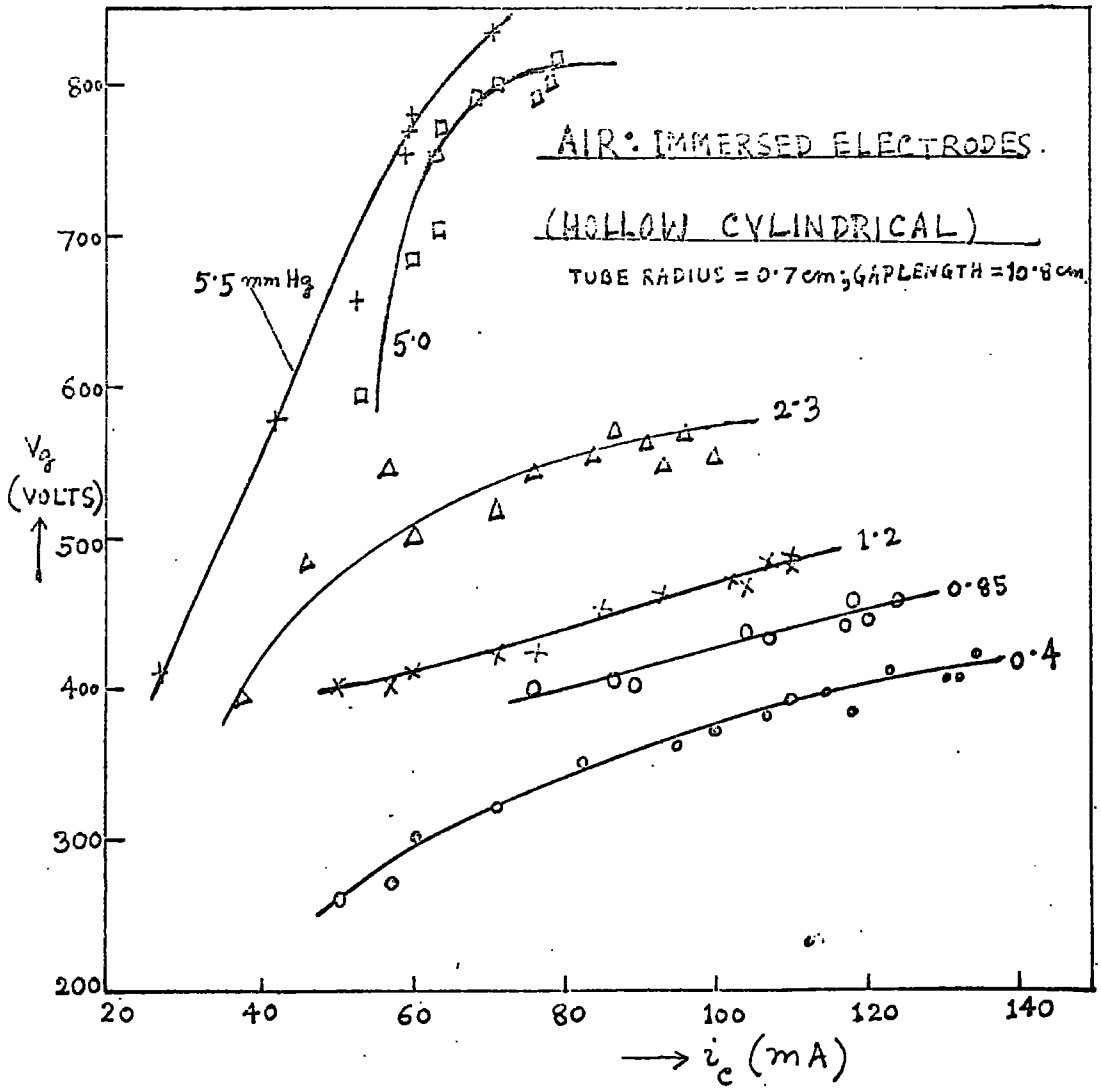
AIR: IMMERSED ELECTRODES.
(HOLLOW CYLINDRICAL)
TUBE RADIUS = 0·7 cm; GAP LENGTH = 10·8 cm.
5·5 mm Hg
5·0
2·3
1·2
0·85
0·4
V_s (VOLTS)
800
700
600
500
400
300
200
20
40
60
80
100
120
140
i_c (mA)

FIG. 8.2.

(i.e. the lower is the pressure), the less should be the total current at a given voltage, according to Eq.(8.1). As the Tables show, there is a clear indication of this being true.

8.4 Experimental Results (With Hollow Cylindrical Electrodes).

(a) Observations in air.

A typical set of V_g vs i_c data is given in Fig.(8.2).

(b) Observations in hydrogen.

Fig.(8.3) shows the V_g - i_c relation at a few pressures.

(c) Observations in neon.

In Fig.(8.4) are given the results of similar observations in neon at pressures of 2.5, 3.9 and 4.9 mm.Hg.

8.5 Discussion of Results.

The results described in the last section all show a few common characteristics, as enumerated below:

(i) The current-voltage characteristic is positive. This is in common with the results in the electrodeless discharge.

(ii) The results are pressure dependent and suggest that the maintaining voltage also like the breakdown voltage

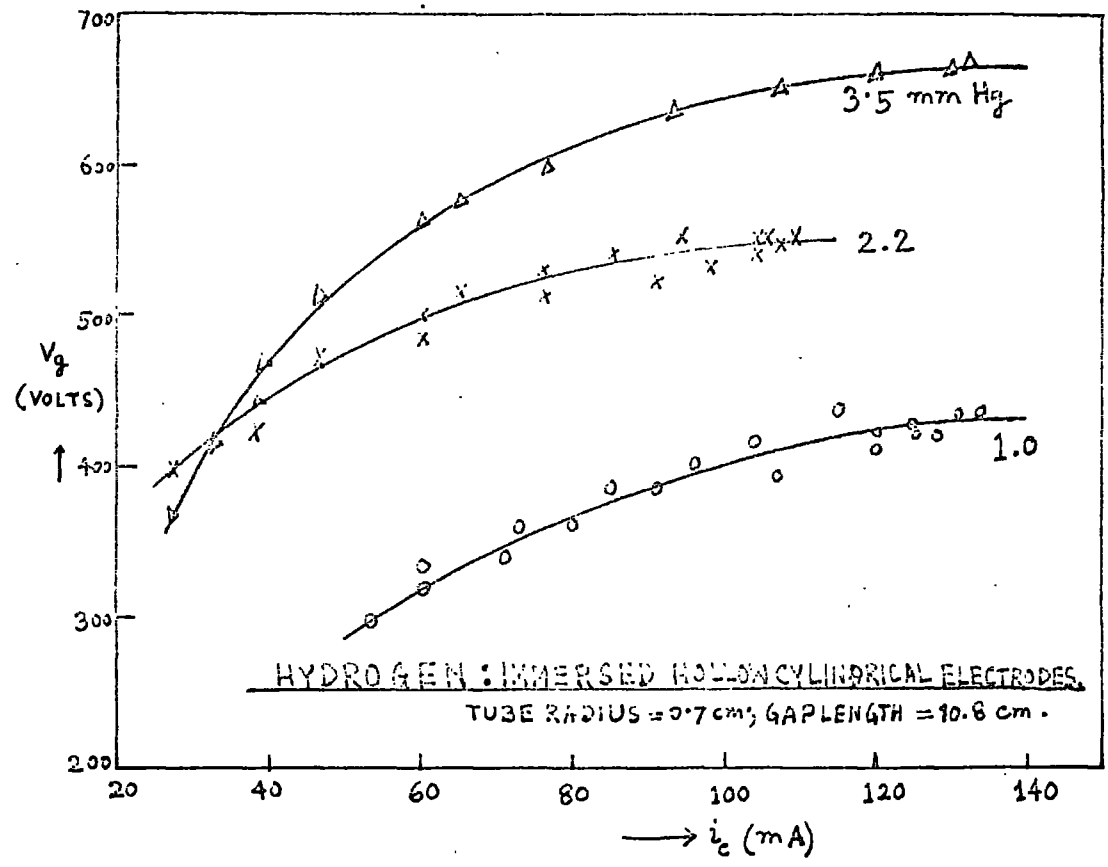

FIG. 8.3

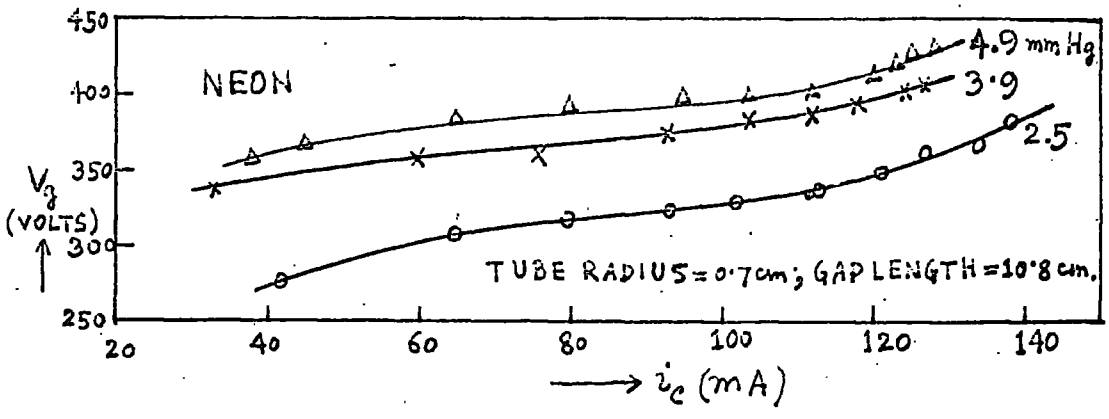

FIG. 8.4: IMMERSED HOLLOW CYLINDRICAL ELECTRODES.

passes through a minimum when plotted against pressure at a given gap current.

TABLE - 8.4.

Values of V_g in volts.

p = 1 mm. Hg.			p = 2.5 mm. Hg.		
i_c mA	air	H_2	i_c mA	H_2	Ne
50	395	290	40	442	265
60	405	322	50	470	287
70	415	350	60	490	300
80	437	372	70	508	307
90	455	390	80	522	315
100	467	405	90	535	320
110	485	415	100	545	325
-	-	-	110	550	330

(iii) The maintaining voltage at a given pressure and for a given gap current is higher in air than in hydrogen and higher in hydrogen than in neon (Table 8.4). This is also common with the results in the electrodeless case.

CHAPTER - IX

OBSERVATIONS ON THE CURRENT-VOLTAGE RELATIONS IN FLAT CAVITIES FITTED WITH INTERNAL ELECTRODES.

9.1 Introduction.

In order to complete the series of observations, one more system remained to be investigated, namely, the flat cavities having internal electrodes fitted to them. Cavities of several aspect ratios were chosen. The gases used were the same as before.

9.2 The Description of the Electrodes and Their Mounting.

As in the case of long tubes, the electrodes in this system consisted of circular discs of mild steel. For electrical connection, a side screw was fitted to each. The smaller diameter electrodes had circular grooves on each face for 'O'-rings, necessary for the QVF coupling, with spacers of different dimensions in between. The mounting arrangement is illustrated in Fig.(4.7).

For electrodes of very large area, it was not suitable to mount them as above. They were mounted as

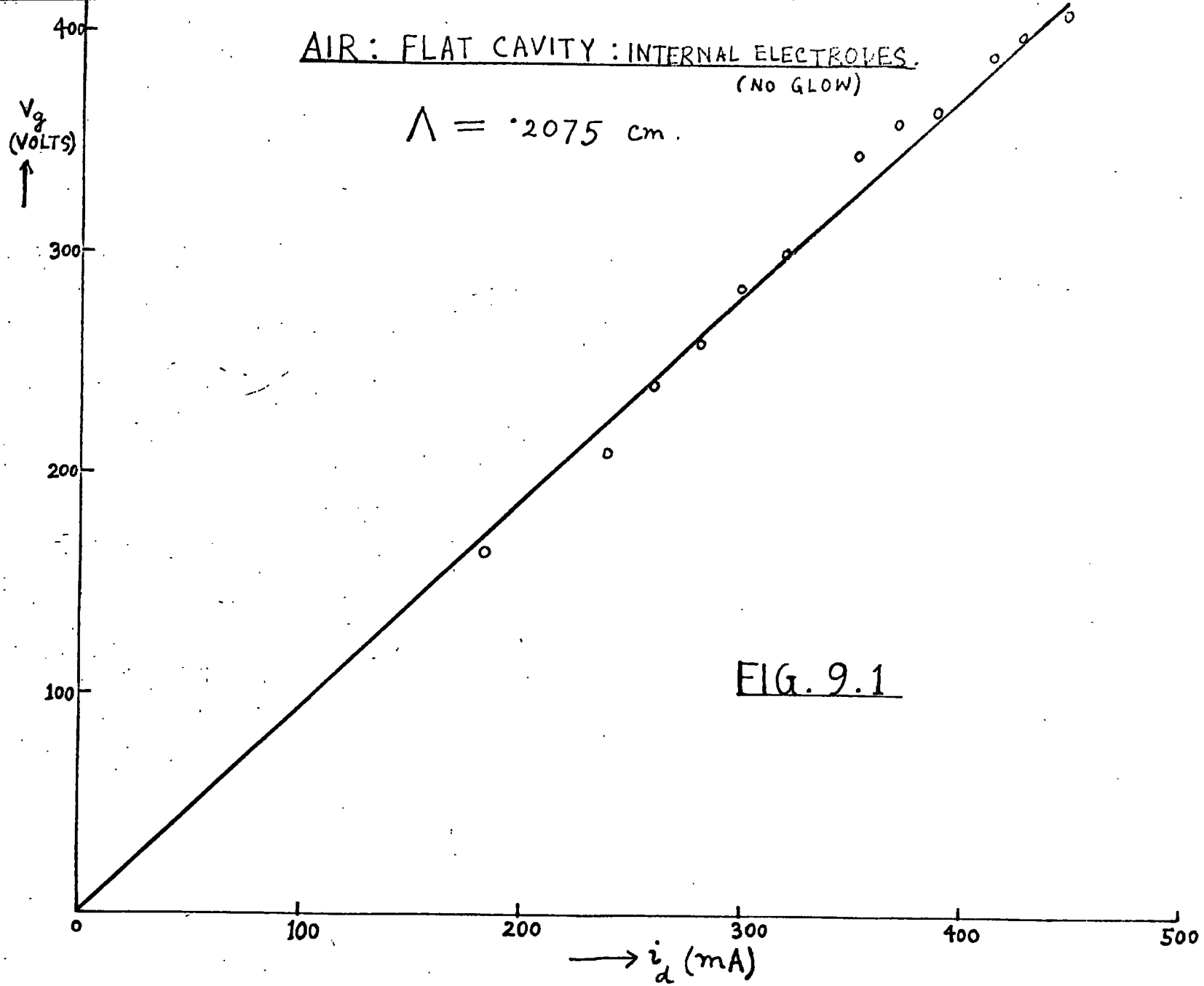
AIR : FLAT CAVITY : INTERNAL ELECTRODES.
(NO GLOW)
Λ = ·2075 cm.
V_g (VOLTS)
400
300
200
100
0
100
200
300
400
500
i_d (mA)

FIG. 9.1

in Fig.(4.8) instead.

9.3 Correction for the Displacement Current.

The displacement current in this system appeared to be far too small in comparison with the conduction current. The method how it was corrected for, is illustrated below:

At first the voltage-current data for the non-glowing cavity were obtained in the usual manner. Since displacement current is proportional to the applied voltage, a straight line is expected if one is plotted against the other. This was in fact found to be true by experiment, as shown in Fig.(9.1). Now, when at a suitable pressure, the tube was glowing, a set of current-voltage data were obtained. For each voltage in the latter case, the current, therefore, represents the total current i. The value of the displacement current i_d for this voltage was noted from Fig.(9.1). Assuming a phase quadrature relation between the conduction and displacement currents, one easily obtains the value of the required conduction current from the simple relation

$$i^2 = i_c^2 + i_d^2 \qquad (9.1)$$

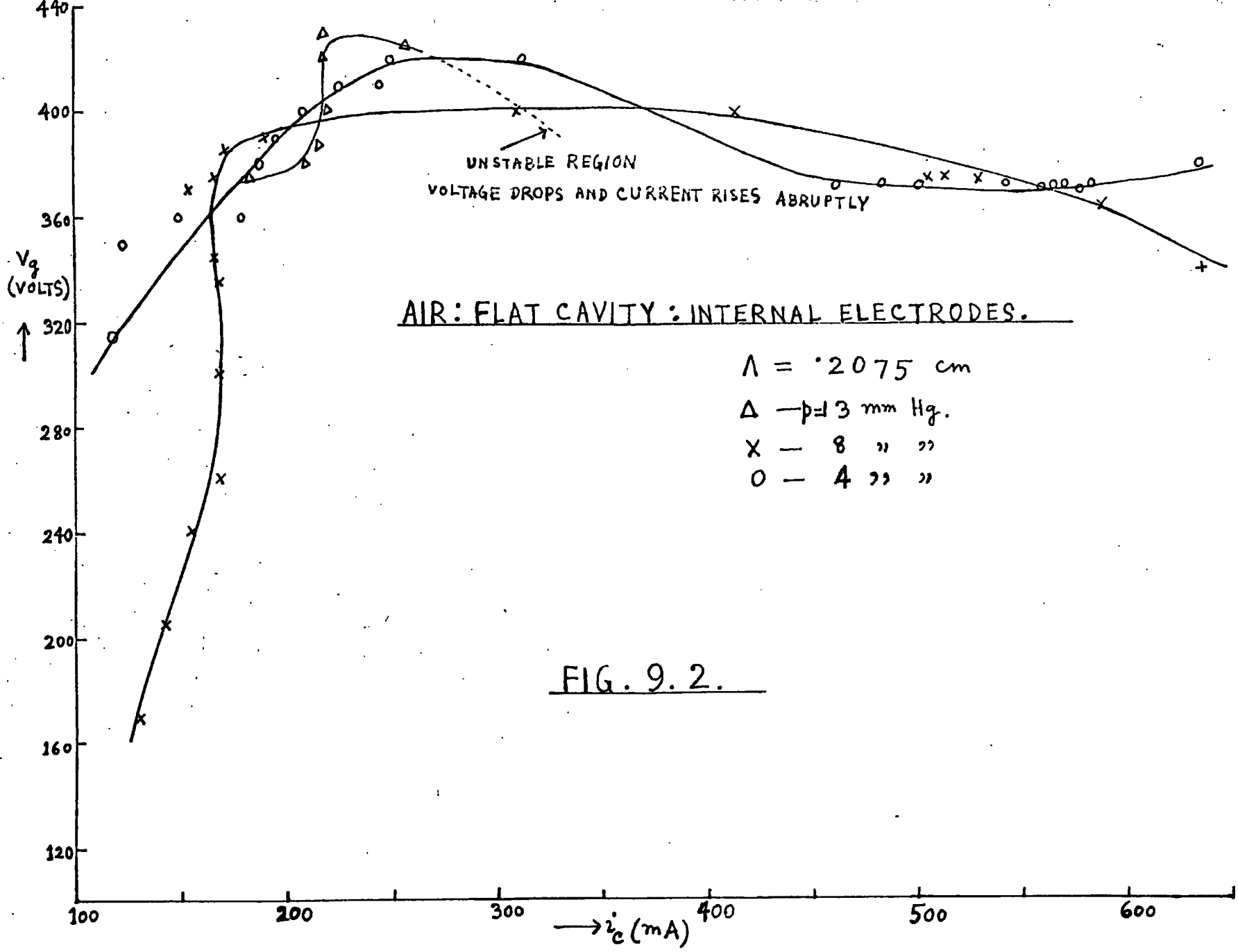
440
400
360
320
280
240
200
160
120
V_g (VOLTS)
UNSTABLE REGION
VOLTAGE DROPS AND CURRENT RISES ABRUPTLY
AIR : FLAT CAVITY : INTERNAL ELECTRODES.
Λ = ·2075 cm
Δ — p=13 mm Hg.
X — 8 " "
O — 4 " "
100
200
300
400
500
600
i_c (mA)

FIG. 9.2.

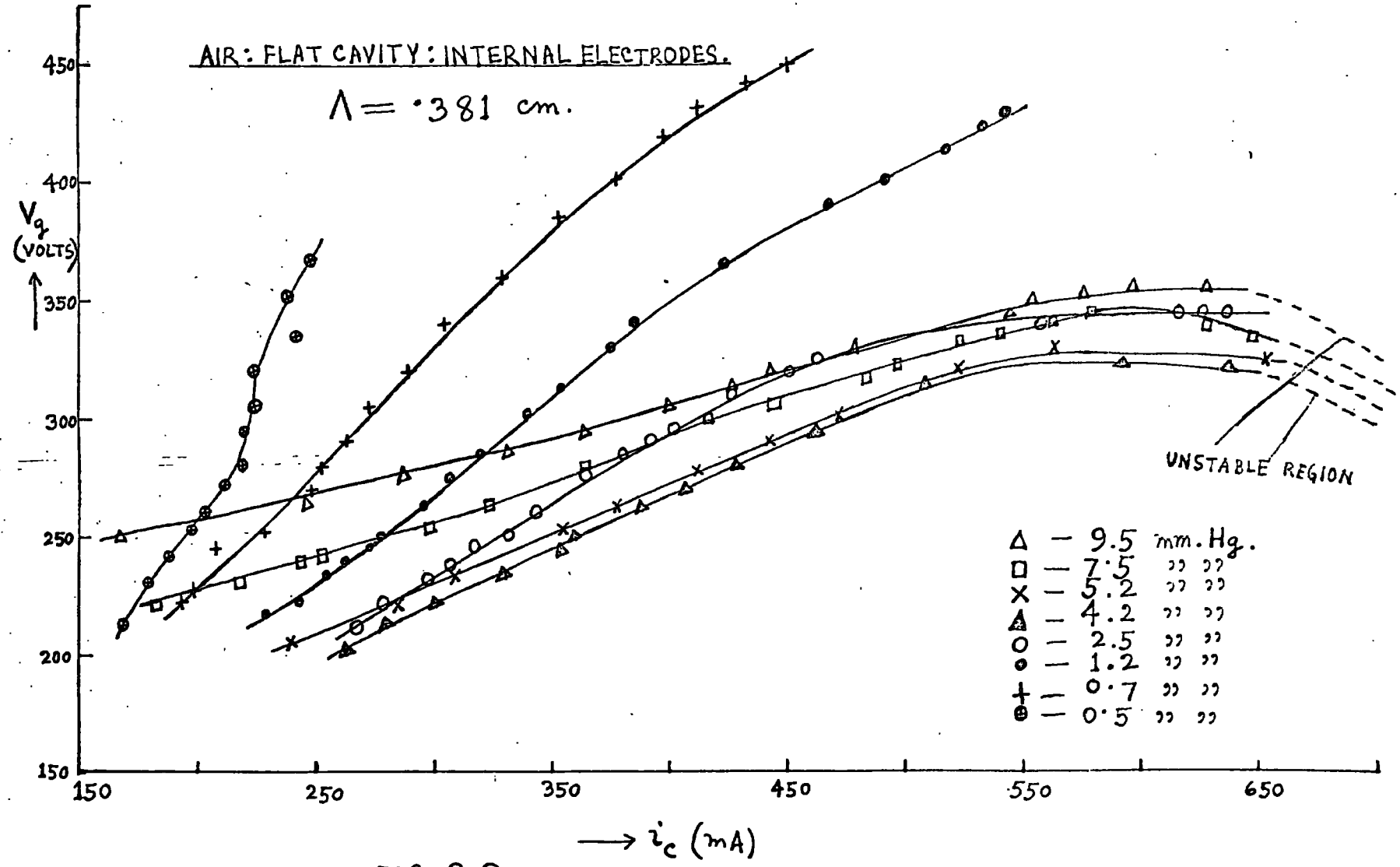
AIR: FLAT CAVITY: INTERNAL ELECTRODES.
Λ = ·381 cm.
V_q (VOLTS)
450
400
350
300
250
200
150
150
250
350
450
550
650
$\longrightarrow i_c$ (mA)
UNSTABLE REGION
Δ — 9.5 mm. Hg.
□ — 7·5 " "
× — 5.2 " "
◭ — 4.2 " "
○ — 2.5 " "
• — 1.2 " "
+ — 0·7 " "
⊕ — 0·5 " "

FIG. 9.3.

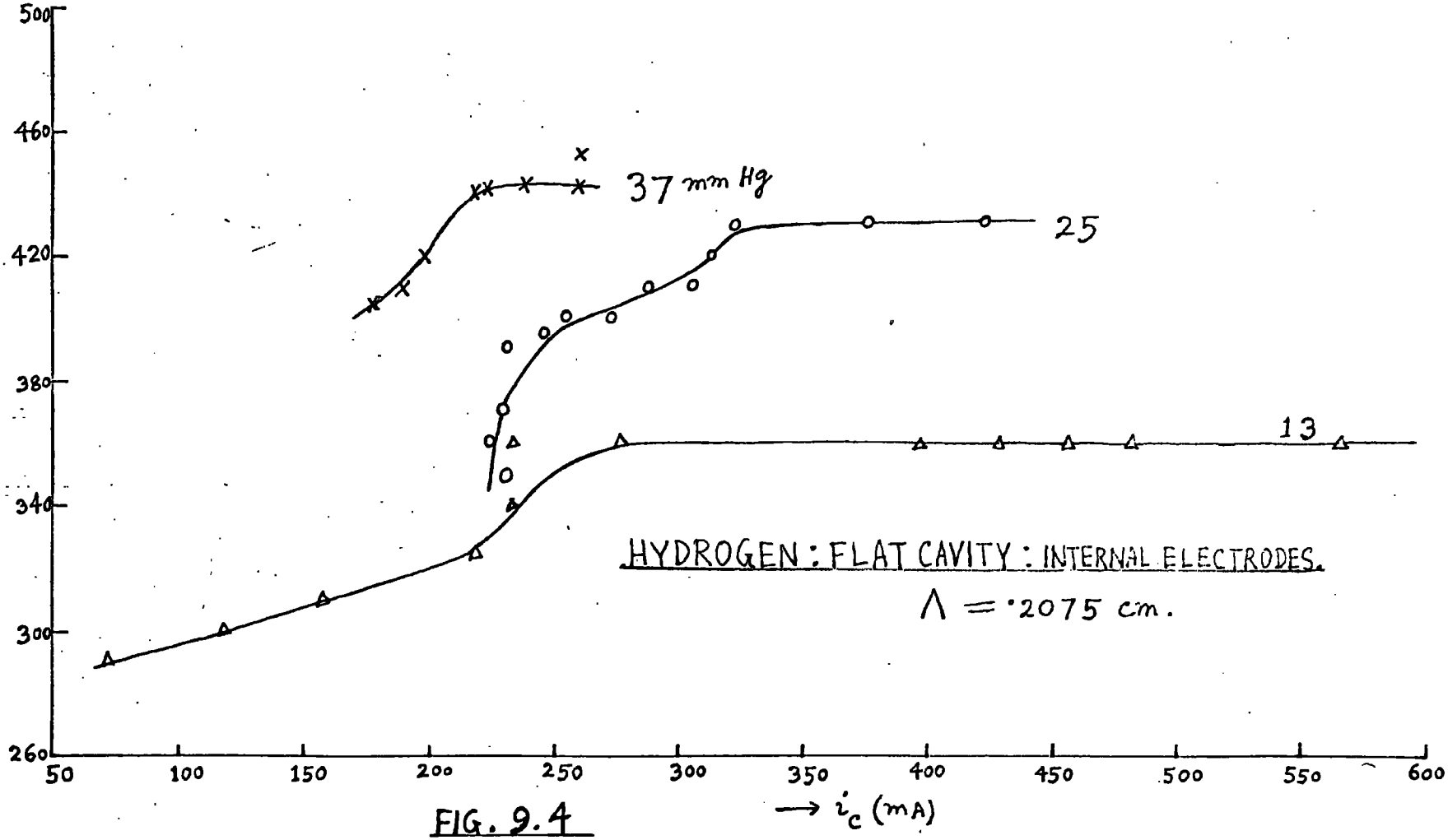
500
460
420
380
340
300
260
37 mm Hg
25
13
HYDROGEN : FLAT CAVITY : INTERNAL ELECTRODES.
Λ = ·2075 cm.
50
100
150
200
250
300
350
400
450
500
550
600
→ i_c (mA)

FIG. 9.4

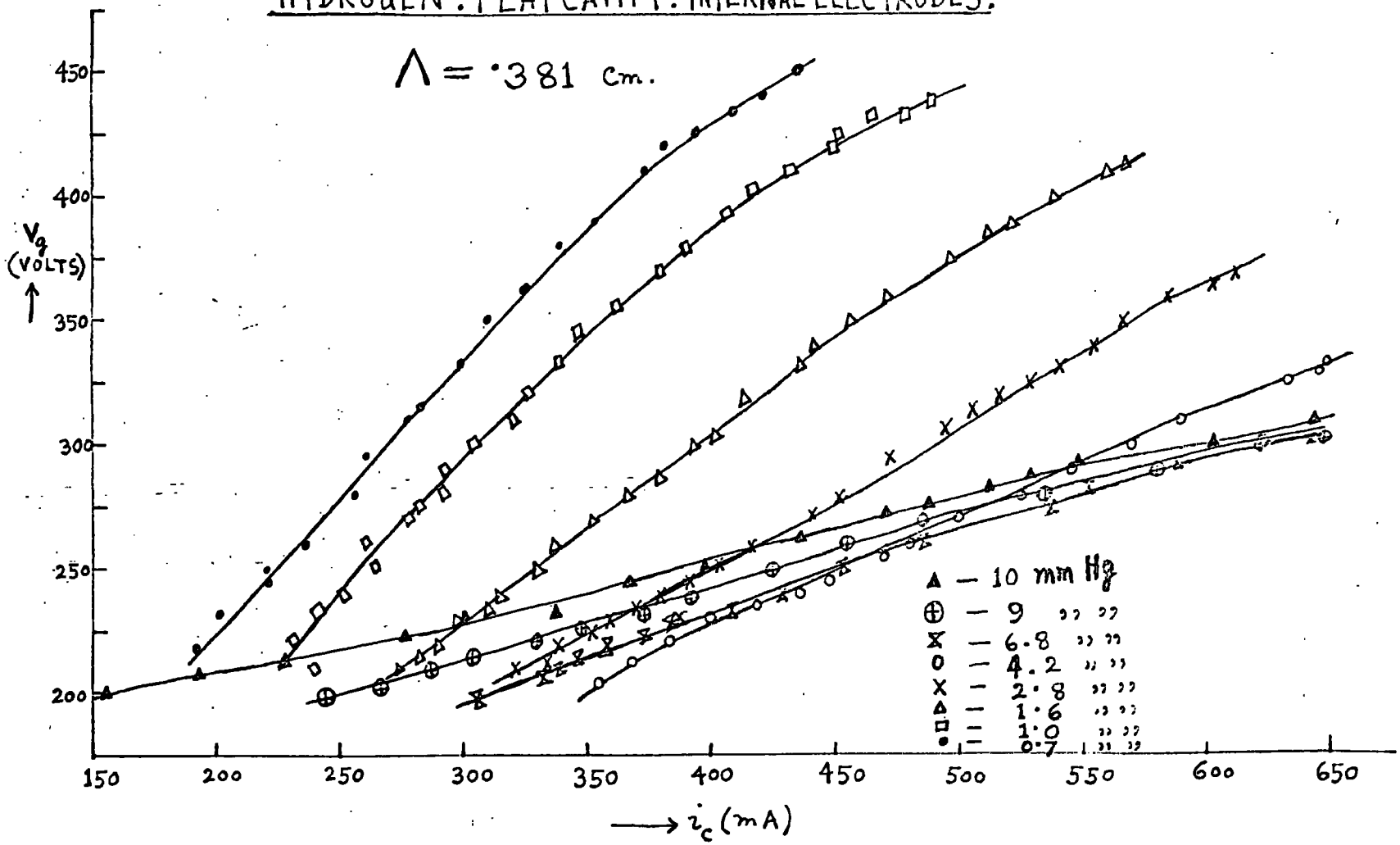
HYDROGEN : FLAT CAVITY : INTERNAL ELECTRODES.
Λ = ·381 cm.
V_g (VOLTS)
450
400
350
300
250
200
150
200
250
300
350
400
450
500
550
600
650
i_c (mA)
▲ — 10 mm Hg
⊕ — 9 " "
⧖ — 6·8 " "
o — 4.2 " "
× — 2·8 " "
△ — 1·6 " "
□ — 1·0 " "
● — 0·7 " "

FIG. 9.5.

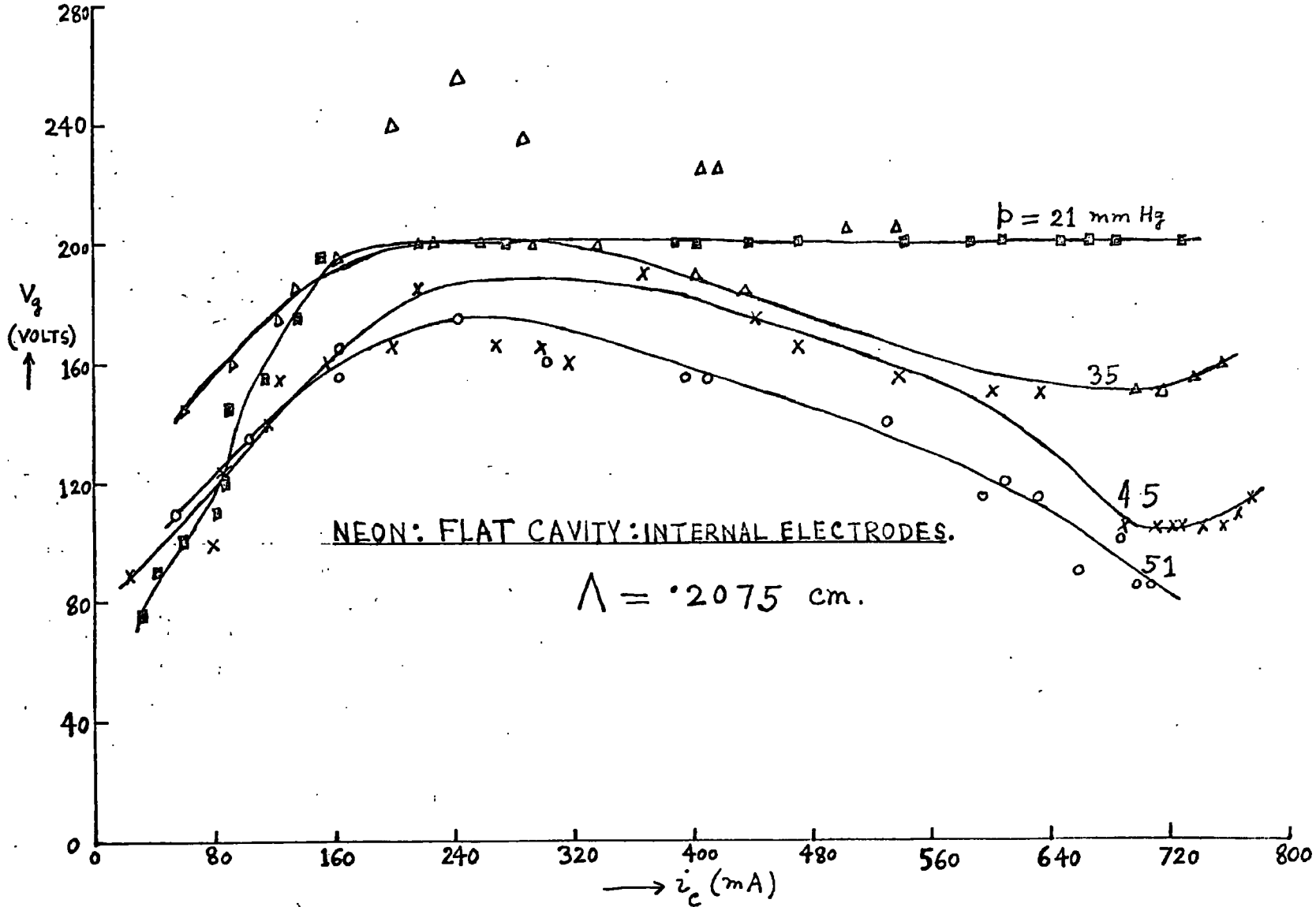
280
240
200
160
120
80
40
0
V_g
(VOLTS)
0
80
160
240
320
400
480
560
640
720
800
$\longrightarrow i_c$ (mA)
p = 21 mm Hg
35
45
51
NEON: FLAT CAVITY: INTERNAL ELECTRODES.
Λ = ·2075 cm.

FIG. 9.6

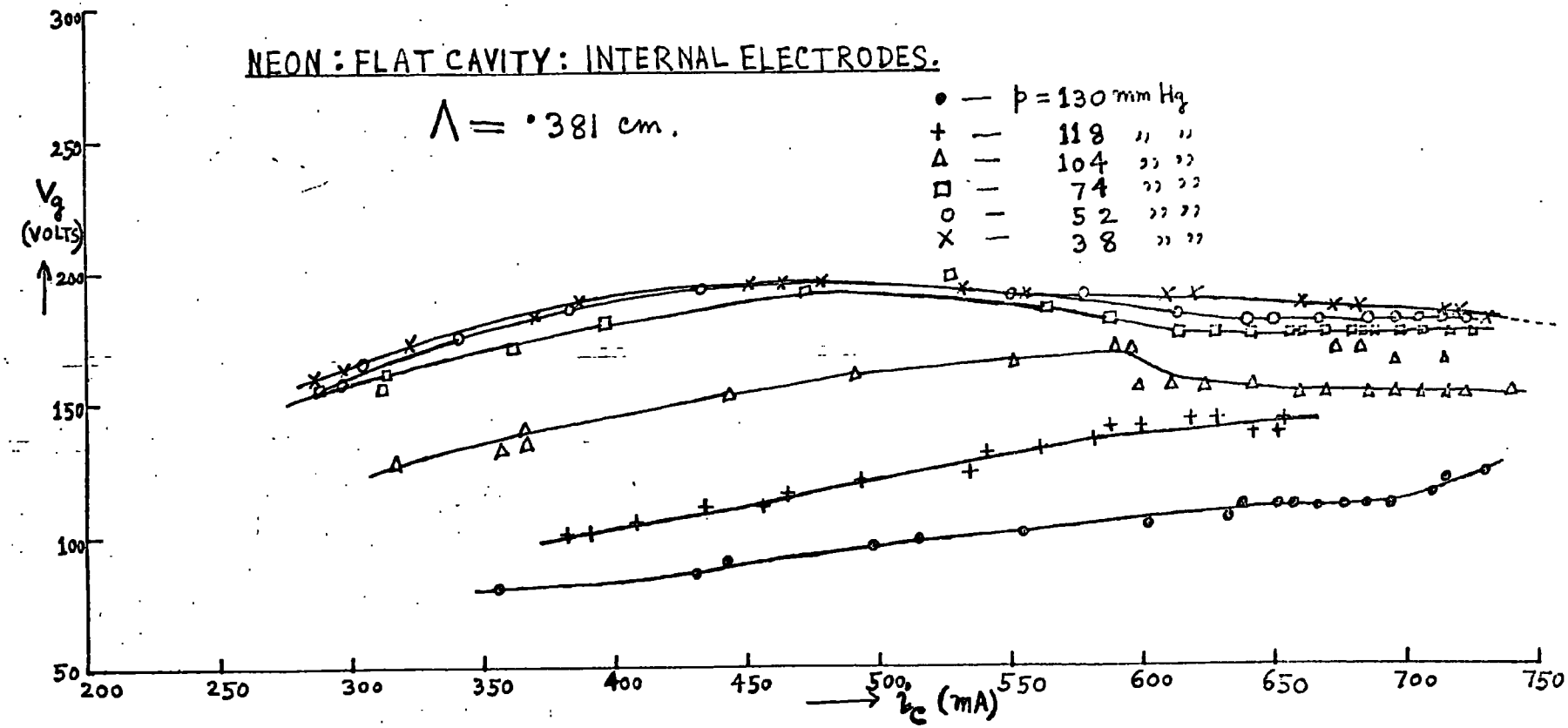
NEON : FLAT CAVITY : INTERNAL ELECTRODES.
Λ = ·381 cm.
● — p = 130 mm Hg
+ — 118 " "
Δ — 104 " "
□ — 74 " "
o — 52 " "
× — 38 " "
V_g (VOLTS)
300
250
200
150
100
50
200
250
300
350
400
450
500
550
600
650
700
750
i_c (mA)

FIG. 9.7.

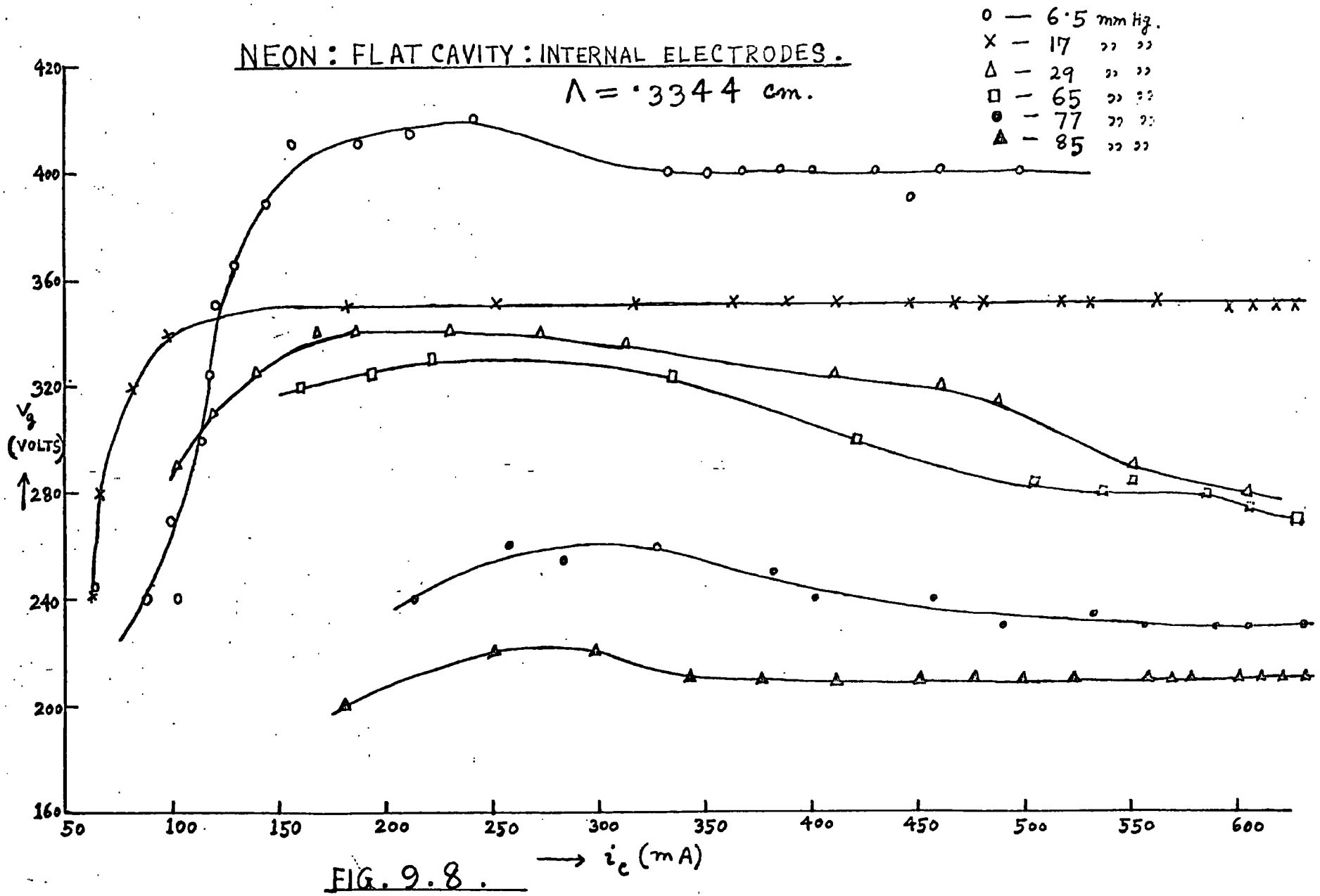
NEON : FLAT CAVITY : INTERNAL ELECTRODES.
Λ = ·3344 cm.
o — 6·5 mm Hg.
× — 17 " "
Δ — 29 " "
□ — 65 " "
● — 77 " "
▲ — 85 " "
420
400
360
320
280
240
200
160
V_g (VOLTS)
50
100
150
200
250
300
350
400
450
500
550
600
i_c (mA)

FIG. 9.8.

9.4 Experimental Results.

(a) Observations in air.

Some readings of gap voltage vs gap current at various pressures are shown graphically in Figs. (9.2 and 9.3) for cavities of which the characteristic diffusion lengths are respectively .2075 and .381 cm,

(b) Observations in hydrogen.

Similarly as in air, some results in hydrogen are represented by Figs.(9.4 and 9.5).

(c) Observations in neon.

Some results in neon are similarly represented by Figs.(9.6 - 9.8).

9.5 Discussion of Results.

An examination of Figs.(9.2 - 9.8) will enable one to draw a few general conclusions. These are enumerated below:

(i) The current-voltage characteristic can be either positive or negative, depending upon the nature of the gas, the cavity dimensions, the gas pressure and the value of the gap current.

(ii) The gap voltage can also be independent of the gap current within a certain range, which, in turn, depends upon the condition in the cavity in respect of the gas pressure and the dimensions of the cavity, or better, the product $p\Lambda$, Λ being the characteristic diffusion length of the cavity.

(iii) In some of the curves, a region of large scatter in the data is noticeable; the region of this scatter is particularly marked in the middle part of the characteristic.

(iv) In some of the characteristics, a discontinuity will be noticed. This is represented by dashes (Figs.9.2, 9.3 and 9.7).

The description of how the discontinuity occurred and what this could possibly mean in physical terms, are given below:

As the current was gradually increased from a low value, the corresponding voltages were noted, till at a certain position, the deflection in the ammeter rose abruptly to a very high value much beyond the ammeter scale. Simultaneously with this abrupt rise of current

there was an instantaneous fall in the voltage reading. The observations were repeated quite a number of times taking particular care while reaching this transition region, namely, very slowly adjusting the position of the control knob of the oscillator and trying to read the ammeter and voltmeter as close to this discontinuity as possible. Each time the discontinuity occurred which could not be avoided.

The discontinuity mentioned above might be due to the possible occurrence of plasma oscillations. The question, however, remains why these oscillations occurred so rarely, though observations were made in the same cavity at other pressures or in other cavities at nearly the same pressures, in other words, it remains to be solved as to how critically the occurrence of plasma oscillations depends on the product of the gas pressure and the characteristic diffusion length, on the gap current and the gap voltage.

(v) As in all previous cases, the maintenance voltage corresponding to a given current, is greater in air than in hydrogen and greater in hydrogen than in neon as shown in Table 9.1 overleaf.

TABLE - 9.1: Flat Cavity: internal electrodes.

Values of V_g in volts

$p\Lambda$ = 1.60 cm. mm.Hg			$p\Lambda$ = 2.22 cm mm Hg			$p\Lambda$ = 1.07 cm mm Hg		
i_c mA	Air	H_2	i_c mA	H_2	Ne	i_c mA	Air	H_2
350	244	200	80	377	232	50	276	252
375	255	215	90	379	248	60	289	268
400	266	228	100	386	269	70	319	285
425	278	238	110	389	290	80	353	305
450	288	248	120	390	340	90	385	328
475	300	260	130	390	366	100	397	354
500	310	271	140	390	384	-	-	-
525	318	282	-	-	-	-	-	-
550	322	293	-	-	-	-	-	-
575	323	305	-	-	-	-	-	-
600	325	315	-	-	-	-	-	-
625	324	325	-	-	-	-	-	-
650	323	323	-	-	-	-	-	-

CHAPTER - X

GENERAL DISCUSSION OF RESULTS AND CONCLUSION.

10.1 Introduction.

In the last few chapters, the experimental results were stated and discussed only briefly. It was also stated how these results fit in well with our two hypotheses, i.e. that (i) in long tubes for which $\ell^2 >> r^2$, the longitudinal gradient and (ii) in flat cavities for which $r^2 >> \ell^2$, the current density, should be constant for constant current and voltage respectively.

Additional support to these ideas will be given in this chapter. From the experimental data, it has been possible to calculate the values of several important quantities, namely, the ambipolar diffusion coefficient, the h.f. ionisation coefficient and the number density of electrons in the central plasma, as a function of the gap current and the gas pressure. The meaning of the end-drop of potential has also been discussed. Arithmetical calculations of the electric field near the electrodes by two independent methods (see Section 10.4(i))

are in satisfactory agreement. Also, the values of the end-drop of potential can be computed from an extension of Schneider's ideas (ref. Chapter II), namely that the end region has a width equal to or nearly equal to the electron ambit (Section 10.4(ii)).

A proposition has been made regarding the possible application of the Langmuir probe theory to the plasma to determine the quantities like concentration of electrons and the electron temperature, the idea being that the electrodes themselves behave as probes and the current-voltage characteristics in our experiments are like the probe characteristic of Langmuir.

Results in the long and flat systems have been combined and calculations of the power dissipation per unit volume in the two systems show that they are in reasonable agreement under identical conditions. Lastly, Poisson's equation has been applied to obtain charge density near the electrodes.

In conclusion, limitations of the work have been pointed out.

10.2 Calculation of the Ambipolar Diffusion Coefficient D_a and the H.F. Ionisation Coefficient ξ.

In the case of diffusion-controlled breakdown, one calculates the breakdown field with the help of the well-known relation (2)

$$\nu_i = \frac{eE_e^2}{mu_i\nu_c} \qquad (10.1)$$

where E_e = effective field in the gap, related to the peak value of the applied field E_p by

$$E_e^2 = \frac{E_p^2}{2}\frac{\nu_c^2}{\nu_c^2+\omega^2} \qquad (10.2)$$

where

e/m = specific charge of the electron,

ν_c = collision frequency between electrons and gas molecules,

ω = angular frequency of the applied h.f. field,

u_i = ionisation potential of the gas in volts

and ν_i = ionisation frequency.

ν_i is also related to the diffusion coefficient of

electrons D^- and the h.f. ionisation coefficient ξ by

$$\frac{\nu_i}{D^-} = \frac{1}{\Lambda^2} \tag{10.3}$$

and

$$\xi = \frac{\nu_i}{D^- E_e^2} = \frac{1}{\Lambda^2 E_e^2} \tag{10.4}$$

where Λ = characteristic diffusion length of the discharge vessel. The above relations are applicable, strictly speaking, to the case of breakdown. To say that these hold good to the sustained discharge as well (as in the present experiments) is not fair. Nevertheless, the reason of using these relations to calculate D_a (D^- being replaced by D_a in sustained discharges) and ξ is obvious, namely, whether or not the values come out of the right order of magnitude, even though the relations may be slightly inaccurate. Another advantage of this might be to see how these quantities vary with the gap current and gas pressure. Calculations were, therefore, carried out according to Eqs. (10.1) - (10.4), using the values of maintaining fields at various currents as given in

Figs.6.23 - 6.25 and Townsend's data (34). Results of such calculations are given in Tables 10.1 and 10.2 for hydrogen and neon respectively.

TABLE - 10.1 : Hydrogen: Electrodeless discharge: Internal diameter of the tube = 1.64 cm.

i_c	p = 9 mm. Hg				p = 6 mm. Hg				p = 3.2 mm. Hg			
mA	E/p V/cm.mm.Hg	ν_i $sec^{-1}(\times 10^6)$	ξ $volt^{-2}(\times 10^{-3})$	D_a $cm^2/sec(\times 10^5)$	E/p V/cm.mm.Hg	ν_i $sec^{-1}(\times 10^6)$	ξ $volt^{-2}(\times 10^{-3})$	D_a $cm^2/sec(\times 10^5)$	E/p V/cm.mm.Hg	ν_i $sec^{-1}(\times 10^6)$	ξ $volt^{-2}(\times 10^{-3})$	D_a $cm^2/sec(\times 10^5)$
80	3.8	7.5	8.2	7.7	4.6	6.5	13.1	6.6	5.4	4.5	32.7	4.6
90	3.7	7.4	8.7	7.6	4.5	6.4	13.4	6.6	5.0	3.9	39.2	4.0
100	3.6	6.8	9.5	6.9	4.5	6.4	13.6	6.5	4.7	3.5	44.6	3.6
110	3.5	6.5	10.0	6.7	4.3	6.0	14.6	6.1	4.5	3.5	46.7	3.5
120	3.3	6.2	10.9	6.3	4.2	5.7	15.6	5.8	4.3	3.2	51.5	3.3
130	-	-	-	-	-	-	-	-	4.1	3.0	57.8	3.0
140	-	-	-	-	-	-	-	-	4.0	2.8	61.3	2.8
150	-	-	-	-	-	-	-	-	3.9	2.7	65.4	2.7

TABLE - 10.2: Neon: Electrodeless discharge: Internal diameter of the tube = 1.64 cm.

i_c	p = 13 mm. Hg				p = 10 mm. Hg				p = 6.5 mm. Hg			
mA	E/p V/cm.mm.Hg	ν_i $sec^{-1}(\times 10^5)$	ξ $volt^{-2}$	D_a $cm^2/sec(\times 10^4)$	E/p V/cm.mm.Hg	ν_i $sec^{-1}(\times 10^5)$	ξ $volt^{-2}$	D_a $cm^2/sec(\times 10^4)$	E/p V/cm.mm.Hg	ν_i $sec^{-1}(\times 10^5)$	ξ $volt^{-2}$	D_a $cm^2/sec(\times 10^4)$
80	0.6	3.4	0.2	3.5	-	-	-	-	0.5	1.6	0.8	1.6
90	0.5	3.1	0.2	3.2	0.3	0.8	1.4	0.9	0.5	1.5	0.8	1.5
100	0.5	2.9	0.2	3.0	0.3	0.7	1.7	0.7	0.5	1.3	1.0	1.3
110	0.5	2.7	0.2	2.8	0.2	0.6	2.0	0.6	0.5	1.2	1.1	1.2
120	0.5	2.4	0.3	2.5	0.2	0.6	2.0	0.6	0.5	1.2	1.1	1.2
130	0.4	2.1	0.3	2.1	0.2	0.5	2.5	0.5	0.4	1.1	1.2	1.1
140	0.4	1.9	0.3	2.0	0.2	0.5	2.5	0.5	0.4	1.1	1.2	1.1
150	0.4	1.7	0.4	1.8	-	-	-	-	0.4	1.0	1.4	1.0
160	0.4	1.6	0.5	1.7	-	-	-	-	0.4	0.9	1.7	0.9
170	0.3	1.3	0.6	1.3	-	-	-	-	0.4	0.9	1.7	0.9
180	0.3	1.2	0.7	1.2	-	-	-	-	0.3	0.5	3.3	0.5

It will be seen from the Tables that the values of D_a in neon are of the expected order of magnitude; in hydrogen, however, they are slightly higher. Further, with increase in gap current, ξ increases and D_a decreases. The pressure variation shows that they may either increase or decrease depending upon the nature of the gas and pressure range itself.

10.3 Calculation of the Electron Ambit and the Electron Concentration in the gap.

If the symbols a, v_d, T and A denote the electron ambit, drift velocity of electrons, period of the applied h.f. field and the cross-sectional area of the discharge space respectively, then

$$a = v_d \frac{T}{2} \qquad (10.5a)$$

and

$$i_c = Nev_dA = \frac{2NeAa}{T} \qquad (10.5b),$$

N being the number density of electrons.

If i_c is in mA, then

$$i_c = \frac{2000\ NeAa}{T}$$

(continued overleaf)

$$= \frac{2000\ N \times 4.8 \times 10^{-10} \times 2.11 \times a \times 17 \times 10^{6}}{3 \times 10^{9}}$$

[Since $A = 2.11\ cm^2$

and $T = \frac{1}{n} = \frac{1}{17 \times 10^{6}}$,

n being 17 Mc/s;

3×10^{9} e.s.u. = 1 coulomb.]

$$\text{or } N = .869 \times 10^{8}\ \frac{i_c}{a} \qquad (10.6)$$

By using Townsend's data (34) for drift velocity v_d, one can thus calculate the value of a and hence N. The values so calculated for various gap currents and gas pressures are presented in Tables 10.3 and 10.4 on the following pages for hydrogen and neon respectively. They are of the expected order of magnitude.

TABLE - 10.3 : Hydrogen: Electrodeless discharge: Internal diameter of the tube = 1.64 cm.

i_c mA	p = 9 mm. Hg				p = 6 mm. Hg				p = 3.2 mm. Hg			
	$E/_p$ V/cm.mm.Hg	a cm.	N ($\times 10^{11}$)	V_{oend} Volts ($\times 10^2$)	$E/_p$ V/cm.mm.Hg	a cm	N ($\times 10^{11}$)	V_{oend} Volts ($\times 10^2$)	$E/_p$ V/cm.mm.Hg	a cm	N ($\times 10^{11}$)	V_{oend} Volts ($\times 10^2$)
80	3.8	.062	1.1	3.3	4.6	.072	1.0	3.3	5.4	.080	0.9	4.0
90	3.7	.062	1.3	3.4	4.5	.071	1.1	3.4	5.0	.073	1.1	4.3
100	3.6	.060	1.4	3.5	4.5	.071	1.2	3.6	4.7	.072	1.2	4.5
110	3.5	.059	1.6	3.6	4.3	.069	1.4	3.8	4.5	.071	1.3	4.7
120	3.3	.057	1.8	3.8	4.2	.068	1.5	4.0	4.3	.069	1.5	4.9
130	-	-	-	-	-	-	-	-	4.1	.066	1.7	5.1
140	-	-	-	-	-	-	-	-	4.0	.065	1.9	5.3
150	-	-	-	-	-	-	-	-	3.8	.063	2.1	5.4

TABLE - 10.4: Neon: Electrodeless discharge: Internal diameter of the tube = 1.64 cm.

i_c	p = 13 mm. Hg				p = 10 mm. Hg				p = 6.5 mm. Hg			
mA	E/p V/cm.mm.Hg	a cm.	N ($\times 10^{11}$)	V_{oend} Volts ($\times 10^2$)	E/p V/cm.mm.Hg	a cm.	N ($\times 10^{11}$)	V_{oend} Volts ($\times 10^2$)	E/p V/cm.mm.Hg	a cm.	N ($\times 10^{11}$)	V_{oend} Volts ($\times 10^2$)
80	0.6	.022	3.1	1.9	-	-	-	-	0.5	.022	3.2	3.1
90	0.5	.022	3.5	2.2	0.3	.016	4.9	3.2	0.5	.021	3.7	3.3
100	0.5	.021	4.1	2.4	0.3	.016	5.6	3.4	0.5	.020	4.3	3.6
110	0.5	.021	4.5	2.5	0.2	.015	6.3	3.6	0.5	.020	4.8	3.9
120	0.5	.020	5.2	2.7	0.2	.015	7.0	3.8	0.5	.020	5.3	4.0
130	0.4	.019	5.8	3.0	0.2	.015	7.7	4.0	0.4	.020	5.7	4.2
140	0.4	.019	6.4	2.4	0.2	.015	8.3	4.1	0.4	.019	6.4	4.4
150	0.4	.018	7.1	2.8	-	-	-	-	0.4	.019	6.9	4.6
160	0.4	.018	7.8	2.8	-	-	-	-	0.4	.019	7.4	4.7
170	0.3	.017	8.8	2.9	-	-	-	-	0.4	.018	8.1	4.9
180	0.3	.016	9.7	3.1	-	-	-	-	0.3	.016	9.6	5.1

10.4 The End-Drop of Potential

Referring back to Figs. (6.13) - (6.22), where V_g vs ℓ are plotted at various gap currents, it is to be noted that there is a considerable amount of end voltage. The magnitudes of the end voltages were found by extrapolating the curves towards the V_g axis ($\ell = 0$). The values so found are given in Tables 10.3 and 10.4 for hydrogen and neon. That the origin of the end-drop is physically explainable can be realised from the two independent approaches, as are described below:

(i) The conduction current i_c produces a voltage drop V_{glass} in glass given by $V_{glass} = i_c/\omega C$, C being the capacitance of the glass tube with respect to the external electrodes. If t_{glass} is the thickness of the tube, $i_c/\omega C t_{glass}$ is the magnitude of electric field inside glass. The electric field in the gas near the electrodes is, therefore, $i_c \varepsilon/\omega C t_{glass}$, where ε is the permittivity of the gas. The field in the gas near the electrodes is also given by $V_{oend}/2a$, where V_{oend} is the peak value of the end-voltage and a is the electron ambit, remembering that there are two end regions near the two electrodes. It has been tacitly assumed that the field near the electrodes is virtually constant over a distance

of the order of an electron ambit. Thus, comparing the values, e.g. $V_{oend}/2a$ and $i_c\varepsilon/\omega Ct_{glass}$, a good agreement will mean that the above picture of the end-drop is essentially correct. Results of calculations, done accordingly, are shown in Table 10.5 and are quite in conformity with the above conception.

TABLE - 10.5: Comparison of values of $V_{oend}/2a$ and $i_c\epsilon/\omega Ct_{glass}$ (V/cm x 10^3)

i_c	Hydrogen						Neon					
	p = 9		6		3.2		13		10		6.5 mm. Hg.	
mA	$\frac{V_{oend}}{2a}$	$\frac{i_c\epsilon}{\omega Ct_{glass}}$	$\frac{V_{oend}}{2a}$	$\frac{i_c\epsilon}{\omega Ct_{glass}}$	$\frac{V_{oend}}{2a}$	$\frac{i_c\epsilon}{\omega Ct_{glass}}$	$\frac{V_{oend}}{2a}$	$\frac{i_c\epsilon}{\omega Ct_{glass}}$	$\frac{V_{oend}}{2a}$	$\frac{i_c\epsilon}{\omega Ct_{glass}}$	$\frac{V_{oend}}{2a}$	$\frac{i_c\epsilon}{\omega Ct_{glass}}$
80	2.7	3.3	2.3	3.3	2.6	3.3	4.4	3.3	-	-	7.1	3.3
90	2.7	3.7	2.4	3.7	2.9	3.7	4.9	3.7	10.2	3.7	7.8	3.7
100	2.9	4.1	2.6	4.1	3.1	4.1	5.7	4.1	11.0	4.1	8.8	4.1
110	3.1	4.5	2.7	4.5	3.3	4.5	6.0	4.5	11.8	4.5	9.6	4.5
120	3.3	4.9	3.0	4.9	3.5	4.9	6.8	4.9	12.7	4.9	10.2	4.9
130	-	-	-	-	3.8	5.3	7.7	5.3	13.6	5.3	10.7	5.3
140	-	-	-	-	4.1	5.7	6.3	5.7	14.1	5.7	11.6	5.7
150	-	-	-	-	4.3	6.2	7.4	6.2	-	-	12.2	6.2
160	-	-	-	-	-	-	7.9	6.6	-	-	12.4	6.6
170	-	-	-	-	-	-	8.8	7.0	-	-	13.5	7.0
180	-	-	-	-	-	-	9.4	7.4	-	-	15.6	7.4

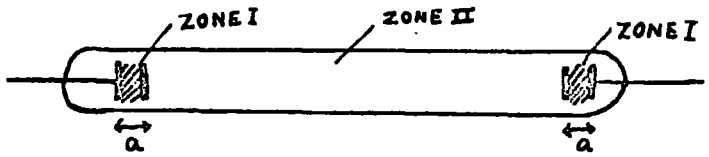

FIG. 10.1.

a = ELECTRON AMBIT

$V_{end} = V_{o\,end} \exp(i\omega t)$

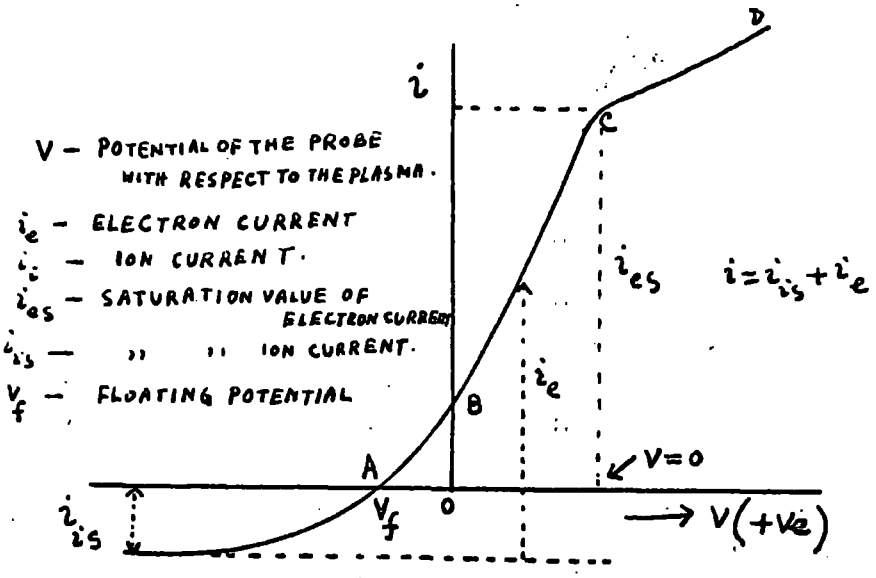

FIG. 10.2. LANGMUIR PROBE CHARACTERISTIC.

(ii) The end-drop of potential can also be explained by an extension of Schneider's theory (7). Let the following assumptions be made:

(a) The zones near the ends (zones I - Schneider) are each of width equal to or of the order of the electron ambit, (Fig.(10.1)).

(b) The time variation of the end-voltage V_{end} is of the form

$$V_{end} = V_{oend} \exp(j\omega t) \qquad (10.7)$$

(c) The field variation in time in zones - I is of the same form as that of V_{end}, and

(d) the conduction current in zone II is the same as the displacement current in zone I, since the same current flows in zones I and II in series (continuity of current - Maxwell).

Thus, if A is cross-section of the conducting channel, then, according to Maxwell's equation for continuity of current,

$$i_c = i_d \quad \text{(assumption d)}$$

$$= \frac{A\varepsilon}{4\pi} \frac{\partial E_{end}}{\partial t}$$

$$= \frac{A\varepsilon\omega}{4\pi} E_{end}, \qquad (10.8)$$

since $E_{end} = E_{oend} \exp(j\omega t)$ (assumptions b and c).

or $$|i_c| = \frac{A\varepsilon\omega}{4\pi} \frac{V_{oend}}{2a} \quad \text{(assumption a)} \qquad (10.8a)$$

Now, in our experiment, A = 2.11 cm^2 and $\omega = 1.07 \times 10^8$ rad/sec. Assuming permittivity of the discharge space nearly unity, if i_c is in mA and V_{oend} in volts then

$$\frac{i_c}{1000} \times 3 \times 10^9 = \frac{2.11 \times 1.07 \times 10^8 \, V_{oend}}{300 \times 4\pi \times 2a}$$

or $$V_{oend} = i_c a \times 100.48 \qquad (10.9)$$

Results of calculations of V_{oend} according to (10.9) can thus be compared with the experimental values of V_{oend} as found by extrapolation (Tables 10.3 and 10.4). These experimental values are again shown against the calculated ones in Table 10.6 on the following page and are found to be in good agreement.

TABLE - 10.6: Comparison of Calculated and experimental values of V_{oend} (x 10^2 volts)

i_c mA	Hydrogen						Neon					
	p = 9		6		3.2		13		10		6.5 mm.Hg	
	V_{oend} Calc.	V_{oend} expt.	V_{oend} Calc.	V_{oend} expt.	V_{oend} Calc.	V_{oend} expt.	V_{oend} Calc.	V_{oend} expt.	V_{oend} Calc.	V_{oend} expt.	V_{oend} Calc.	V_{oend} expt.
80	5.0	3.3	5.8	3.3	6.4	4.0	1.8	1.9	-	-	1.7	3.1
90	5.6	3.4	6.4	3.4	6.6	4.3	2.0	2.2	1.4	3.2	1.9	3.3
100	6.1	3.5	7.1	3.6	7.2	4.5	2.1	2.4	1.6	3.4	2.0	3.6
110	6.5	3.6	7.6	3.8	7.8	4.7	2.3	2.5	1.7	3.6	2.2	3.9
120	6.9	3.8	8.2	4.0	8.3	4.9	2.4	2.7	1.8	3.8	2.4	4.0
130	-	-	-	-	8.6	5.1	2.5	3.0	1.9	4.0	2.6	4.2
140	-	-	-	-	9.1	5.3	2.7	2.4	2.1	4.1	2.7	4.4
150	-	-	-	-	9.5	5.4	2.8	2.8	-	-	2.8	4.6
160	-	-	-	-	-	-	2.9	2.8	-	-	3.0	4.7
170	-	-	-	-	-	-	2.9	2.9	-	-	3.1	4.9
180	-	-	-	-	-	-	2.9	3.1	-	-	2.9	5.1

10.5 Possibility of Application of Langmuir's Probe Theory.

As is well-known, the probe is a very useful tool for exploration of the plasma. Its achievement in determining the important quantities like electron temperature and electron concentration is indeed remarkable. The theory of the plane probe is equally applicable to the cylindrical and spherical probes (24).

Let us examine whether the probe theory can be applied to the present experiments. A typical probe characteristic (35) is represented by Fig.(10.2). Let us make the following assumptions:

(i) the end electrodes can be imagined to act as plane probes,

(ii) the point A corresponding to zero current corresponds to the situation when the electronic and ionic currents to the probes are equal; this then should represent the state when loss of both types of charged carriers is due to ambipolar diffusion,

(iii) the point C in the characteristic represents the state when the probe is at the same potential as the plasma. In that state, the sheath of positive ions on the surface

of the probe vanishes and is replaced by a much more dense sheath of electrons. Now, in order to base our argument regarding the end drop of potential on the possible existence of a positive ion sheath (not of electrons), we must make the assumption that the end electrodes (or rather the end probes) are at a negative potential with respect to the plasma. This, therefore, means that we are concerned with the region ABC of the characteristic. (In any case, the $V_g - i_c$ characteristics in our experiments are of similar shape as the probe characteristic of Fig.(10.2)).

Up to C the probe is always negative; the current density in this part i.e. part ABC is given by

$$j^- = eN^- \sqrt{\frac{KT_e}{2\pi m}} \exp\left(-\frac{eV}{KT_e}\right) \qquad (10.10)$$

$$\text{or} \quad \ell n j^- = \text{constant} - \frac{eV}{KT_e}$$

$$\text{or,} \quad \left|\frac{\partial(\ell n j^-)}{\partial V}\right| = \frac{e}{KT_e} \qquad (10.11)$$

Using (10.11) a few typical calculations for electron temperature and electron density have been done. The results of such calculations are of the expected order of magnitude, as shown in Table 10.7 below:

TABLE - 10.7: Calculations from the Probe Theory.

gas	i_c mA	$p\Lambda$ cm. mm. Hg.	T_e ($x10^2$eV)	N^- ($x10^9$ cm^{-3})
Hydrogen	250	0.27	7.2	0.3
	300	3.81	1.5	5.3
	400	2.59	2.1	2.8
Neon	400	28.19	12.8	0.3
	500	44.95	6.0	0.7
	500	49.52	5.8	20.0

10.6 Results in Long Cylindrical Tubes and Flat Cavities Combined.

It would be very instructive to examine how the results in the two systems can be co-ordinated together to allow some useful comparison of a physical variable. One such variable is obviously the power dissipation in either system under identical conditions. It is expected that for the same value of $p\Lambda$ the power dissipation per unit volume in the two systems should be comparable; in other words,

$$\frac{E_1 i_{c_1}}{A_1} = \frac{E_2 i_{c_2}}{A_2} \qquad (10.12)$$

where the suffix 1 refers to long tubes and 2 to flat cavities.

If V_2 denotes the total voltage in system 2, then the voltage drop in the gas in this system should be given by

$$V_{g_2} = V_2 - V_{oend_2} \qquad (10.13)$$

where V_{oend2} is the appropriate end drop of potential in this system. If the width of the cavity is d, then, assuming that there are two distinct end regions in this system also, of the same order of magnitude as the electron ambit a, the thickness of the central plasma is

$$t_{g2} = d - 2a \tag{10.14}$$

so that the axial field in the plasma of this system should be

$$E_2 = \frac{V_{g2}}{t_{g2}} = \frac{V_2 - V_{oend2}}{d - 2a} \tag{10.15}$$

Now, according to Eq.10.8(a), for a given conduction current i_c, V_{oend} is inversely proportional to the cross-sectional area of the electrodes and therefore, one can write

$$V_{oend1} A_1 = V_{oend2} A_2 \tag{10.16}$$

or,

$$E_2 = \frac{V_2 - V_{oend1} \frac{A_1}{A_2}}{d - 2a} \tag{10.17}$$

The procedure of verifying Eq. (10.12) is illustrated as follows:- A_1 and A_2 are known quantities; the pressures and the electrode areas in the two systems are so chosen that $p_1A_1 = p_2A_2$. Now, for a given current in system 1, i_{c_1} say, one can obtain E_1, V_{oend_1} and a from Tables 10.1 - 10.4; for the same current in system 2 i.e. $i_{c_1} = i_{c_2}$, the total voltage V_2 is found out from the appropriate $V_g \div i_c$ characteristic of system 2; one can, thus obtain the value of E_2 by using Eq.(10.17). Such calculations have been done for hydrogen and neon. Results given in Tables 10.8 and 10.9 on the following pages show that the values of power dissipation per c.c. in the two systems under identical conditions are in good agreement.

TABLE - 10.8: Comparison of power dissipation per c.c. in both systems.

gas	pΛ cm. mm. Hg.	i_c mA	Long tube: electrodeless $A_1 = 2.11$ cm^2 $\frac{E_1 i_{c_1}}{A_1}$ (x 10^{-1} watt per c.c)	Flat Cavity: electrodeless $A_2 = 18.4$ cm^2 $d = 2.06$ cm. $\frac{E_2 i_{c_2}}{A_2}$ (x 10^{-1} watt per c.c)
Neon	3.44	100	1.7	3.4
	"	110	1.7	4.1
	2.22	80	1.9	2.5
	"	100	2.1	3.7
	"	110	2.2	4.4
	"	140	2.6	6.4
Hydrogen	2.05	100	18.0	4.6
	1.09	100	10.1	4.8
	"	110	10.6	5.9
	"	140	11.9	8.8

TABLE - 10.9: Comparison of power dissipation per c.c. in both systems

gas	$p\Lambda$ cm. mm. Hg	i_c mA	Long tube: electrodeless $A_1 = 2.11$ cm^2 $\frac{E_1 i_{c_1}}{A_1}$ (x 10^{-1} watt per c.c)	Flat Cavity: immersed electrodes $A_2 = 5.54$ cm^2 $d = 1.32$ cm $\frac{E_2 i_{c_2}}{A_2}$ (x 10^{-1} watt per c.c)
Hydrogen	1.09	100	10.0	28.1
	"	120	11.2	39.5
	2.05	80	14.7	24.5
	"	90	16.3	29.8
	"	100	18.1	35.0
Neon	2.22	80	1.9	12.9
	"	90	2.1	15.4
	"	100	2.2	17.1

10.7 Comparison of Data in Tubes of Different Diameters (D) and Flat Cavities of Different diffusion Lengths (Λ)

In Tables 10.10 and 10.11 on the following pages are shown values of voltage gradients, $dV_g/d\ell$ for different tubes and maintaining voltages V_g for different cavities, at various pressures and gap currents.

It appears that neither $\left(\frac{dV_g}{d\ell}\right)_{i_c,p = \text{const.}}$ versus D

nor $\left(V_g\right)_{i_c,p = \text{const.}}$ versus Λ, obeys any simple functional relation and that both are dependent upon gas pressure and gap current. The scatter in the data could, however, partly be attributed to the fact that it is difficult to vary the tube diameter or the cavity length without any change of other conditions in the system.

TABLE - 10.10

Values of voltage gradients, $\frac{dV_g}{d\ell}$ (V/cm)

Gas	pressure mm. Hg.	i_c mA	Tube diameters (D) cm				
			.525	.93	1.28	1.455	1.64
Air	1.5	70	41	50	63	45	-
	"	80	35	44	63	43	30
	"	90	37	37	48	34	-
	3.5	60	69	73	85	49	44
	"	80	58	56	54	44	43
Hydrogen	3	80	62	58	62	73	-
	"	100	63	54	57	41	-
	"	120	75	58	53	-	-
	8	60	102	-	101	-	85
	"	70	102	-	102	-	91
	"	80	-	-	99	-	93
Neon	5.5	100	43	11	20	-	16
	"	120	38	14	11	-	13
	8.5	100	-	13	15	-	23
	"	120	-	15	16	-	17
	"	140	-	17	20	-	13
	"	160	-	19	18	14	13

TABLE - 10.11

Hydrogen

Values of Maintaining Voltages, V_g (x 10^2volts)

p	i_c	Diffusion length (Λ) of cavities (cm)		
mm. Hg.	mA	.208	.334	.422
1.5	90	-	3.7	3.0
"	100	-	3.8	3.5
"	110	-	3.8	4.3
3.5	80	-	3.2	3.4
"	90	.9	3.3	3.9
"	100	-	3.7	4.3
"	110	1.0	3.8	4.7
"	120	-	4.0	4.9
"	200	1.5	-	-
"	250	1.8	-	-
5.5	80	-	3.3	2.9
"	90	-	3.5	3.2
"	100	-	3.7	3.5
"	110	-	3.8	3.8
"	120	-	3.9	4.1
"	130	-	4.0	4.3
"	140	-	4.1	4.5
7	50	1.3	3.7	-
"	60	1.4	3.7	-
"	70	1.5	3.7	-

10.8 Variation of Maintaining Voltage with Gas Pressure at Constant Gap currents.

From the current-voltage characteristics of the maintained discharge, one can study the variation of the maintaining voltage with pressure of the gas at various constant gap currents. Typical sets of data presented in Tables 10.12 and 10.13 on the following page show that as in Paschen's curves, there is a minimum, the value of which depends upon the gap current.

TABLE - 10.12

Air: Internal Electrodes: Λ = .381 cm

p mm. Hg	Values of V_g (volts) for i_c = 275	300	325	350	375	400	425	450 mA
9.5	274	280	285	291	298	305	312	320
7.5	247	254	262	271	280	291	300	310
5.2	219	229	240	250	260	271	281	292
4.2	209	220	232	244	256	266	278	288
2.5	217	234	249	265	280	294	307	320
1.2	247	266	289	310	330	350	365	381
0.7	304	331	356	380	400	420	437	450

TABLE - 10.13

Hydrogen; Internal Electrodes: Λ = .381 cm.

p mm. Hg.	Values of V_g (volts) for i_c = 350	375	400	425	450 mA
10.0	235	242	248	254	261
9.0	221	229	236	242	250
6.8	206	215	224	233	241
4.2	200	215	228	238	249
2.8	224	237	250	264	277
1.6	267	285	304	324	343
1.0	344	366	386	405	420
0.7	386	410	429	445	457

10.9 Application of Poisson's Equation to determine the Density of Charges near the Electrodes.

Poisson's equation, which applies to any point of space where there is a charge density, is given in the one-dimensional case by

$$\frac{d^2V}{dx^2} = 4\pi\rho = 4\pi Ne \qquad (10.18)$$

where V is the potential at a distance x from an electrode and ρ is the volume density of charges and N is their number density.

Now, for H_2 at 9 mm. Hg, for example, the average value of the potential gradient near the electrodes (zone I) is of the order of 10^3 (Table - 10.5) and that in the plasma (zone II) is about 30 (Table - 10.1) or,

$$\left(\frac{dV}{dx}\right)_I \simeq \frac{V_{oend}}{2a} \simeq 10^3 V/cm; \left(\frac{dV}{dx}\right)_{II} \simeq 30 \text{ V/cm.} \qquad (10.19)$$

Thus, there is a very sharp change of the gradient within a distance of the order of an electron ambit; more clearly, at the electrode or very near to it, the gradient is high (10^3 V/cm) and constant, i.e. the spatial rate of change of gradient is zero (and hence the charge density at the electrode should be zero according to Poisson's equation), whereas at a distance nearly equal to the electron ambit, the change in the gradient is $10^3 - 30 \simeq 10^3$. Therefore, the average spatial rate of change of the gradient is given by

$$\left(\frac{d^2V}{dx^2}\right)_{av} = \frac{\left(\frac{dV}{dx}\right)_I - \left(\frac{dV}{dx}\right)_{II}}{2a} \qquad (10.20)$$

$$\simeq \frac{10^3}{.12} = 8.3 \times 10^3 = 4\pi Ne$$

$$= 4 \times 3.14 \times N \times 4.8 \times 10^{-10} \times 300$$

$$\text{or } N = 5 \times 10^9 \qquad (10.21)$$

The value of N thus calculated can be compared with that found by using the relation

$$N = N_o J_o \left(\frac{2.4r}{R}\right) \qquad (10.22)$$

where N_o is the number density of charges in the central plasma, N, that at a distance r from the axis, R is the radius of the tube and J_o is Bessel function of the zeroeth order. In our experiments, N_o is of order 10^{11} (Table - 10.3), R = 1.64 cm, r = R - a; the argument of J_o is then

$$2.4 \times \frac{1.58}{1.64} = 2.31 \quad (a \simeq .06, \text{ see Table 10.3})$$

From Table of Functions,

$$J_o\ (2.31) = .055$$

so that

$N = 5.5 \times 10^9$, in conformity with the value obtained in Eq.(10.21).

Similar calculations for neon at 10 mm. Hg are given below and on the following page:
In this case,

$$\left(\frac{dV}{dx}\right)_I \simeq \frac{V_{oend}}{2a} \simeq 10^4 \text{ V/cm.} \qquad \text{(Table 10.5)}$$

and $\left(\frac{dV}{dx}\right)_{II} \simeq 2$ (Table 10.2)

so that, arguing as before, one can write

$$\left(\frac{d^2V}{dx^2}\right)_{av} \simeq \frac{10^4 - 2}{2a} \simeq \frac{10^4}{.04} \quad \text{(since a} \simeq .02 \text{ cm, see Table 10.4)}$$

$$= 4\pi Ne$$

$$= 4 \times 3.14\ N \times 4.8 \times 10^{-10} \times 300$$

$$\text{or } N = 1.4 \times 10^{11} \qquad (10.23)$$

The argument of J_o in this case is

$$2.4 \times \frac{(1.64 - .02)}{1.64} = 2.37$$

From Table of Functions, J_o (2.37) = .02

N_o in this case is of the order of 10^{12} (Table 10.4)

Therefore, $N \simeq 0.2 \times 10^{11}$, which is one-seventh of the value given in Eq. (10.23)

10.10. Conclusion

Results presented in this thesis are obtained by a method which has not been used before. For the first time the current-voltage relations in a high-frequency discharge have been studied in detail, taking into account the phase quadrature between the voltage drop across the tube wall and the gap voltage (it may be recalled that Townsend's school did some work on this problem only at a very low current range, e.g. a few mA, without considering the phase quadrature).

That the hypothesis of ambipolar diffusion as the main operating process in the sustained h.f. discharge has been justified by the experimental results is a definite step forward towards our understanding of the mechanism of the discharge. In spite of the success, it should be pointed out that there is ample scope for refinement of the experiment. Certain facts, namely, occasional occurrence of plasma oscillations, variation of the longitudinal electric field with the gap current (Figs. 6.23 - 6.25), the exact phase relation between the conduction and displacement currents, the edge effect giving a rise of the current density in the gap for lower

electrode areas etc. need more accurate and thorough investigation.

Appendix I

Elimination of the Slow Drift of Ammeter Readings

The reduction of ammeter deflection with time might be due to the dielectric heating of the material of the discharge tube and its assembly. In order to test this a dummy electrode (a hollow cylindrical tube of brass) was suspended in air near one end of the discharge tube (the ammeter end) and connections to it were made. As Table I-1 below shows, this did not improve the situation.

TABLE - I-1: Air: p = 3.7 mm.Hg.

Controlling Knob of the oscillator fixed at a convenient position.

Observations with proper electrodes		Observations with dummy electrodes	
Maximum deflection (mm)	deflection after 2 minutes (mm)	Maximum deflection (mm)	deflection after 2 minutes (mm)
19	9	30	11
23	10	31	11

Observations were, therefore, continued with the proper electrodes. When the above method failed, the voltmeter circuit was suspected. It was soon found that without the voltmeter circuit in operation, the deflection remained steady in time. It was next thought that the ammeter and voltmeter readings should be taken separately. Accordingly, the procedure adopted was as follows:

Set the controlling knob of the oscillator at any convenient position; switch on the oscillator; note the ammeter deflection and switch off the oscillator; complete the voltmeter circuit, switch on the oscillator and note the voltmeter reading. Repeat this procedure for several settings of the controlling knob. A set of data taken according to this procedure had a large scatter.

The trouble in the voltmeter circuit lay in fact with the batteries used for the filament supply. So long dry cells were being used; it was decided to use freshly charged storage cells instead and this nearly eliminated the difficulty.

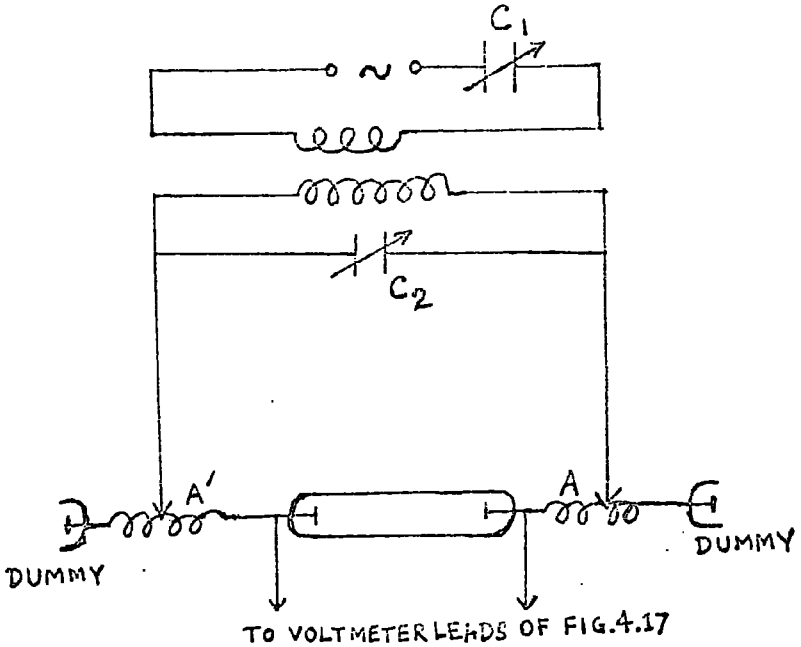

FIG. II - 1

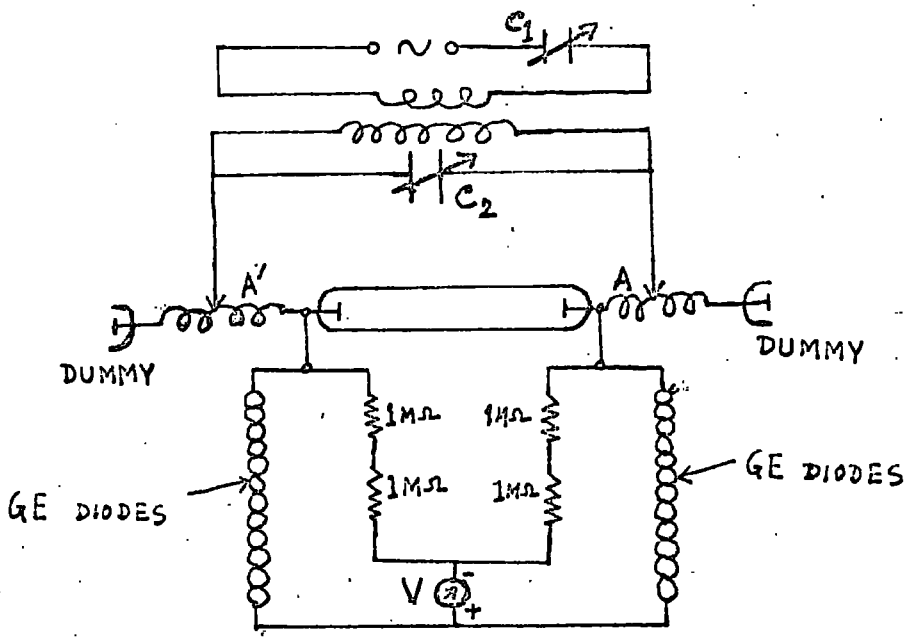

FIG. II - 2.

Appendix - II

Difficulties with the Strays.

A number of steps were taken to deal with the difficulties introduced by the strays. They are enumerated below:

(i) Use of the dummy electrode.

As shown in Fig. II-1, the input terminals from the secondary were connected to the mid-regions of the coil A and A^1, the free ends of the coils being connected to dummy electrodes. The idea was that the displacement currents in the two halves of each coil, would in all circumstances flow in opposite directions and by adjustment of the position of the input points these two oppositely flowing displacement currents could be balanced or brought to near balance. When this could be achieved, breakdown of the gap would show a deflection corresponding to the conduction current through the gap.

This, however, did not work in practice, partly because of the reduction in the ammeter sensitivity produced.

(ii) Use of germanium diodes.

Instead of the EY51 diodes, a string of germanium diodes were used (a dozen on each side, as shown in

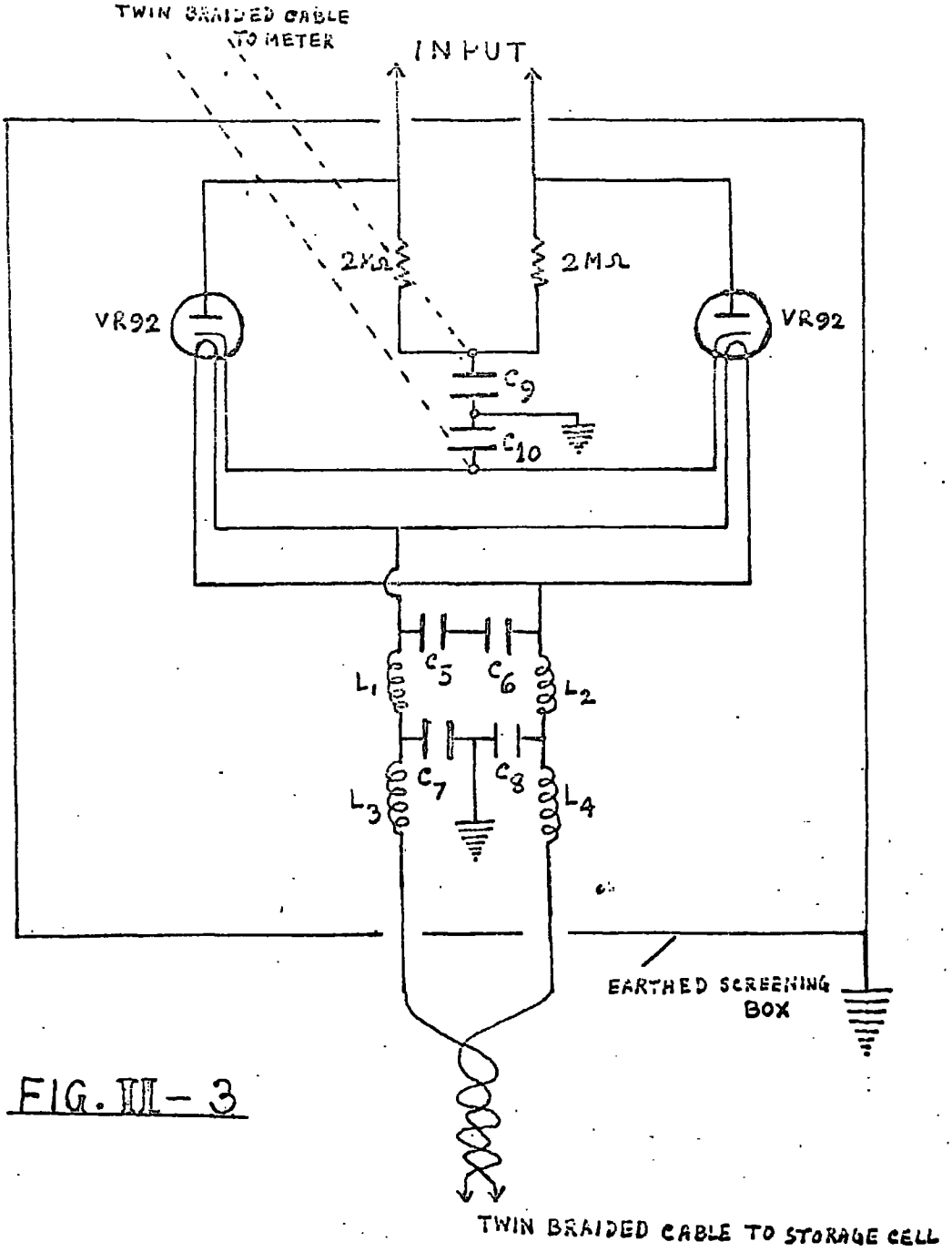
TWIN BRAIDED CABLE TO METER
INPUT
2MΩ
2MΩ
VR92
VR92
C9
C10
L1
C5
C6
L2
L3
C7
C8
L4
EARTHED SCREENING BOX
TWIN BRAIDED CABLE TO STORAGE CELL

FIG. III - 3

Fig.II-2) with the idea that this would reduce the effective self-capacity (and hence the displacement current); but this did not work owing to increase in the stray capacitances of these diodes to earth.

(iii) Shifting of the voltmeter circuit.

The voltmeter circuit was placed between the discharge tube and the capacitor C_2, rather than the previous arrangement of the tube in between the voltmeter circuit and C_2. By this change of the physical laying out of the entire electrical assembly, it was found that the displacement current was much reduced.

(iv) Use of a tuning condenser.

A small tuning condenser was next placed in series with coil A at its dummy end with the hope of reducing the deflection due to the displacement current further. It was found, however, that though by adjusting this condenser, the deflection could be further reduced, this adjustment affected the intensity of discharge within the tube and so it was subsequently removed.

(v) Modification of the voltmeter circuit.

A few modifications in the voltmeter circuit were done (Fig.II-3) for reducing the strays e.g. the capacitances C_5 - C_8 and the chokes L_1 - L_4reduced strays

from battery to ground, C_9 and C_{10} bypassed strays from the meter case to ground. By these modifications, slight improvement was noticed, but complete elimination of the strays was not achieved.

Incidentally, during this exploratory period, use of an electrostatic voltmeter or an absolute voltmeter based on the balance method was thought about. The balance method, however, was soon ruled out from the point of view of too small a force (due to the electric field) to make it work. The electrostatic voltmeter was ruled out for the reason that the one that was available had divisions not small enough to read 5 or 10 Volts.

REFERENCES.

1. Townsend, J.S. and Nethercot, W., Phil. Mag..7, 600, 1929.
2. Brown, S.C., Handbuch der Physik 22, 531, 1956.
3. Boyer, M.F., Ph.D. Thesis, University of Durham, 1965.
4. Oskam, H.J. and Mittlestadt, V.R., 31, 940, 1960.
5. Mulcahy, M.J. and Lennon, J.J., Proc. Phys.Soc. 80,626,1962.
6. Eckert, H.U., Ionisation Phenomena in Gases, Conference paper. Munich, Vol.I, 537, 1961.
7. Schneider, F., Z.Ang. Phys. 6, 456, 1954.
8. Allis, W.P, Brown, S.C. and Everhart, E., Phys. Rev. 84, 519, 1951.
9. von Engel, A., Ionised Gases, 2nd Edition, Clarendon Press, Oxford, p.145, 1965.
10. Gill, E.W.B. and von Engel, A., Proc. Roy. SOC. Lond., Ser A 197, 107, 1949.
11. Francis, G. and von Engel, A., Phil. Trans. Roy.Soc. A 246, 143, 1953.
12. Hatch, A.J. and Williams, H.B., J.Appl.Phys. 25, 417, 1954; Phys. Rev. 100, 1228, 1955; Phys. Rev.89, 339, 1953.
13. Townsend, J.S. and Jones, F.L., Phil. Mag 12, 815, 1931.
14. Hayman, R.L., Phil.Mag 7, 586, 1929.
15. Phelps, A.V. and Brown, S.C., Phys.Rev 86, 102, 1952.
16. Thompson, J.B., Proc.Phys.Soc. 73, 818, 1959.
17. Schulz-Du Bois, E., Z.Phys. 145, 269, 1956.

18. Romig, M.F., The Physics of Fluids, 3, 129, 1960.

19. Allis, W.P. and Rose, D., Phys. Rev. 93, 83, 1954.

20. Fowler, R.G., Proc.Phys. Soc. 80, 620, 1962.

21. Golovanivskii, K.S. and Kuzovnikov, A., Sov.Phys.Tech.Phys., 6, 645, 1962.

22. Perel, V.I. and Pinskii, Ya. M., Sov.Phys.Tech.Phys. 8, 197, 1963.

23. Loeb, L.B., Basic Processes of Gaseous Electronics, University Press, Chap. V, 1955.

24. Francis, G. Ionisation Phenomena in Gases, Butterworth, p.163, 1960.

25. Brown, S.C., International Symposium on Electrical Discharge in Gases, Delft, p.97, 1955.

26. Nicholls, M.J., Ph.D. Thesis, University of Durham, p.41, 1960.

27. Maxwell, J.C., Electricity and Magnetism, Oxford, vol.II, 1904.

28. Thornton, W.M. and Thompson, W.G., J.I.E.E. 71,1,1932.

29. Hund, A., High Frequency Measurements, McGraw-Hill Book Co. Inc. New York and London, p.101, 1933.

30. Gill, E.W.B. and von Engel, A., Proc.Roy.Soc, Lond., Ser. A, 192, 446, 1948.

31. Richards, R.C., Phil.Mag. 2, 508, 1926.

32. Pekarek, L. and Krejci, V., Czech, J. Phys. B12, 722, 1962.

33. Nakata, J., TaKenaka, E. and Masutari, T., J.Phys.Soc. Japan, 20, 1698, 1965.

34. Townsend, J.S.E., Electrons in Gases, Hutchinson's Scientific and Technical Publications,p.72-73,1947.

35. Papoular, R., Electrical Phenomena in Gases, Iliffe, English Edition, p.188, 1965.